Jahn-Teller effect and topological Jahn-Teller Mott insulators in magic-angle twisted-bilayer graphene

Michele Fabrizio (SISSA)

Outline of the lectures

- peculiar features of the band structure of magic-angle twisted bilayer graphene with relaxed atomic positions

  Phys. Rev. B **98**, 235137 (2018)

- effects of special phonon displacements on the tight-binding band structure: emergence of an $e \times E$ Jahn-Teller effect?

  Phys. Rev. X **9**, 041010 (2019)

- explicit construction of the Jahn-Teller model in the continuum representation of Bistritzer and MacDonald

  Eur. Phys. J. Plus (2020) 135:630

- interplay between Coulomb repulsion and Jahn-Teller phonon mediated electron-electron attraction: Hartree-Fock phase diagram and dynamical Jahn-Teller effect

  preprint, arXiv:2204.05190

Most of the work done by

Mattia Angeli, former SISSA student,
currently post doc at Harvard

Andrea Blason, current SISSA student

bilayer graphene

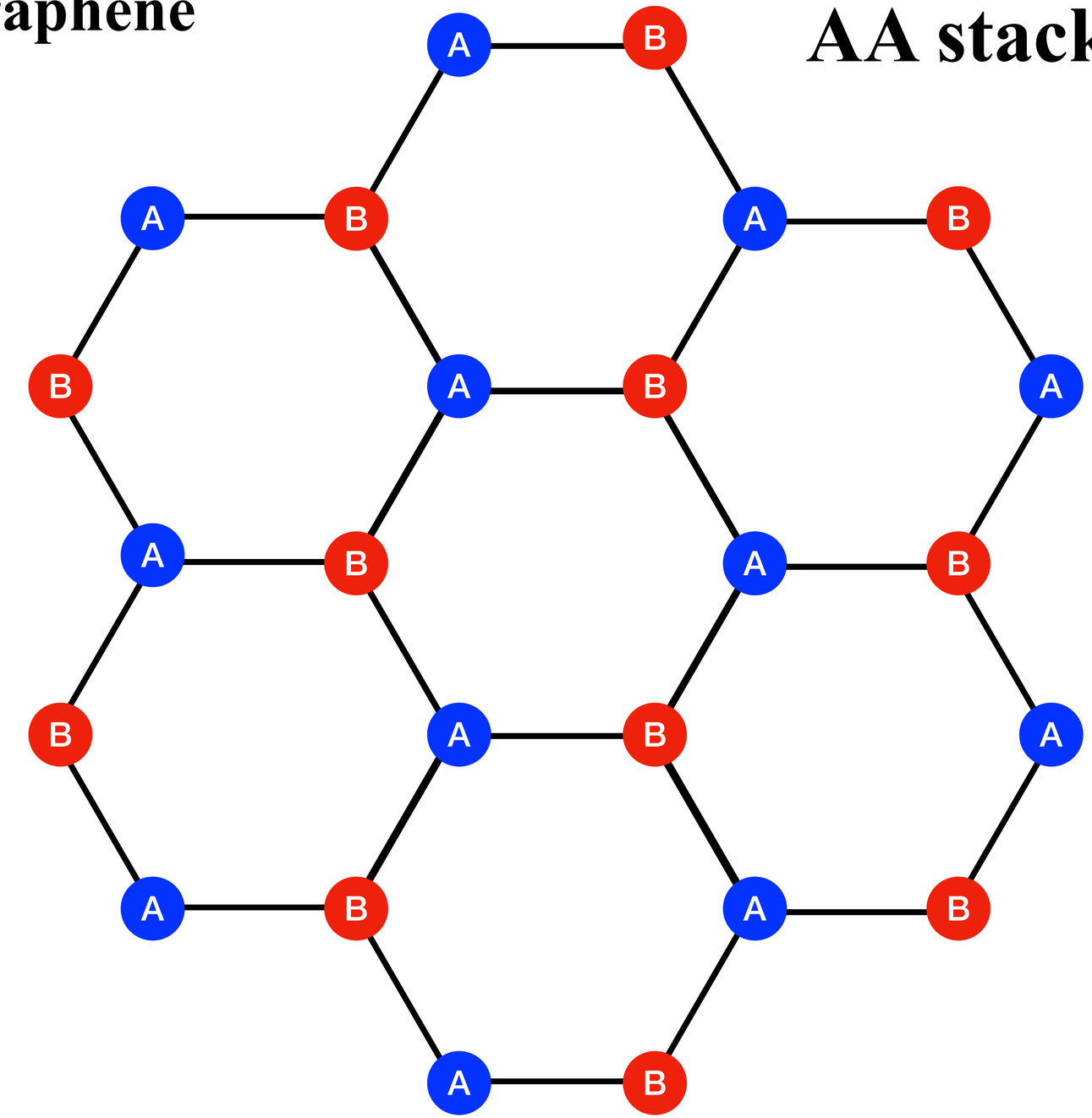

bilayer graphene

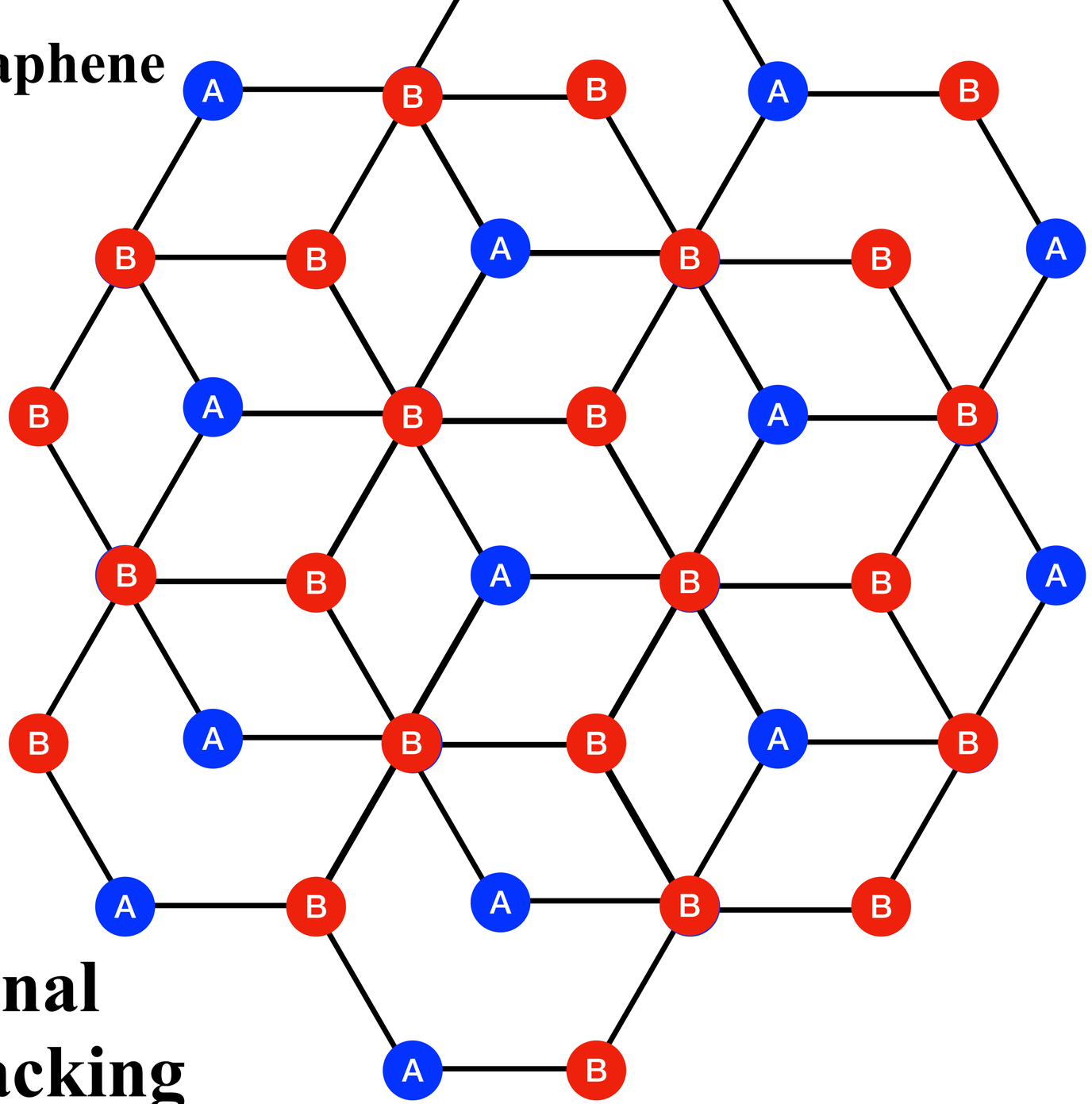

Bernal
AB stacking

bilayer graphene

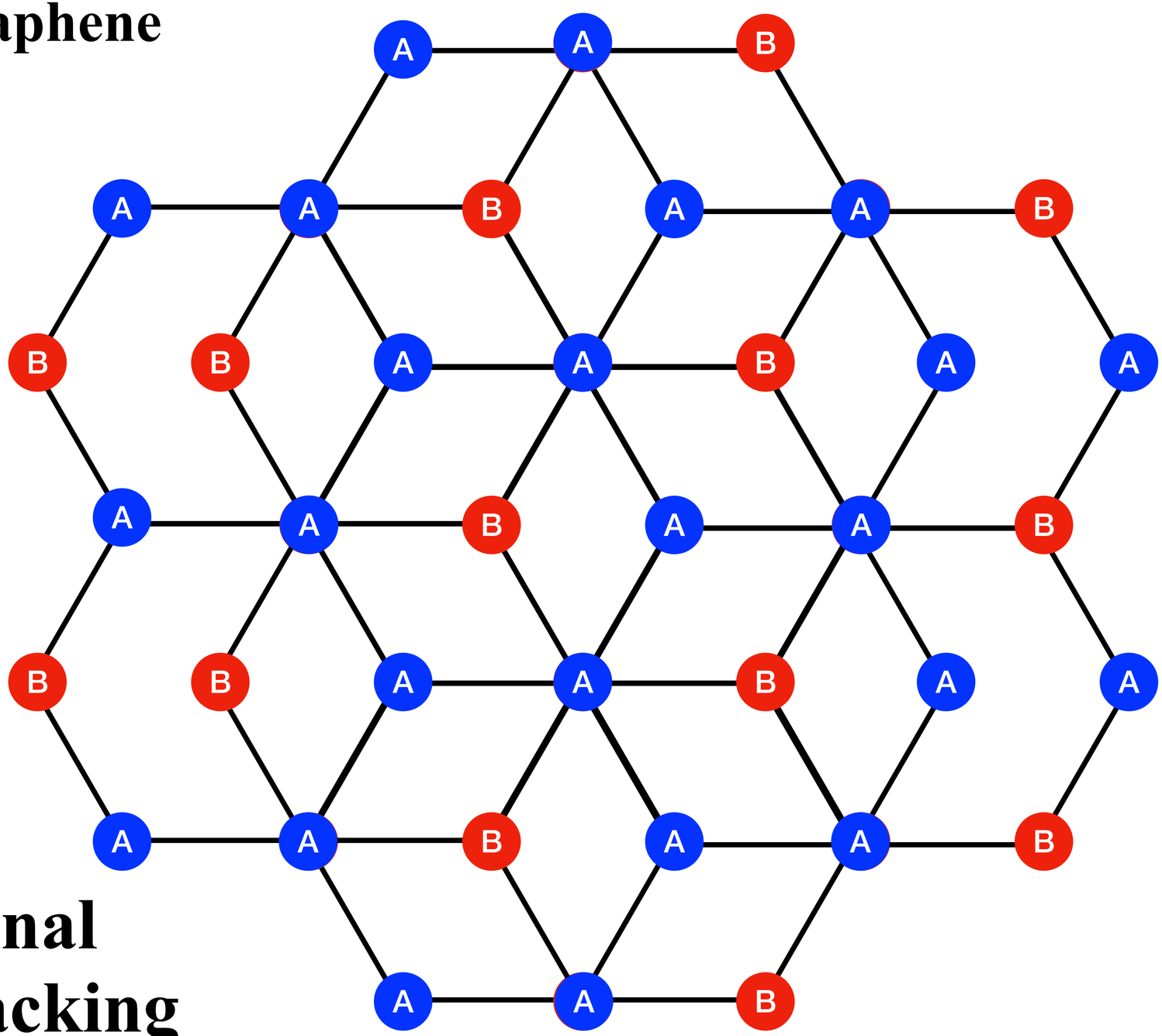

Bernal
BA stacking

Twisted bilayer graphene

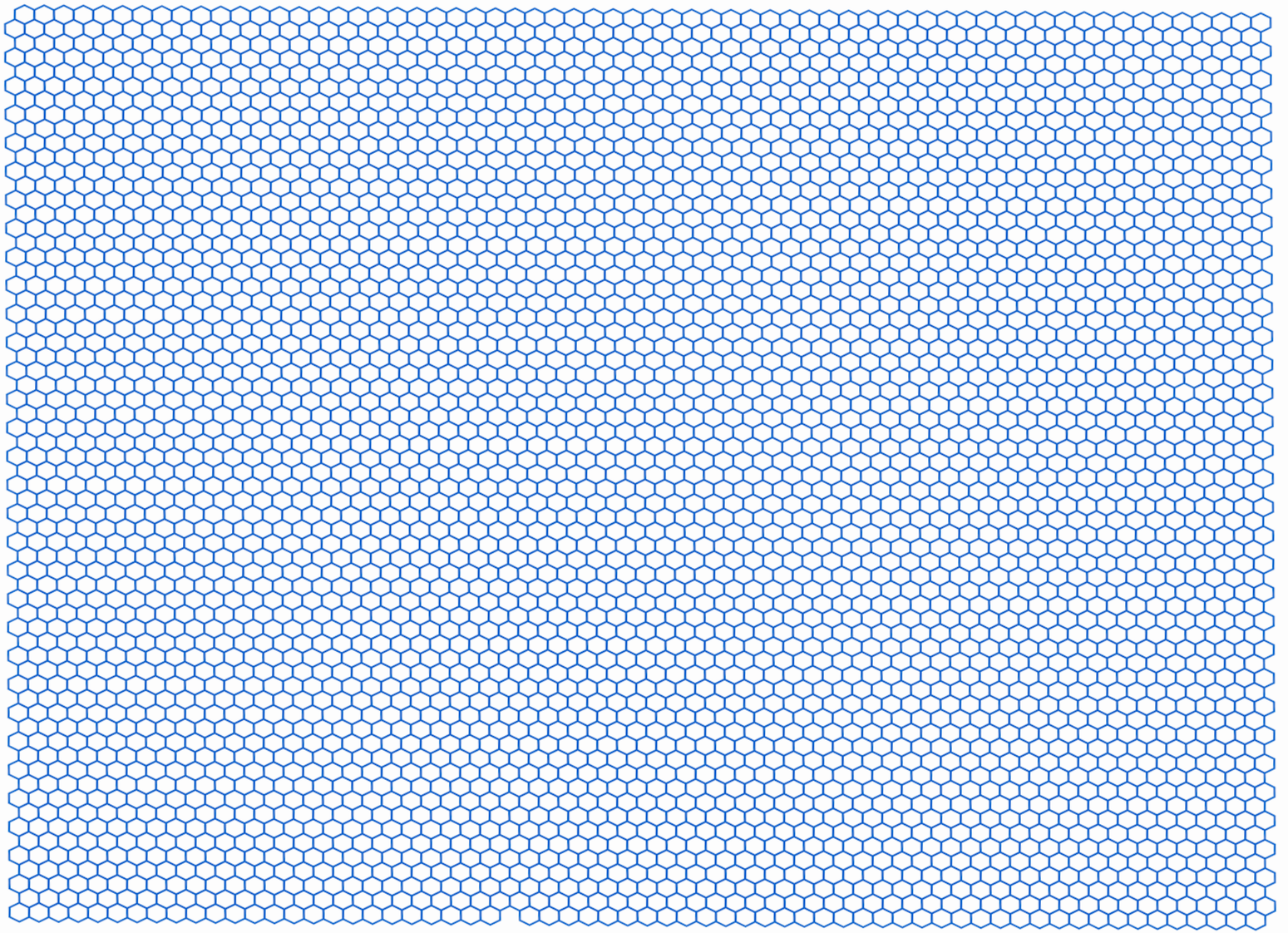

take a graphene AA stacked bilayer and rotate one sheet of an angle θ with respect to the other sheet

Twisted bilayer graphene

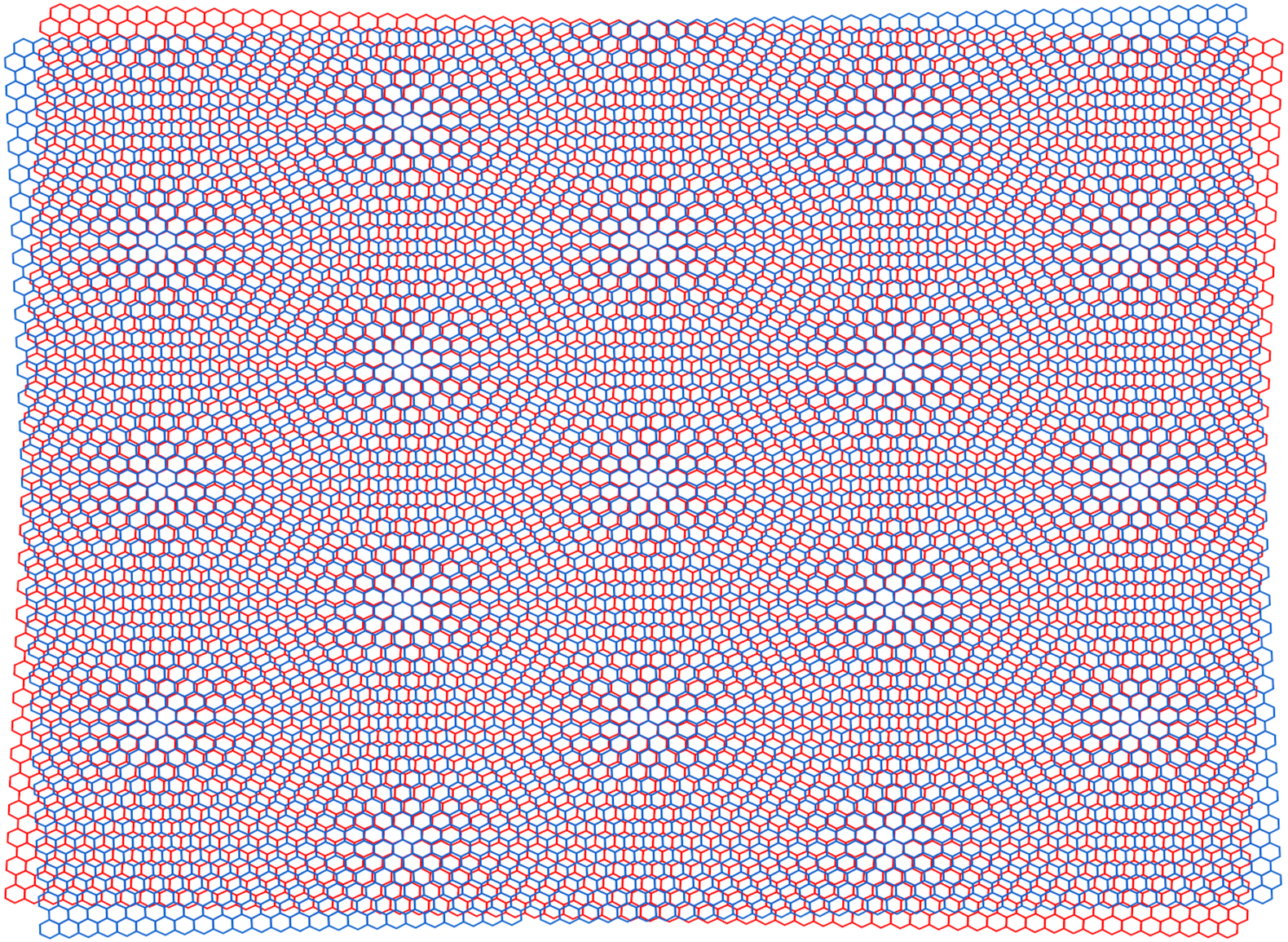

moiré pattern

Twisted bilayer graphene

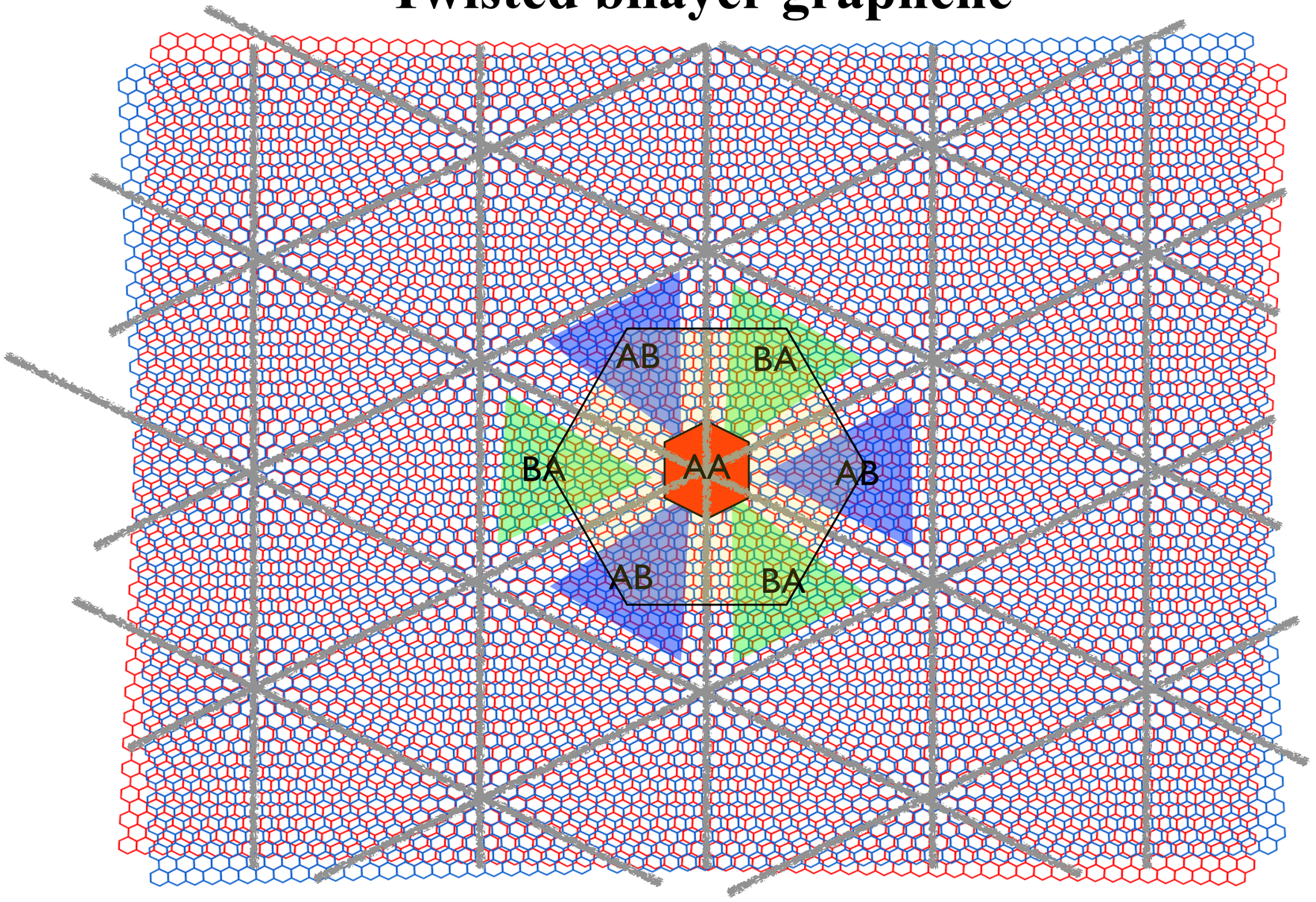

moiré pattern

Band structure of unrelaxed twisted bilayer graphene

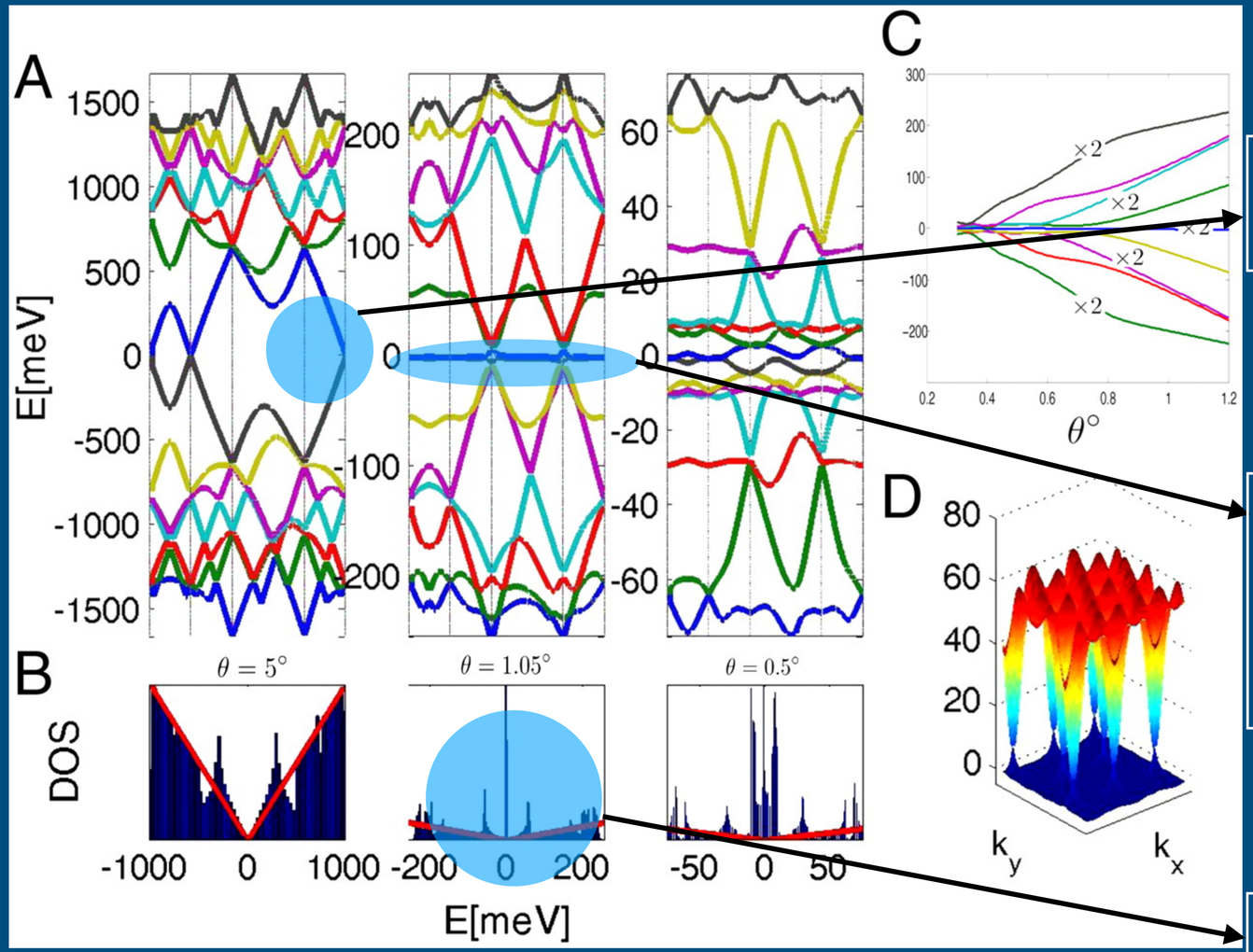

there are still Dirac nodes

there are magic angles where the velocity at the Dirac nodes vanishes

no gap in the spectrum at the magic angle

R. Bistritzer and A.H. MacDonald, PNAS 108, 12233 (2011)

First question: why experimentally the twisted bilayer near the magic angle is insulating for $n = \pm 4$ electrons per moiré unit cell, whereas band structure calculations predict a metallic behaviour.

Answer: atomic relaxation

Lucignano et al., PRB 99, 195419 (2019)

Since Bernal stacking has lower energy, the twisted bilayer relaxes so as to maximise AB and BA Bernal stacked regions and minimise AA ones

Phys. Rev. B 98, 235137 (2018)

AA **Bernal** **domain wall**

$\theta = 1.08^{o}$

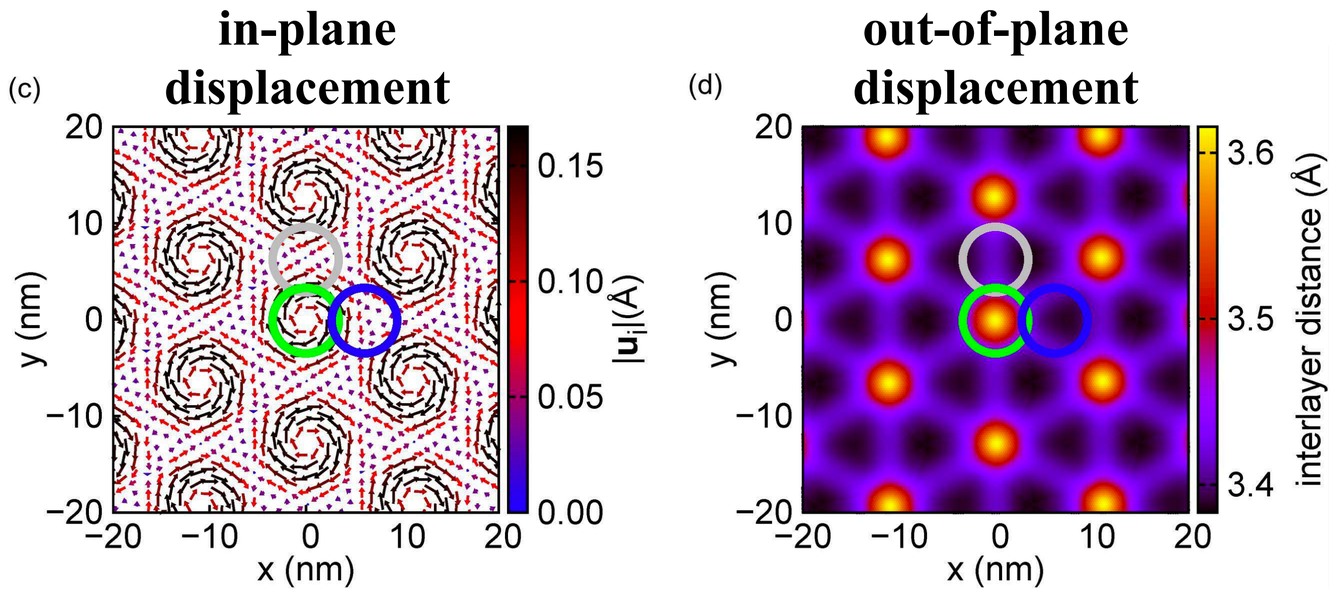

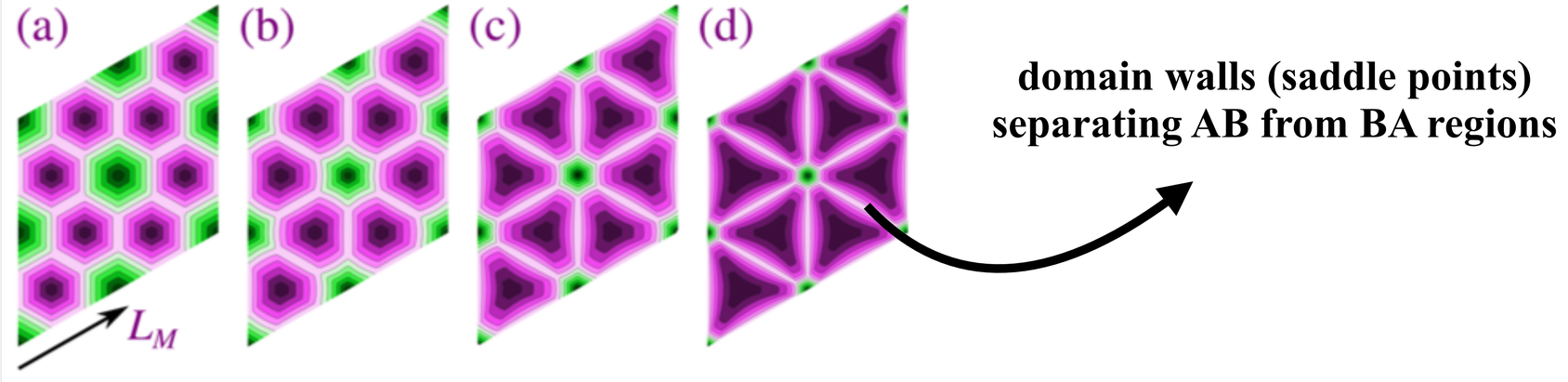

next step: tight-binding calculation with realistic Slater-Koster parameters describing hopping between p_z orbitals of carbon atoms in the relaxed positions

$$t(\mathbf{r}) = V_{pp\sigma}(r)\,\frac{\mathbf{r}\cdot\boldsymbol{e}_z}{r} + V_{pp\pi}(r)\left(1 - \frac{\mathbf{r}\cdot\boldsymbol{e}_z}{r}\right)$$

$$V_{pp\sigma(\pi)}(r) = V^0_{pp\sigma(\pi)}\,\mathrm{e}^{-r/r_0}$$

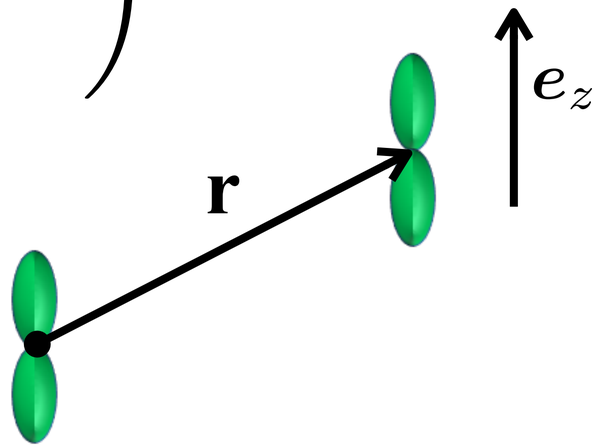

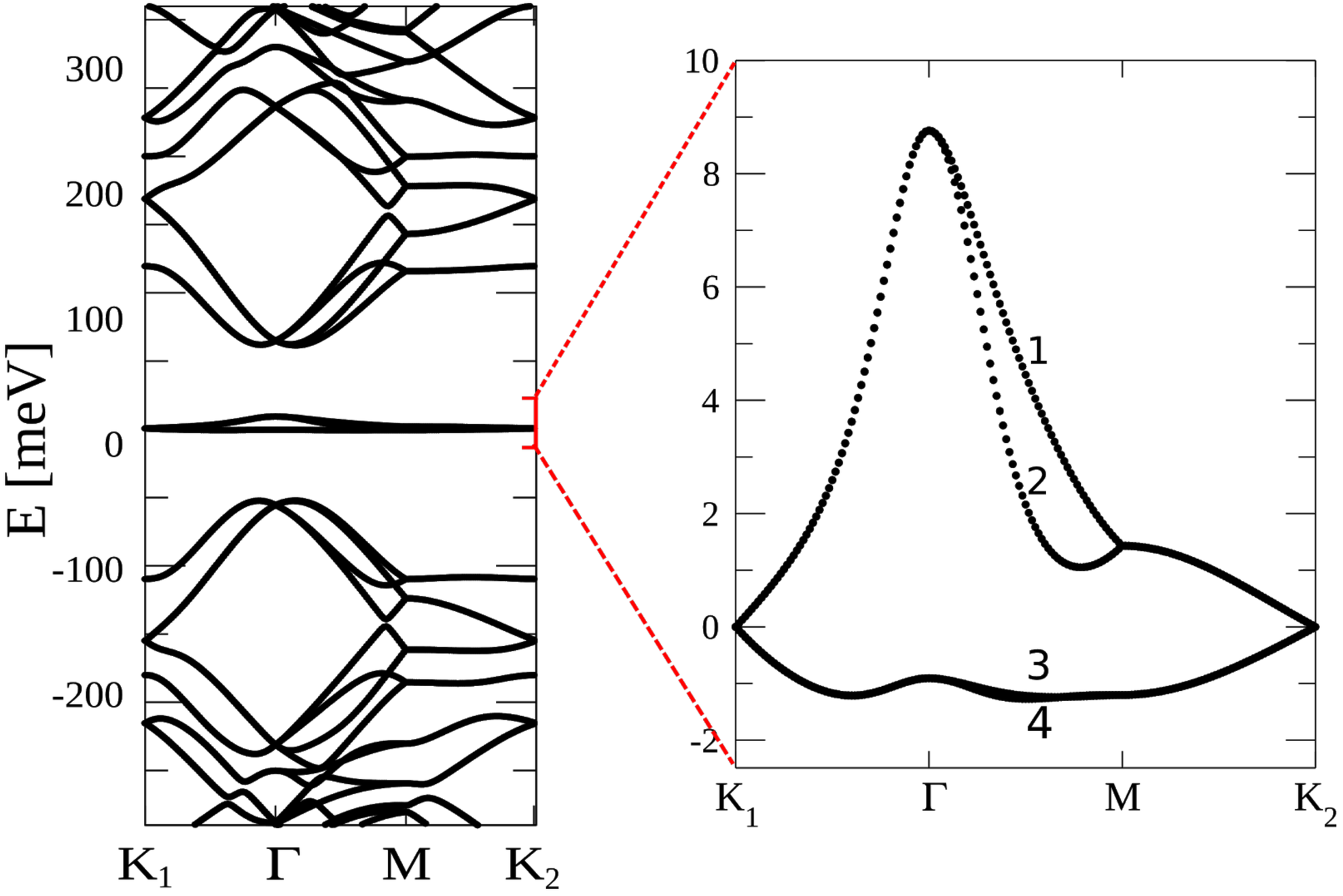

indeed four flat bands around charge neutrality, separated by a gap from all other bands

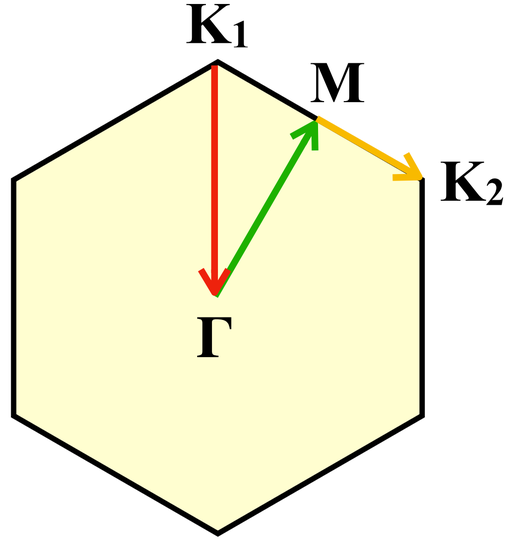

mini Brillouin zone

Common approach to narrow bands:

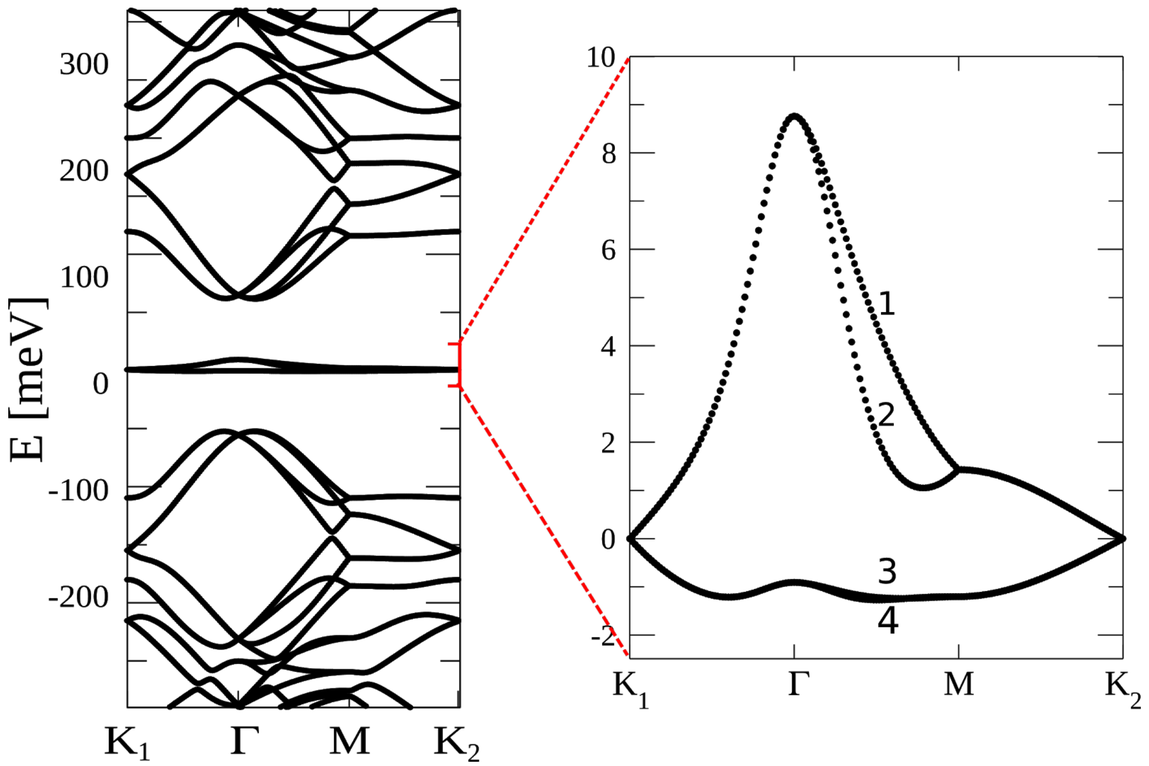

- build a tight-binding model with short range hopping for the 4 mini-bands, add interaction, and study the model by many-body tools

need to construct Wannier orbitals

Symmetries

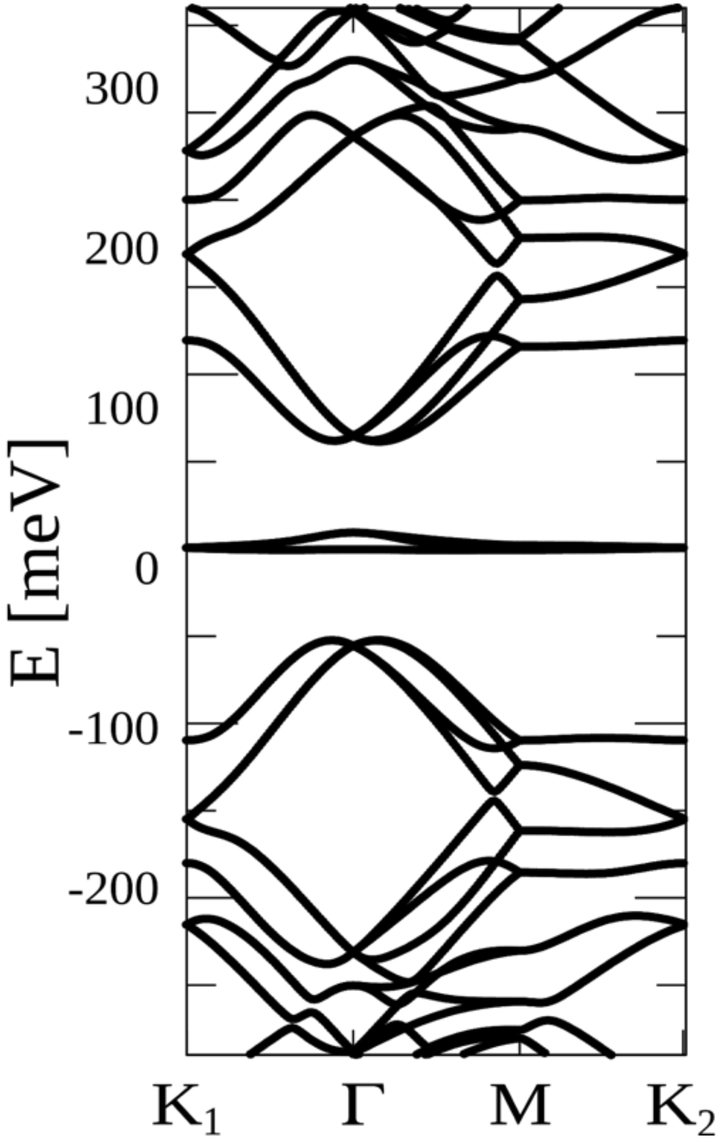

- full D_6 space group symmetry (C_{3z} , C_{2z} , C_{2x} , C_{2y})

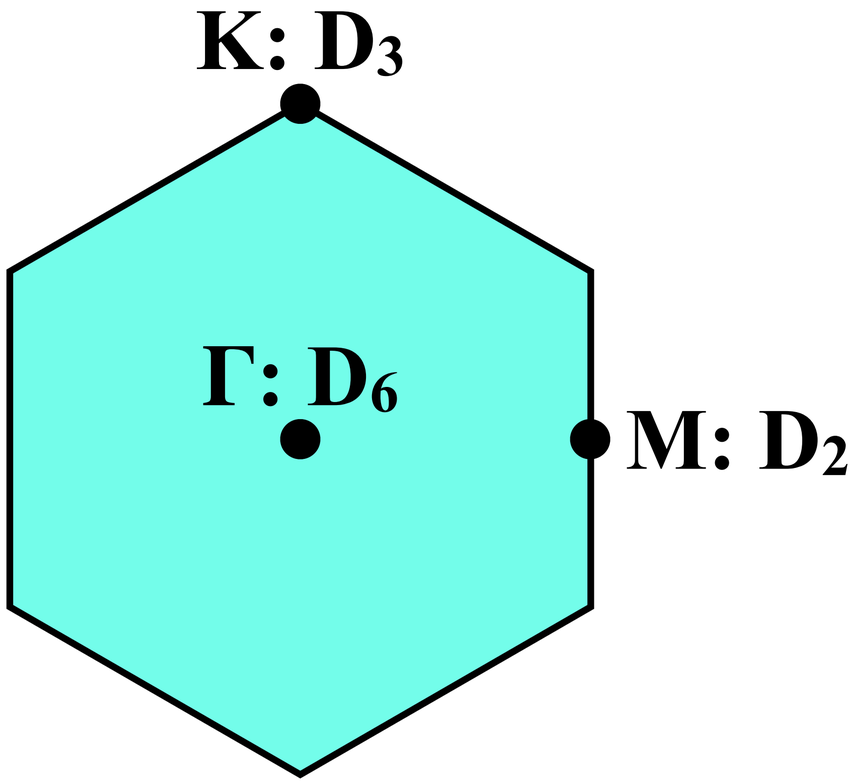

irreducible representations of D_6 space group

(little group at **Γ**)

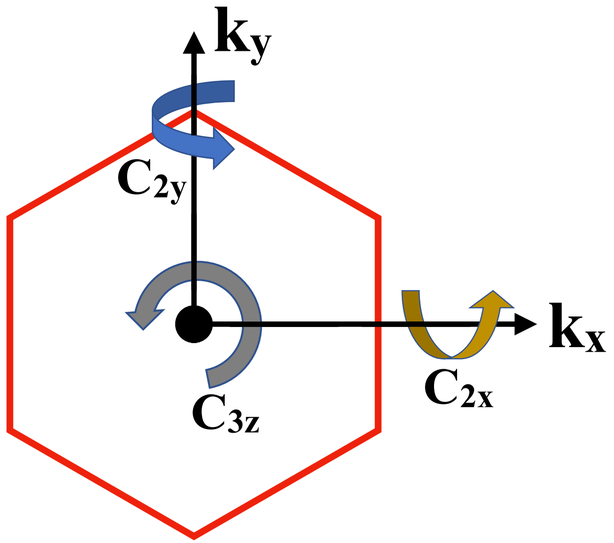

	C_{3z}	C_{2x}	C_{2y}	functions
$A_1(1)$	+1	+1	+1	x^2+y^2
$A_2(1)$	+1	-1	-1	z
$B_1(1)$	+1	+1	-1	$x(x^2-3y^2)$
$B_2(1)$	+1	-1	+1	$y(3x^2-y^2)$
$E_1(2)$	$\begin{pmatrix} e^{2i\pi/3} & 0 \\ 0 & e^{-2i\pi/3} \end{pmatrix}$	$\begin{pmatrix} 0 & 1 \\ 1 & 0 \end{pmatrix}$	$\begin{pmatrix} 0 & -1 \\ -1 & 0 \end{pmatrix}$	$\begin{pmatrix} x+iy \\ x-iy \end{pmatrix}$
$E_2(2)$	$\begin{pmatrix} e^{2i\pi/3} & 0 \\ 0 & e^{-2i\pi/3} \end{pmatrix}$	$\begin{pmatrix} 0 & 1 \\ 1 & 0 \end{pmatrix}$	$\begin{pmatrix} 0 & 1 \\ 1 & 0 \end{pmatrix}$	$\begin{pmatrix} x^2-y^2-ixy \\ x^2-y^2+ixy \end{pmatrix}$

irreducible representations of D_3 space group

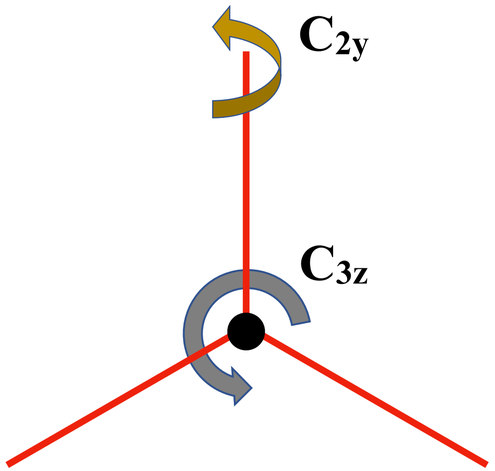

(little group at **K**)

	C_{3z}	C_{2y}
$A_1(1)$	$+1$	$+1$
$A_2(1)$	$+1$	-1
$E(2)$	$\begin{pmatrix} e^{2i\pi/3} & 0 \\ 0 & e^{-2i\pi/3} \end{pmatrix}$	$\begin{pmatrix} 0 & 1 \\ 1 & 0 \end{pmatrix}$

irreducible representations of D_2 space group

(little group at **M**)

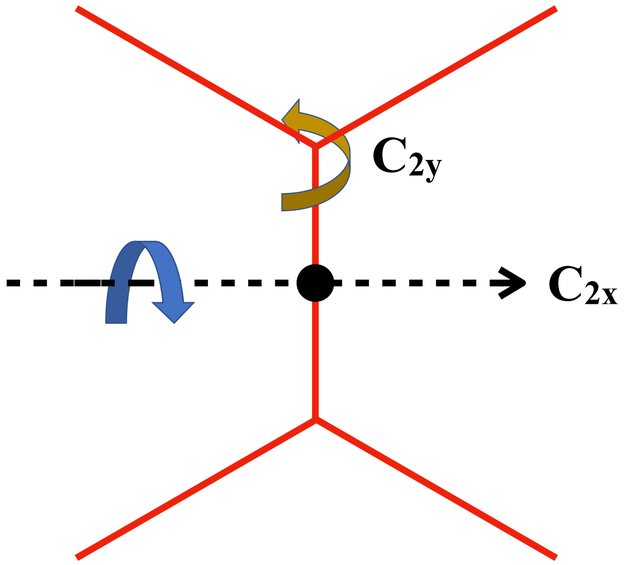

	C_{2y}	C_{2x}
$A(1)$	$+1$	$+1$
$B_1(1)$	-1	-1
$B_2(1)$	$+1$	-1
$B_3(1)$	-1	$+1$

Emergent U(1) valley symmetry

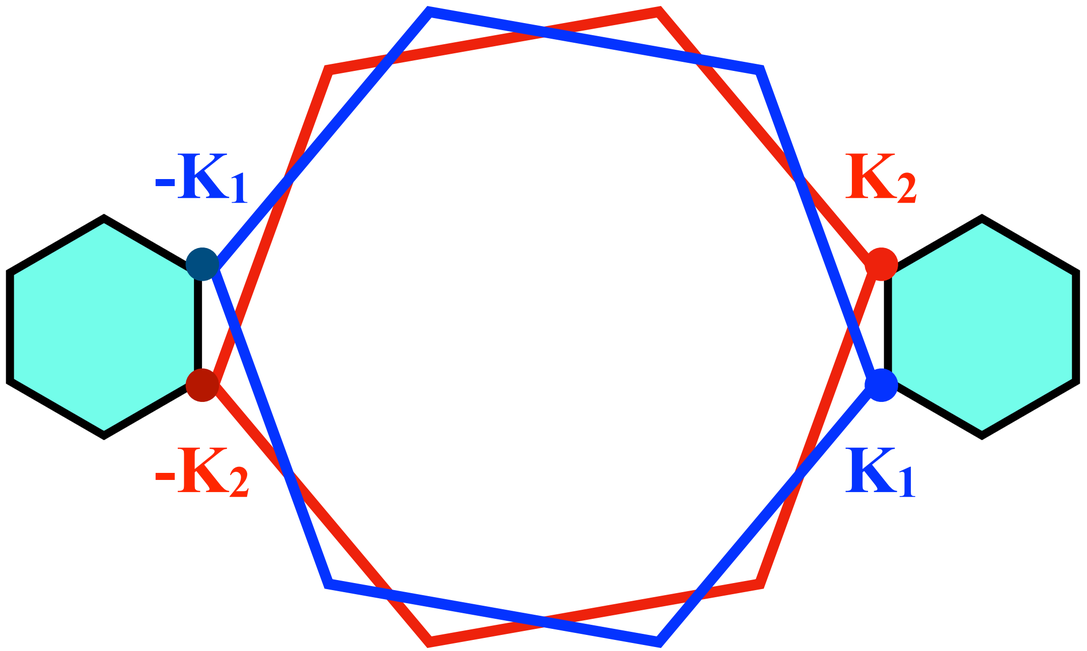

$\mathbf{K_1}$ of layer 1 and $\mathbf{-K_2}$ of layer 2 fold into $\mathbf{K_1}$ of the mini Brillouin zone

&

$\mathbf{K_2}$ of layer 1 and $\mathbf{-K_1}$ of layer 2 fold into $\mathbf{K_2}$ of the mini Brillouin zone

In spite of that, $\mathbf{K_1}$ (valley $\tau_3 = +1$) and $\mathbf{-K_2}$ ($\tau_3 = -1$) are uncoupled at small twist angle, as well as $\mathbf{K_2}$ ($\tau_3 = +1$) and $\mathbf{-K_1}$ ($\tau_3 = -1$).

The tight-binding Hamiltonian effectively commutes with τ_3 that becomes the generator of a valley $U_v(1)$

Symmetries

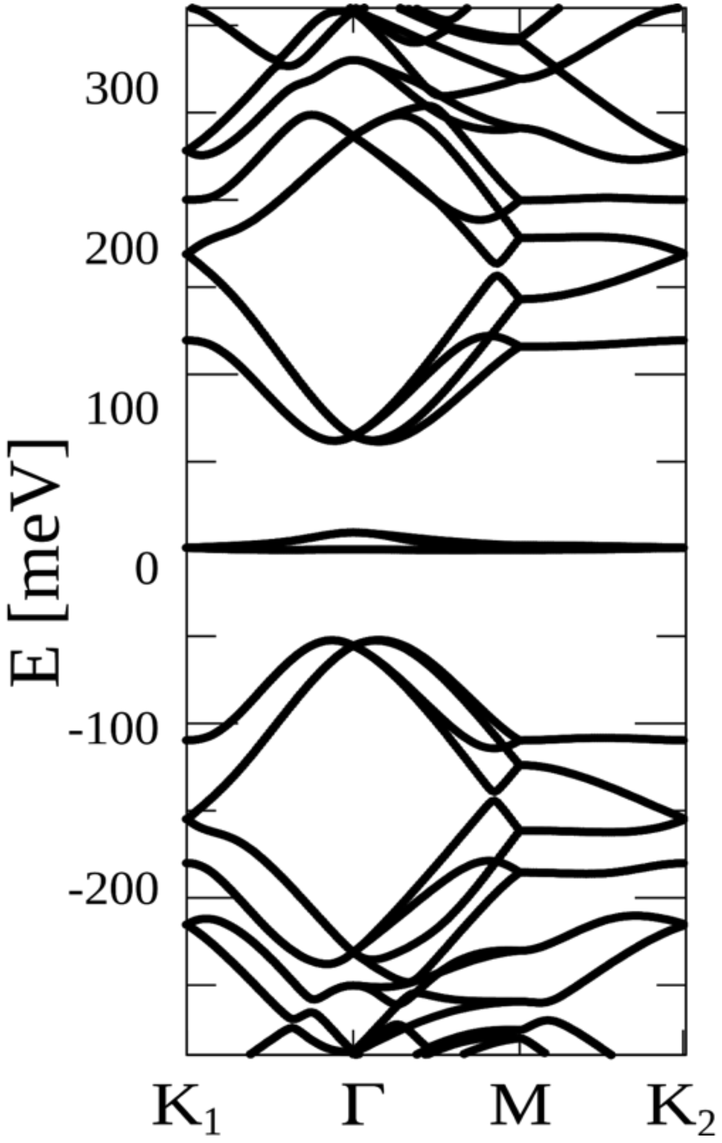

- D_6 space group symmetry (C_{3z} , C_{2z} , C_{2x} , C_{2y})
- time reversal T
- Valley U(1) symmetry

Symmetry analysis of the flat bands Bloch waves

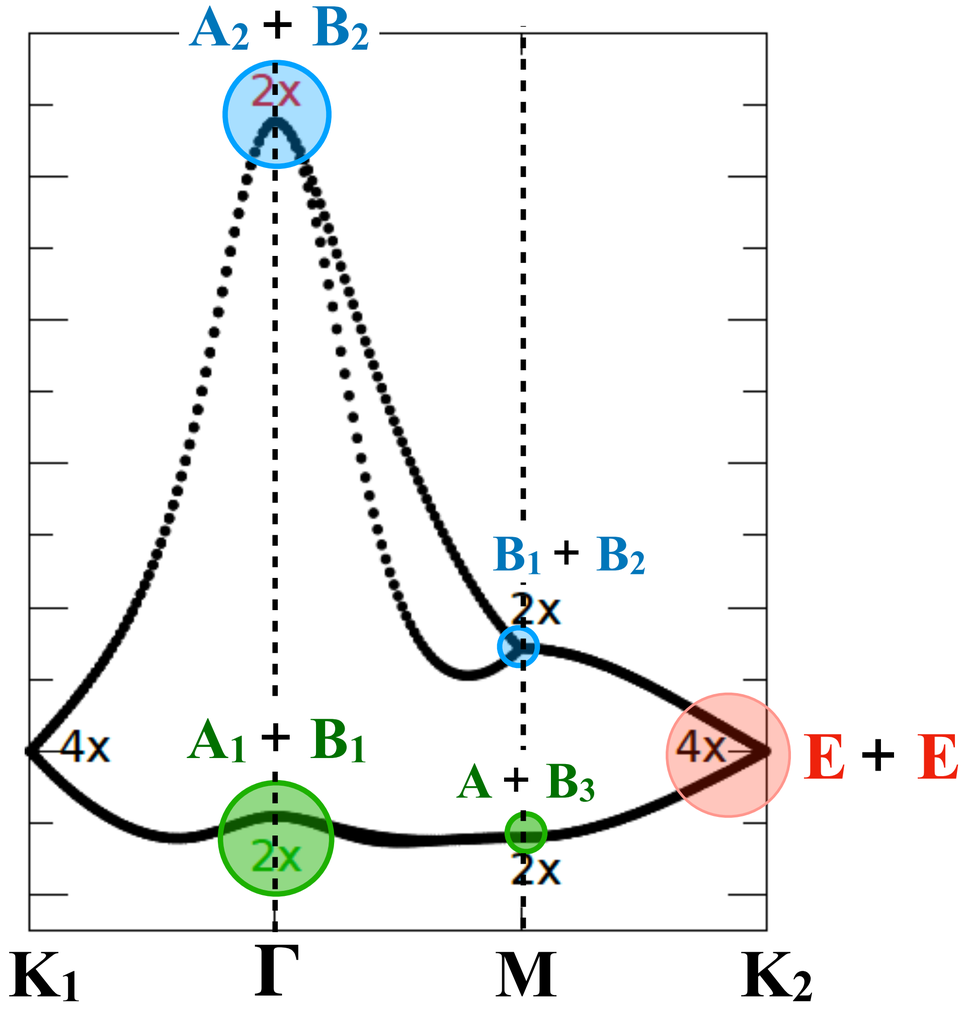

Γ: D_6

K: D_3

M: D_2

- Elementary band representation cannot reproduce the symmetry properties of Bloch waves. No Wannierization of the flat bands may yield short-range hoppings (Wannier obstruction), which hints at non trivial topology [Zou et al., Phys. Rev. B **98**, 085435 (2018)]

Symmetry analysis of the flat bands Bloch waves

finite winding number

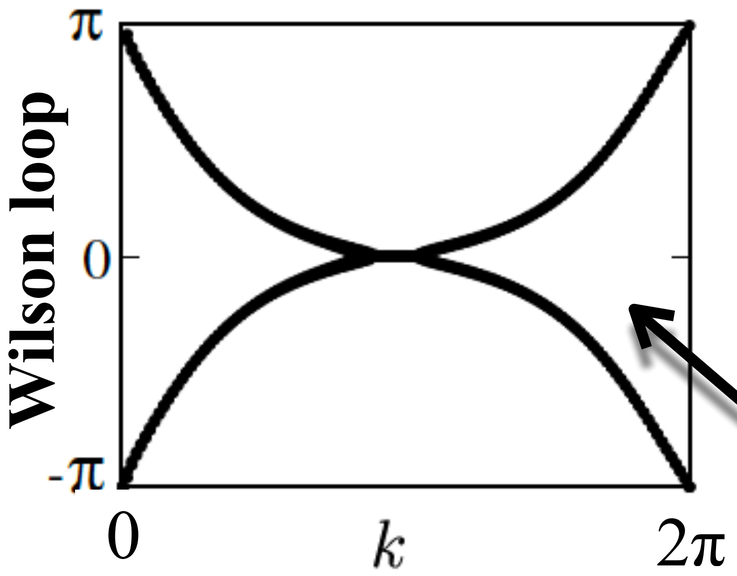

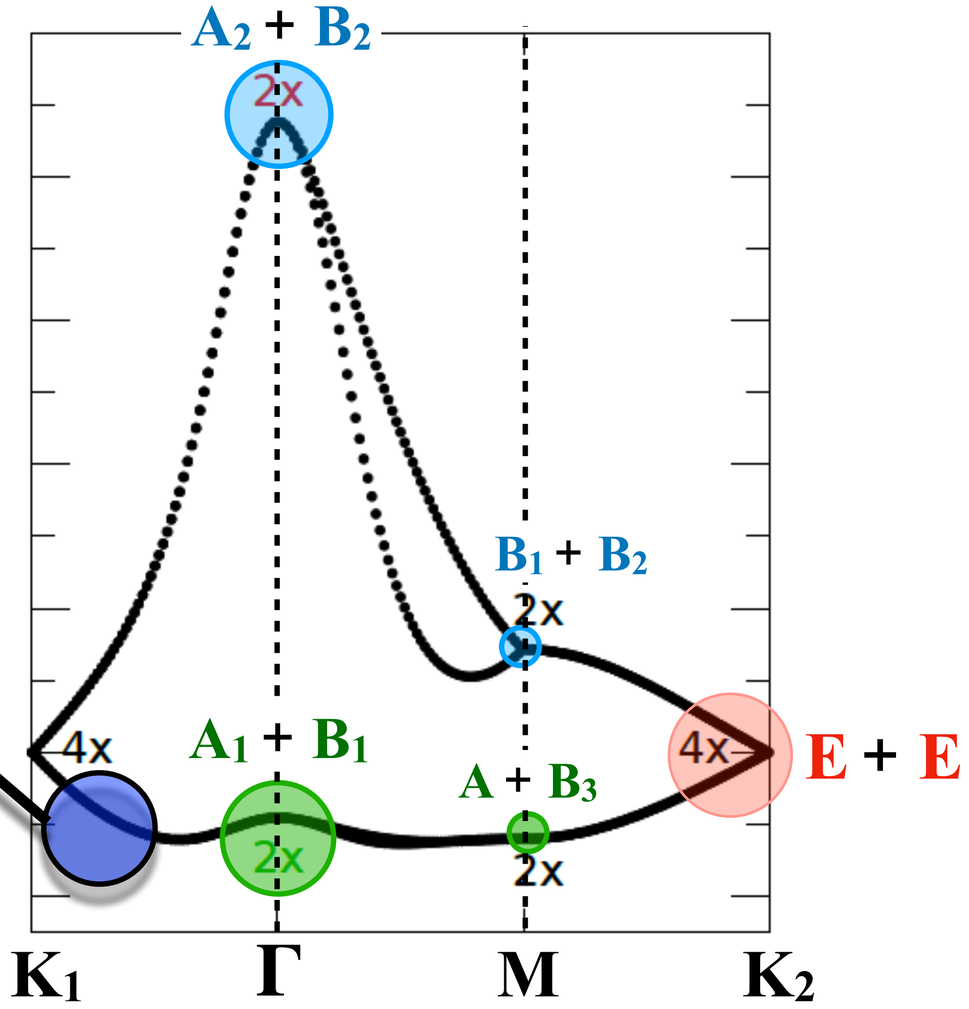

Γ: D_6

K: D_3

M: D_2

- Elementary band representation cannot reproduce the symmetry properties of Bloch waves. No Wannierization of the flat bands may yield short-range hoppings (Wannier obstruction), which hints at **non trivial topology**

Symmetry analysis of the flat bands Bloch waves

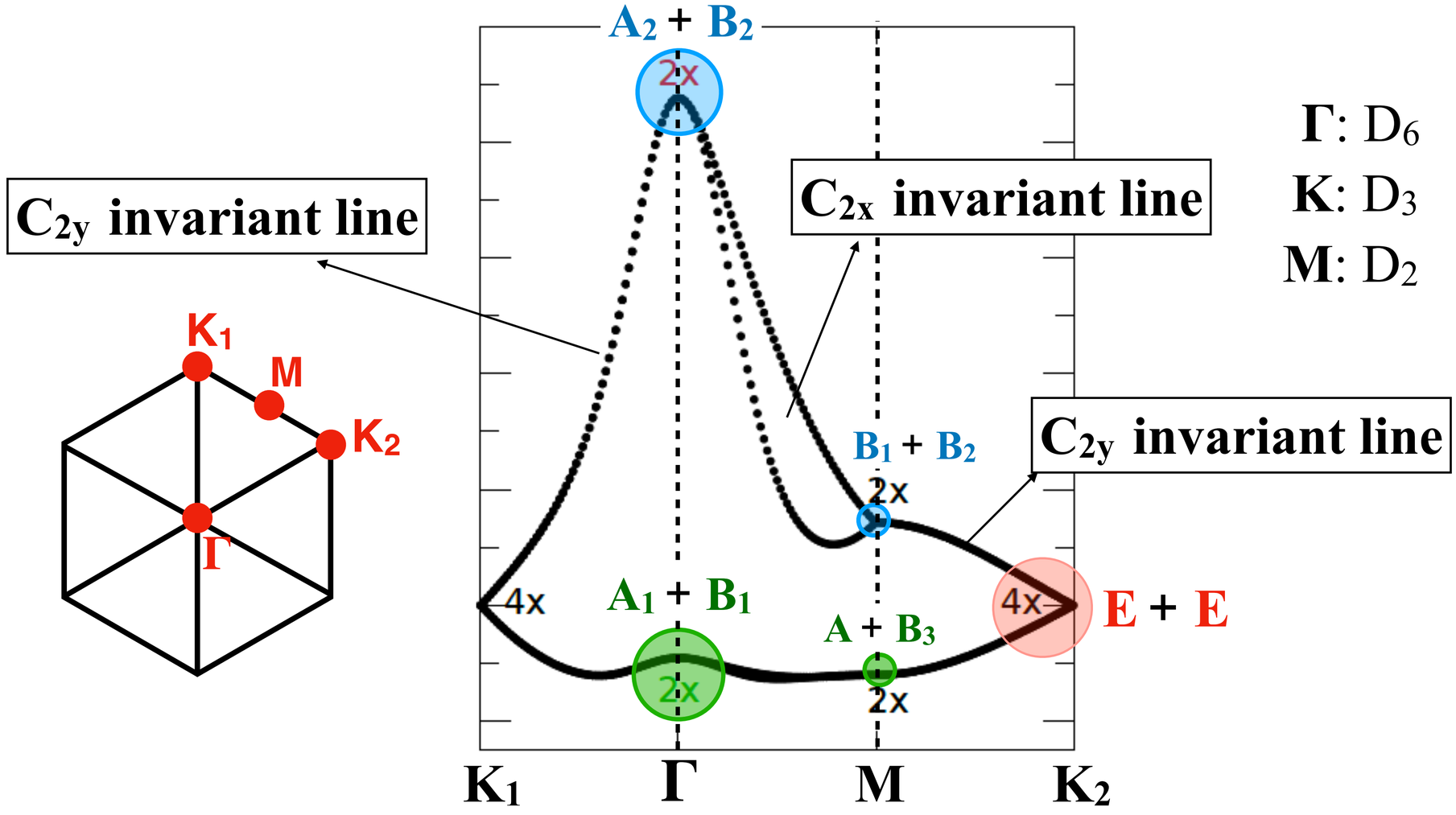

- accidental degeneracy along all lines invariant under C_{2y}. **WHY**?

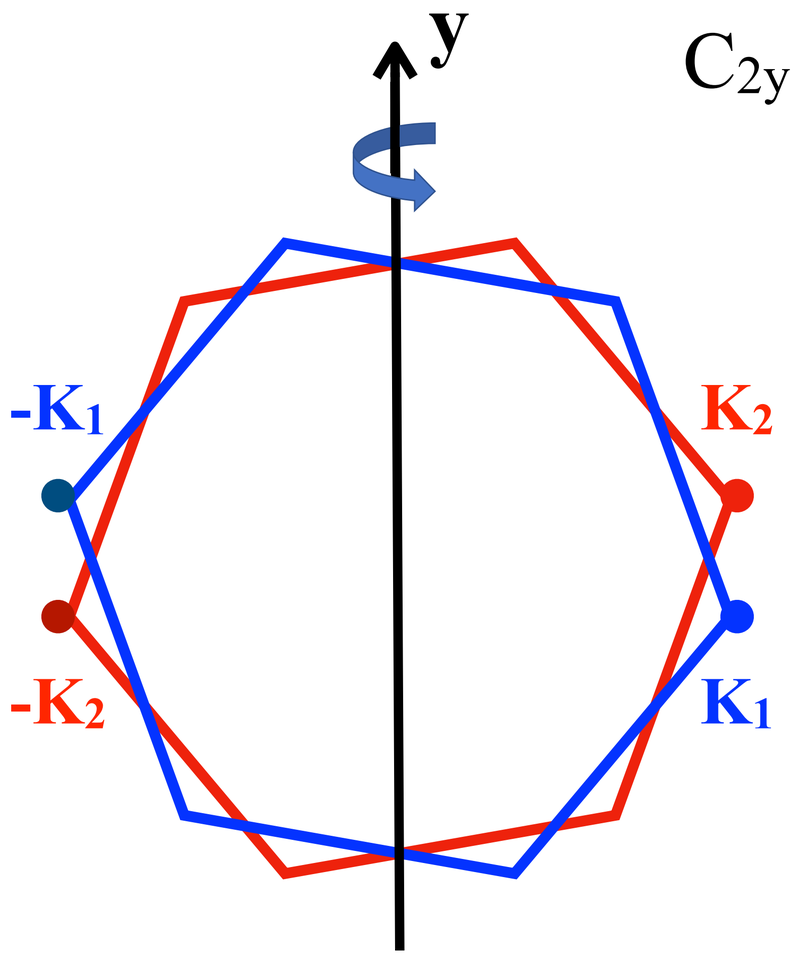

C_{2y} exchanges the valleys

$$\mathbf{C_{2y}} \equiv \tau_1 \times \left(\mathbf{k} \rightarrow C_{2y}(\mathbf{k})\right)$$

on the C_{2y} invariant lines

$$\mathbf{C_{2y}} \equiv \tau_1$$

- on the C_{2y} invariant lines, $H(\mathbf{k})$ commutes with τ_3 as well as with $C_{2y} \equiv \tau_1$, thus also with their product τ_2. Therefore, on those lines $U_v(1) \otimes C_{2y} \sim SU(2)$, which forces states with opposite parity w.r.t. C_{2y} to be degenerate.

There is wide consensus that magic-angle TBLG are insulators at all integer fillings of the flat bands. For that one needs first to get rid of the accidental degeneracy along C_{2y} invariant lines.

Coulomb repulsion can do the job driving spontaneous breakdown of $U_v(1)$.

What about atomic displacement?

Phys. Rev. X 9, 041010 (2019)

ad-hoc displacement field at Γ:

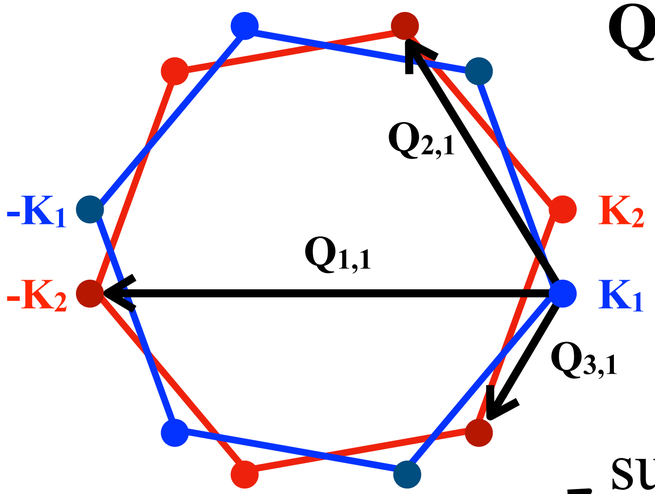

$\mathbf{Q}_{n,2} = C_{3z}(\mathbf{Q}_{n,1}) \quad \mathbf{Q}_{n,3} = C_{3z}(\mathbf{Q}_{n,2}) \quad n=1,2,3$

- the set of all $Q_{i,j}$'s, which are multiples of the primitive reciprocal lattice vectors of the mini BZ, is invariant under C_{3z} and C_{2x}, and odd under C_{2y} and C_{2z}

sum over all C atoms

$$\mathbf{u}(\mathbf{r}) = \sum_{\mathbf{R}} \sum_{i,j=1}^{3} \mathbf{u}_{ij}(\mathbf{R}) \sin\left(\mathbf{Q}_{i,j} \cdot \mathbf{R}\right) \delta(\mathbf{r} - \mathbf{R}) \quad \text{with} \quad \mathbf{u}_{ij}(\mathbf{R}) \parallel \mathbf{Q}_{i,j}$$

such displacement field is invariant under D_6

$$g\big(\mathbf{u}(\mathbf{r})\big) = \mathbf{u}\big(g(\mathbf{r})\big) \qquad \forall\, g \in D_6$$

$$\mathbf{u}(\mathbf{r}) = \sum_{\mathbf{R}} \sum_{i,j=1}^{3} \mathbf{u}_{ij}(\mathbf{R}) \sin\left(\mathbf{Q}_{i,j} \cdot \mathbf{R}\right) \delta(\mathbf{r} - \mathbf{R}) \qquad \text{with} \qquad \mathbf{u}_{ij}(\mathbf{R}) \parallel \mathbf{Q}_{i,j}$$

- recall that problems arise on C_{2y} invariant directions. In real space, those are the directions of the domain walls separating AB from BA Bernal stacked regions. We therefore take $\mathbf{u}_{ij}(\mathbf{R})$ finite only in proximity of the domain walls, thus affecting around 1% of the total number of atoms.

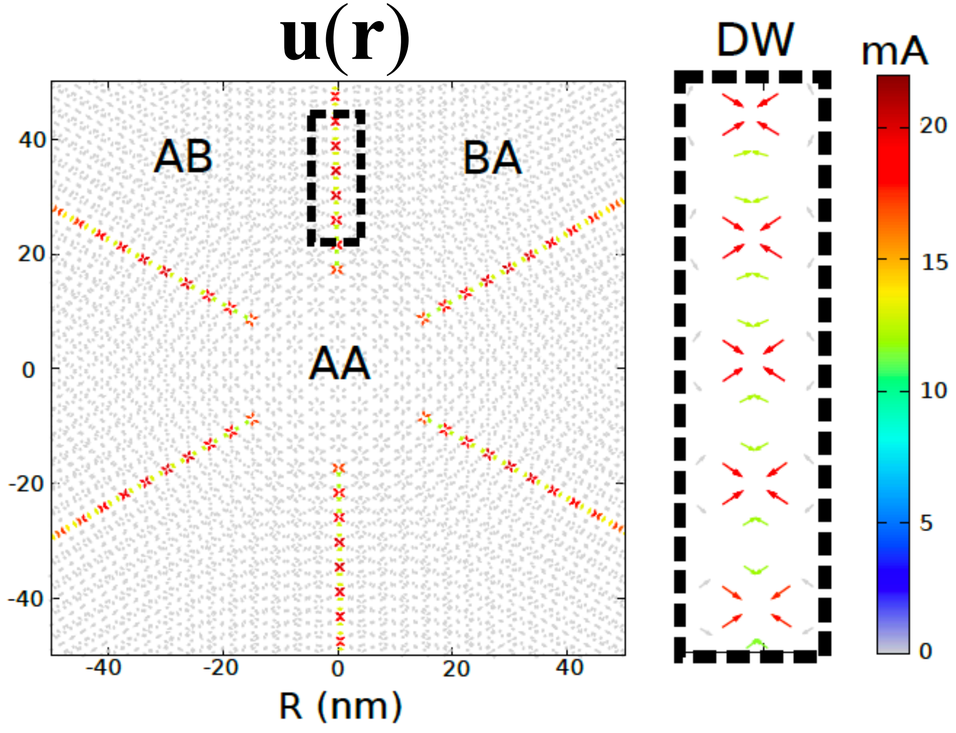

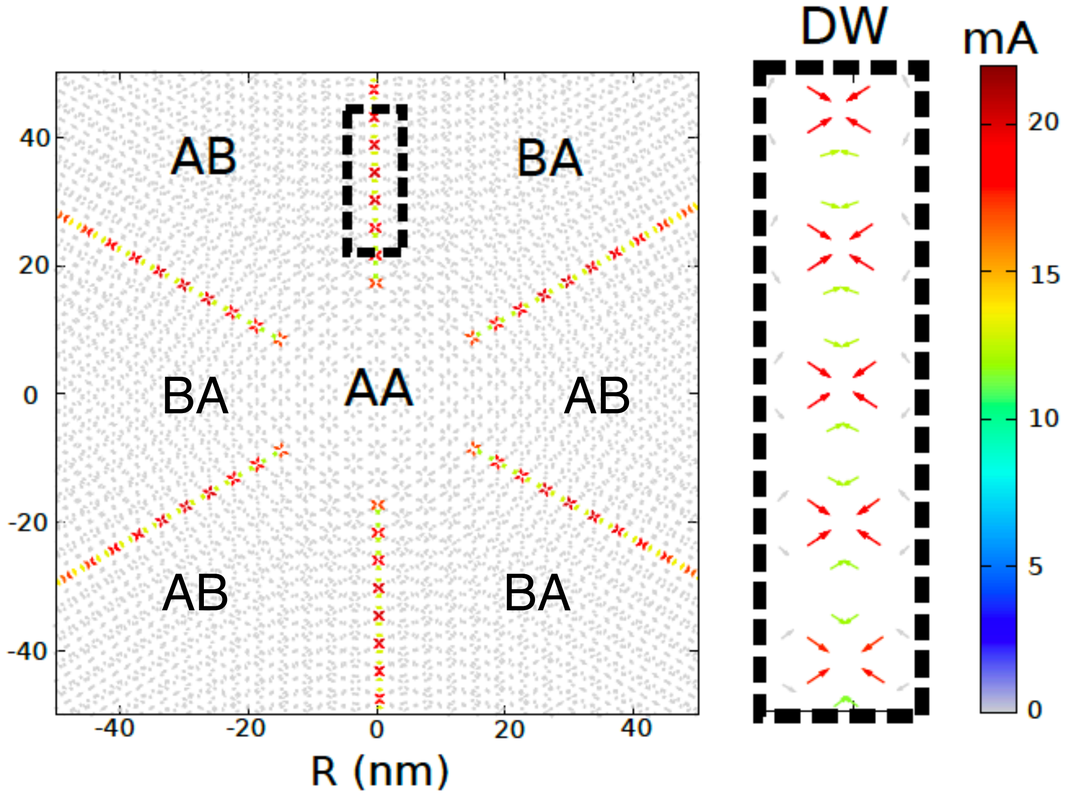

- only atoms around the domain walls are displaced from their equilibrium positions

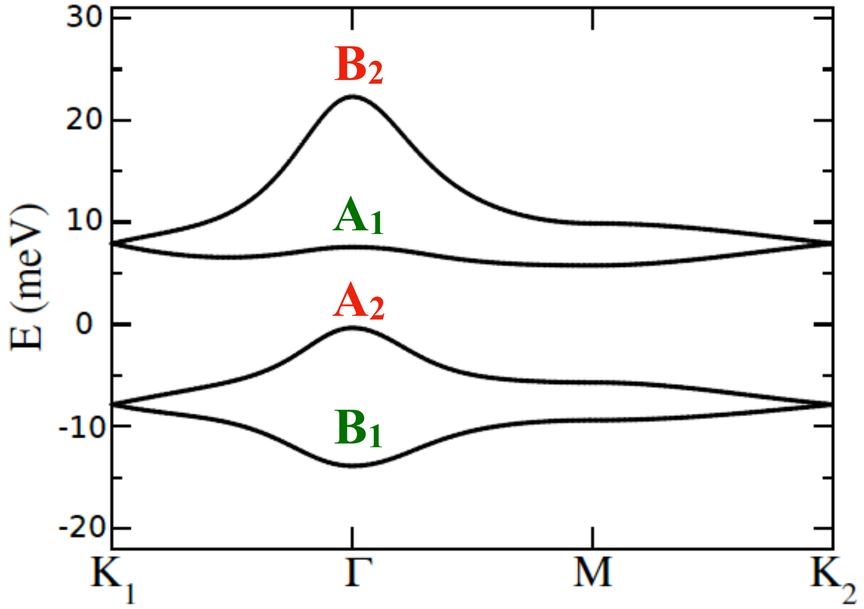

- yet the effect on the mini bands is remarkable: the accidental degeneracy along all lines invariant under C_{2y} is fully lifted. Moreover, the lower flat bands have still non trivial topology

Given that promising result, we do a better job and calculate the phonon spectrum of the relaxed structure

Phonon spectrum

- ✓ we calculate the phonon spectrum comprising 33492 modes
- ✓ there are special modes that resemble global vibrations of the moiré supercell, as it were a single ultralarge molecule

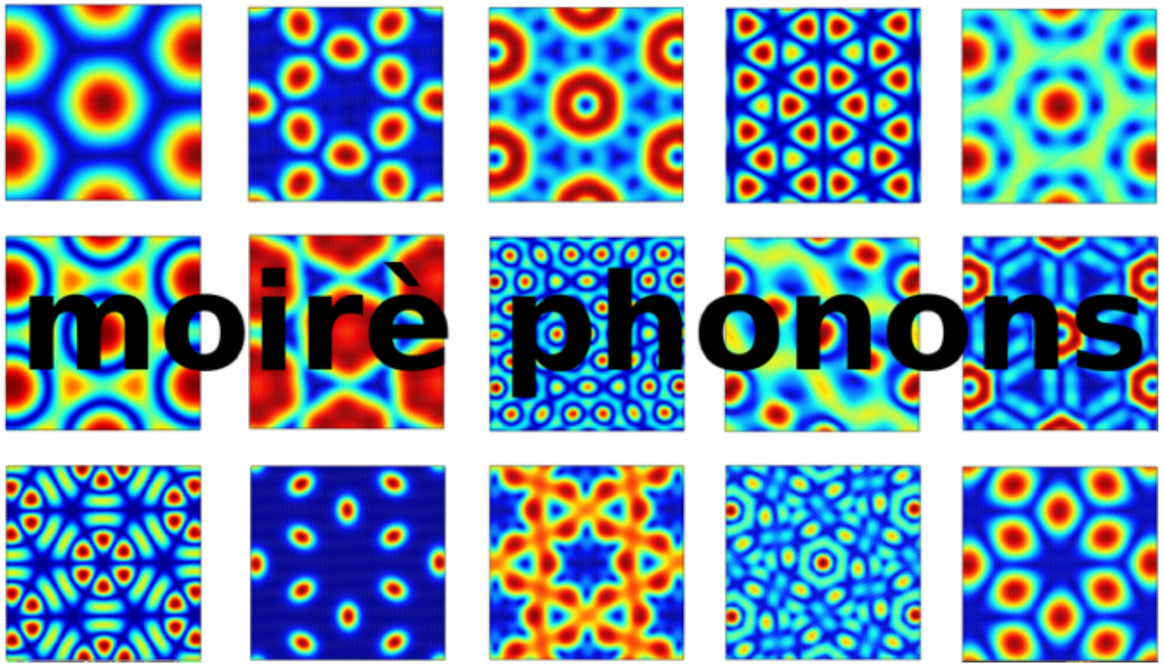

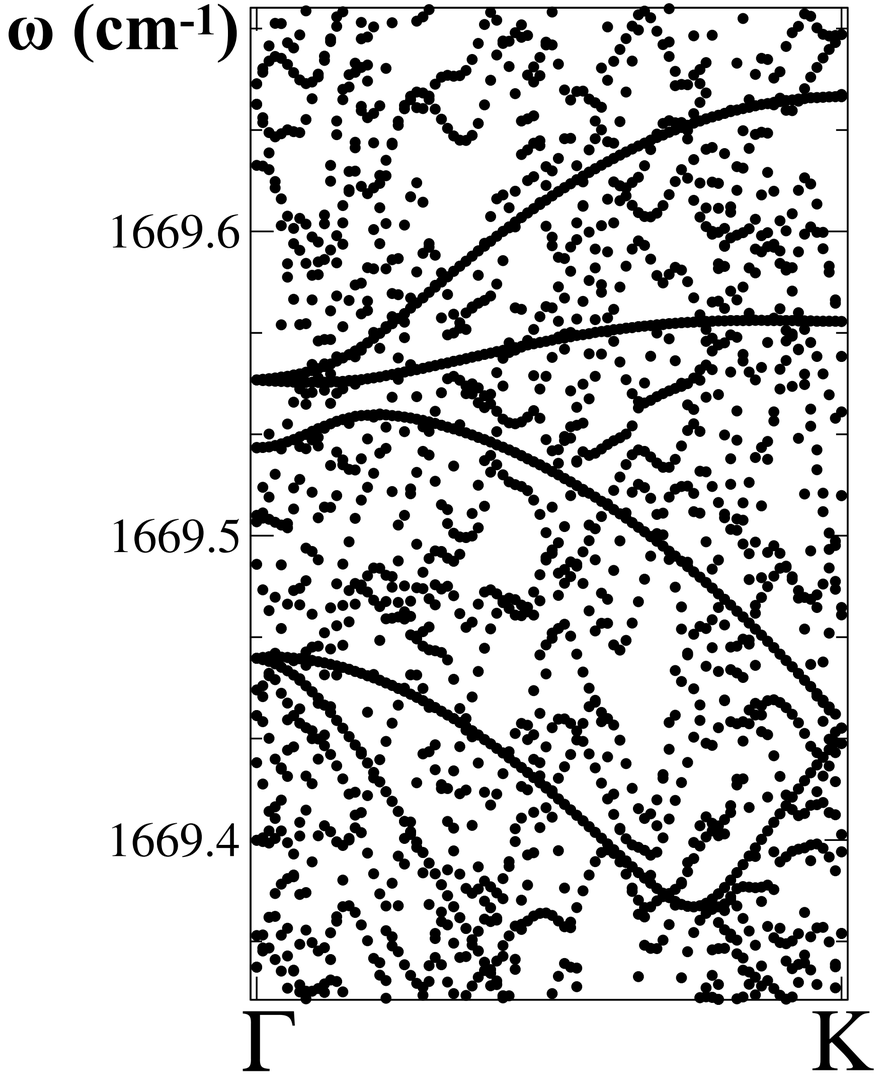

Phonon spectrum

- ✓ we calculate the phonon spectrum comprising 33492 modes
- ✓ there are special modes that resemble global vibrations of the moiré supercell, as it were a single ultralarge molecule
- ✓ remarkably, these modes have the same accidental double degeneracy as the electronic bands

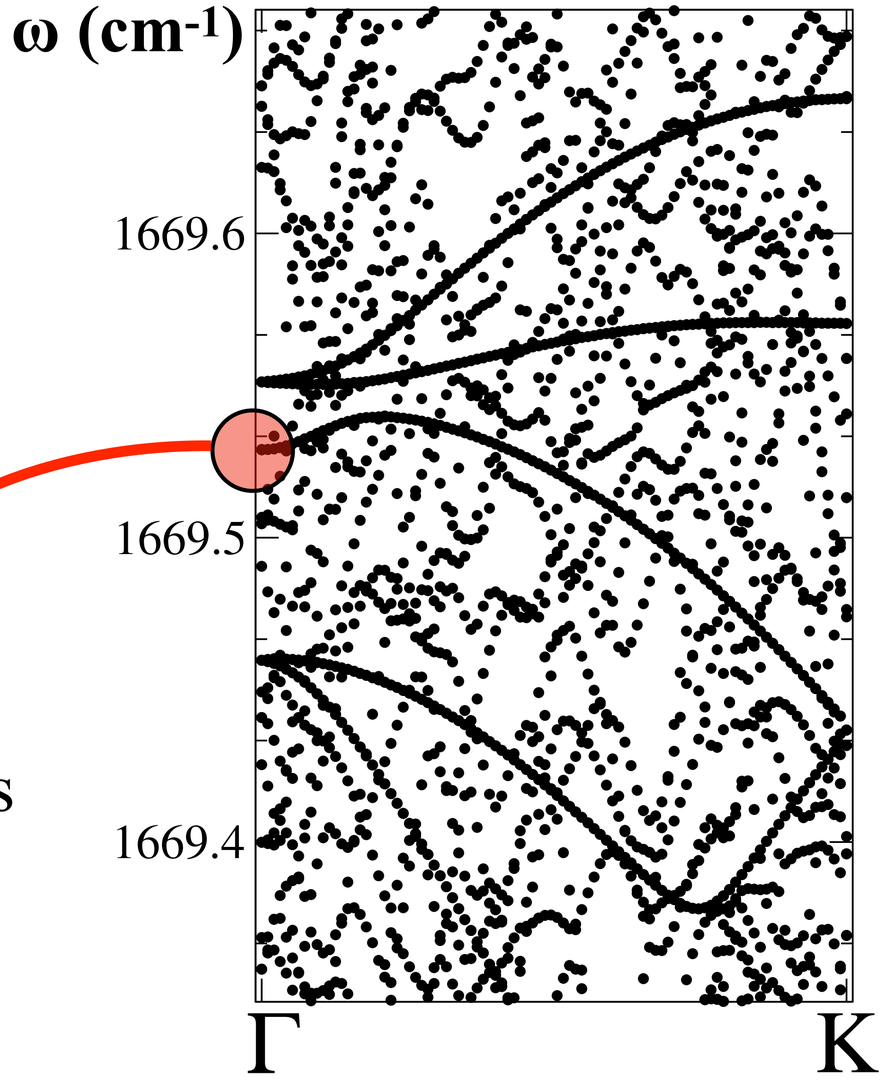

- this doubly degenerate phonon at **Γ** comprises one A_1 mode even under C_{2y} and the other B_1 mode odd. The A_1 mode has more than 90% overlap with the ad-hoc distortion.

Phonon spectrum

- ✓ we calculate the phonon spectrum comprising 33492 modes
- ✓ there are special modes that resemble global vibrations of the moiré supercell, as it were a single ultralarge molecule
- ✓ remarkably, these modes have the same accidental double degeneracy as the electronic bands

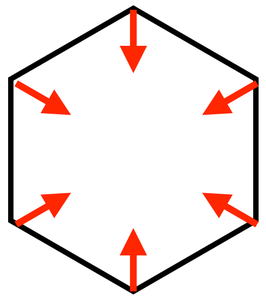

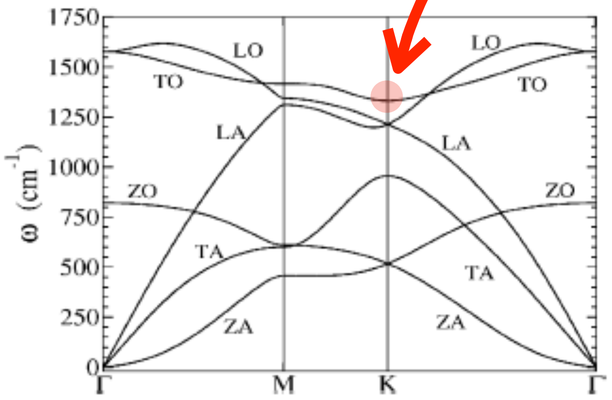

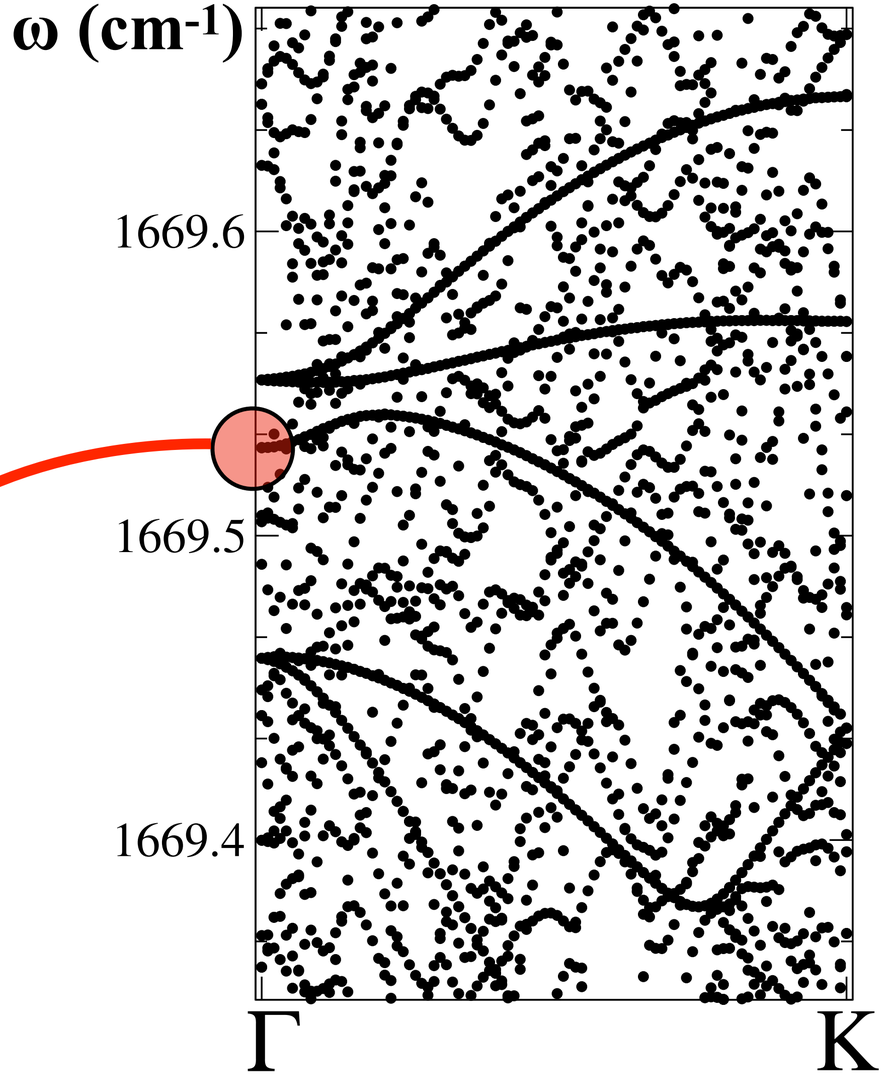

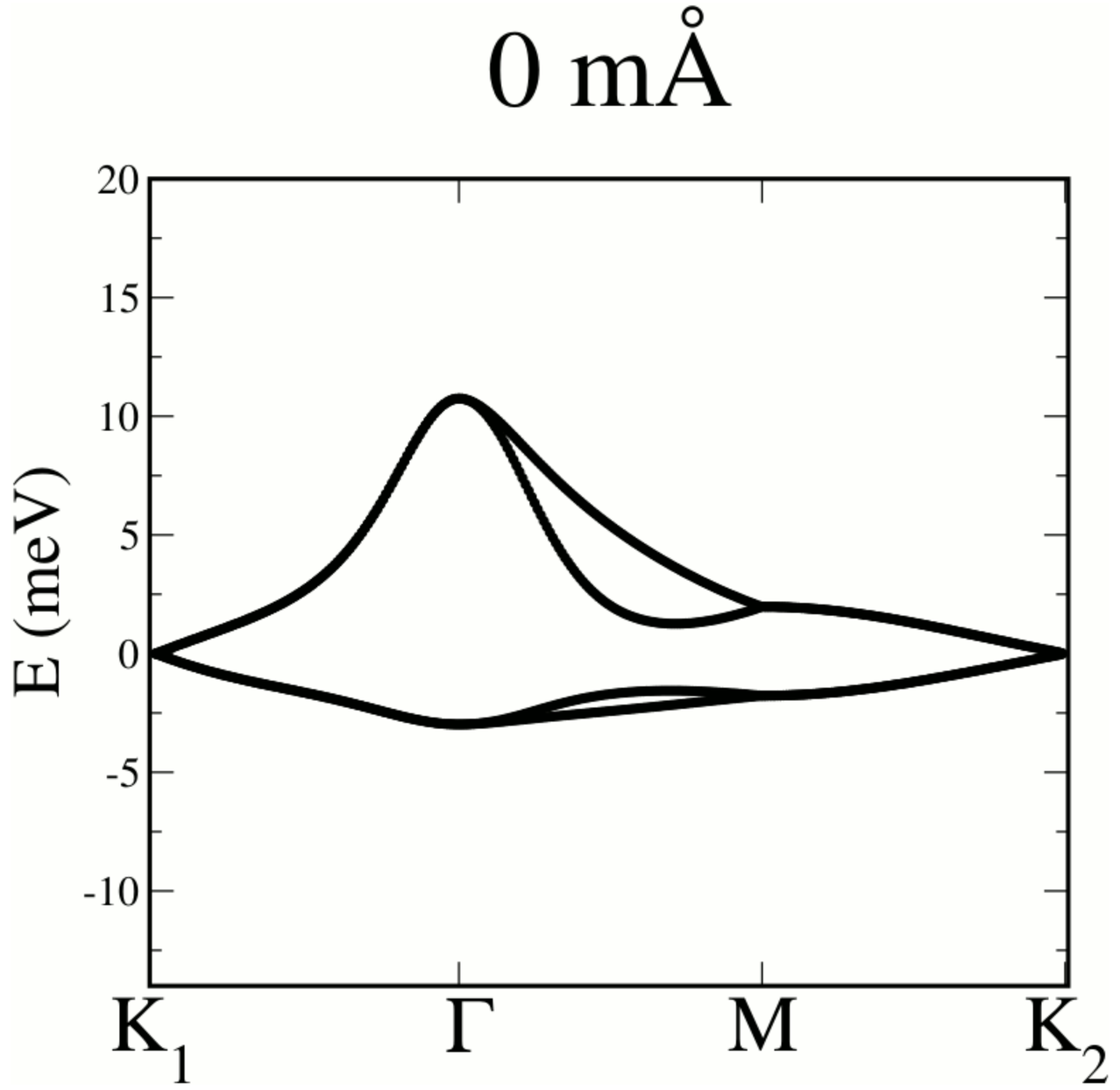

C-C distance in graphene = 1.42 Å

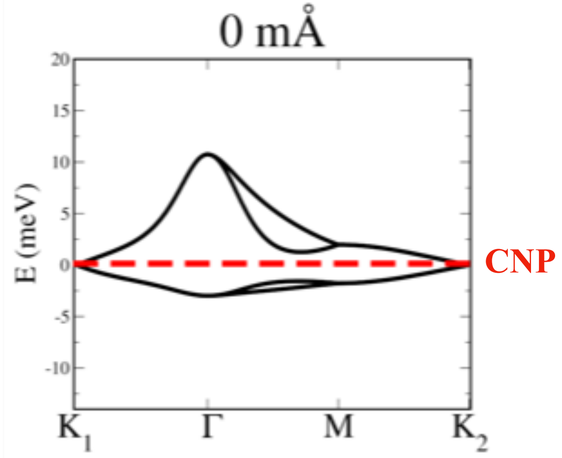

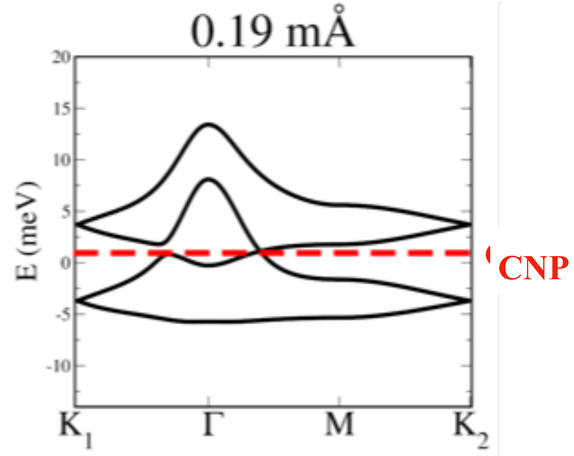

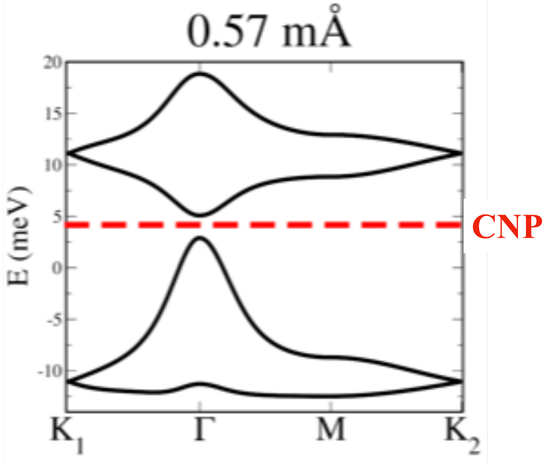

- both A_1 and B_1 modes produce the same bands
- very efficient lifting of the accidental degeneracy
- huge electron-phonon coupling compared with the width of the flat bands and the graphene C-C distance of 1.42 Å
- non-trivial topology of the insulator above 0.5 mÅ

edge states

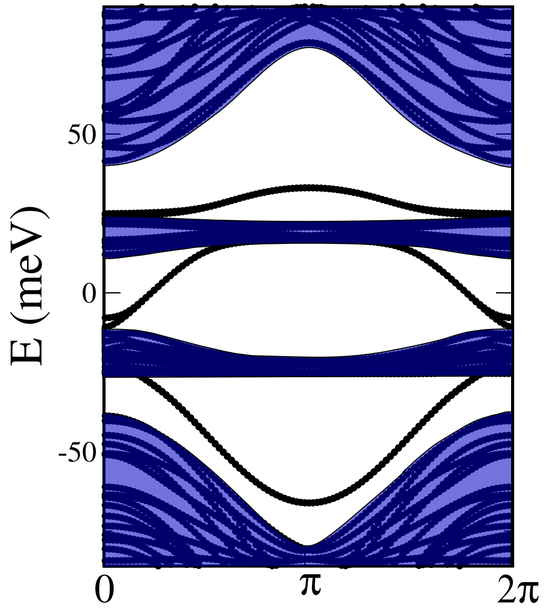

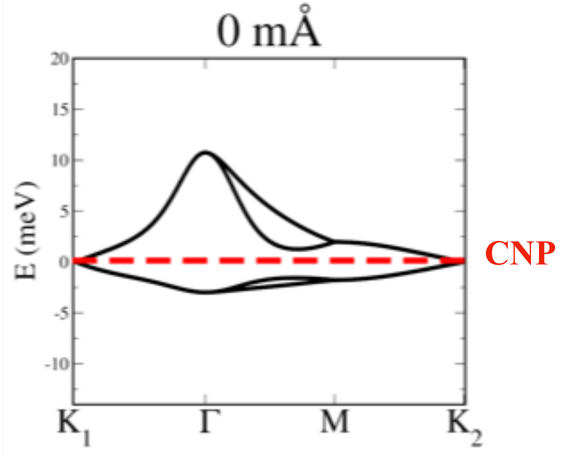

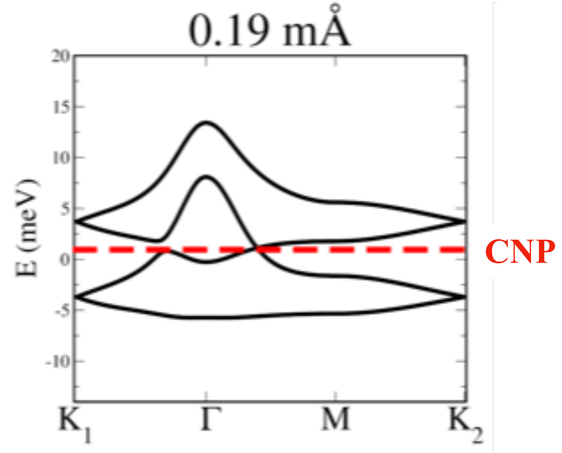

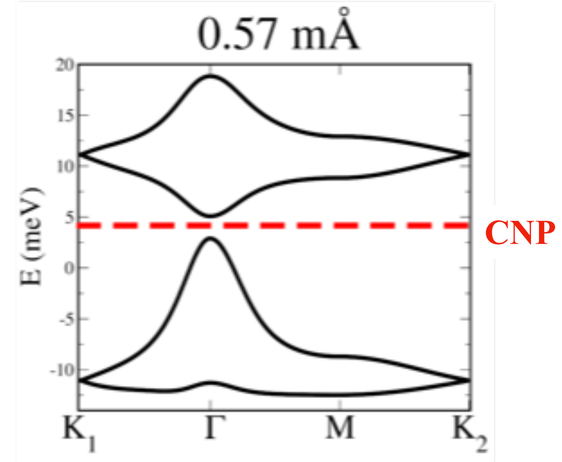

- both A_1 and B_1 modes produce the same bands

This is strongly suggestive of an **E×e** Jahn-Teller effect: a doubly degenerate mode $\mathbf{q} = (q_1, q_2)$ coupled to a doubly degenerate band in a $U_v(1)$ symmetric way:

$$H_{\text{J-T}} \sim -g\, \mathbf{q} \cdot \boldsymbol{\tau} = -g\, \left(q_1\, \tau_1 + q_2\, \tau_2 \right)$$

$U_v(1)$ generator: $L_3 = \dfrac{\tau_3}{2} + \mathbf{q} \wedge \mathbf{p}$

$\mathbf{p}$: momentum conjugate to $\mathbf{q}$

$E \times e$ Jahn-Teller effect in short

• take, e.g., degenerate p_x  and p_y  atomic-like orbitals in D_4 symmetry

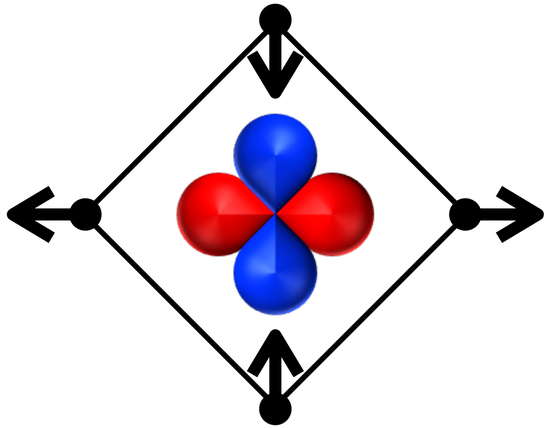

B_1 mode q_1: coupling τ_3

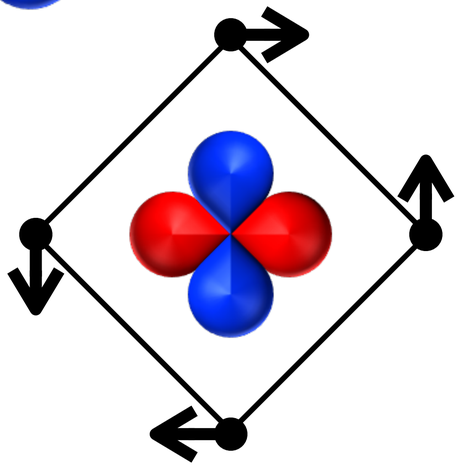

B_2 mode q_2: coupling τ_1

$$H_{\text{J-T}} = -g\left(q_1\,\tau_3 + q_2\,\tau_1\right) + \sum_{i=1}^{2}\left(\frac{p_i^2}{2M} + \frac{K\,q_i^2}{2}\right) = -g\,\boldsymbol{q}\cdot\boldsymbol{\tau} + \left(\frac{\boldsymbol{p}^2}{2M} + \frac{K\,\boldsymbol{q}^2}{2}\right)$$

U(1) generator: $L = \dfrac{\tau_2}{2} + \boldsymbol{q}\wedge\boldsymbol{p}$

Born-Oppenheimer potential

- if $\boldsymbol{q}$ is fixed then $\boldsymbol{\tau} = n\,\boldsymbol{q}/q$
  with $n = 0, 1, 2$ the electron number mod(4),
  and thus $V(\boldsymbol{q}) = \frac{K}{2}\,q^2 - g\,n\,q + u\,q^4$

- kinetic energy $= \frac{1}{2M}\,\boldsymbol{p}^2$

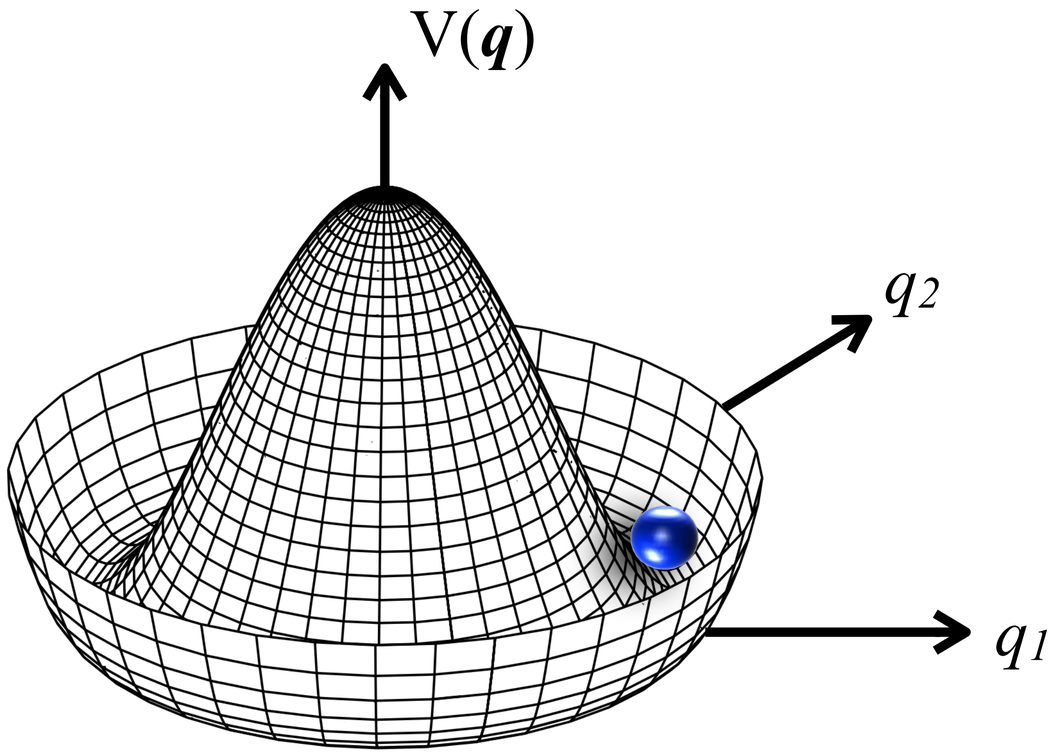

- Static Jahn-Teller effect

  – if $M \to \infty$ the phonon distortion locks into a generic point of the potential valley

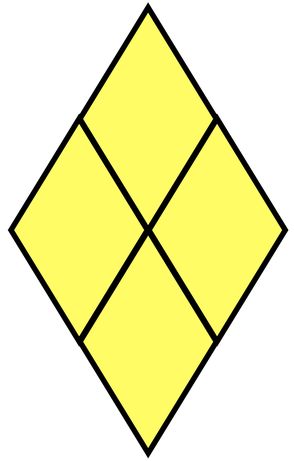

collective distortion of the lattice

Born-Oppenheimer potential

- if $\boldsymbol{q}$ is fixed then $\boldsymbol{\tau} = n\,\boldsymbol{q}/q$
  with $n = 0, 1, 2$ the electron number $\mathrm{mod}(4)$,
  and thus $V(\boldsymbol{q}) = \frac{K}{2}\,q^2 - g\,n\,q + u\,q^4$

- kinetic energy $= \frac{1}{2M}\,\boldsymbol{p}^2$

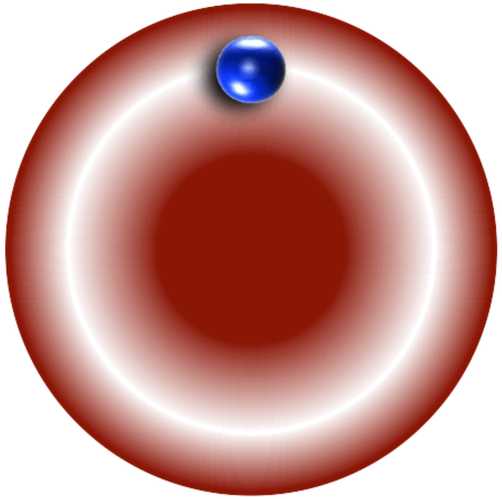

- Dynamic Jahn-Teller effect

  - if M is finite the phonon displacement moves coherently along the potential valley

  - the U(1) symmetry is instantaneously broken but, on average, dynamically recovered

  - the motion is akin a rigid rotor in $2d$ with a caveat: when the number of electrons is odd, there is a Berry phase that forces the angular momentum to be half an odd integer

easy way to describe a dynamical Jahn-Teller effect

- integrate the phonons out and neglect retardation effects

$$-g\,\boldsymbol{\tau}\cdot\boldsymbol{q} \;\longrightarrow\; -\frac{g^2}{\omega_0}\left(\tau_3\,\tau_3+\tau_1\,\tau_1\right)=-\frac{g^2}{\omega_0}\left(\boldsymbol{\tau}\cdot\boldsymbol{\tau}-\tau_2\,\tau_2\right)$$

- U(1) generator: $\tau_2/2$ = integer or half an odd integer for even or odd number of electrons

- the lowest energy configuration of two electrons is a spin-singlet τ-triplet state, with $\tau_2 = 0$

$$\frac{1}{\sqrt{2}}\left(p^\dagger_{x\uparrow}\,p^\dagger_{x\downarrow}+p^\dagger_{y\uparrow}\,p^\dagger_{y\downarrow}\right)\,|0\rangle\equiv\Delta^\dagger\,|0\rangle$$

dynamical Jahn-Teller effect inverts Hund's rules and yields spin-singlet pairing

- consider a lattice of such molecules, 2 electrons per site, and the Hamiltonian

$$H = H_0 - \frac{g^2}{2\omega_0} \sum_{\mathbf{R}} \left(\boldsymbol{\tau}_{\mathbf{R}} \cdot \boldsymbol{\tau}_{\mathbf{R}} - \tau_{2\mathbf{R}}\, \tau_{2\mathbf{R}} \right) + \frac{U}{2} \sum_{\mathbf{R}} n_{\mathbf{R}} \left(n_{\mathbf{R}} - 1 \right)$$

H_0: tight-binding preserving the D_4 symmetry

- weak U: superconductor with coupling constant $g^2/2\omega_0$ - U and s-wave order parameter

$$\Delta^\dagger = \sum_{\mathbf{k}} \psi_{\mathbf{k}} \left(p^\dagger_{x\mathbf{k}\uparrow}\, p^\dagger_{x-\mathbf{k}\downarrow} + p^\dagger_{y\mathbf{k}\uparrow}\, p^\dagger_{y-\mathbf{k}\downarrow} \right) \quad \psi_{\mathbf{k}} = \psi_{-\mathbf{k}} \quad \sum_{\mathbf{k}} \left| \psi_{\mathbf{k}} \right|^2 = 1$$

- large U: **Jahn-Teller Mott insulator** (PRB **55**, 13465 (1997)) with two electrons localised on each site into the $\mathbf{S} = 0$, $\boldsymbol{\tau} = 1$ and $\tau_2 = 0$ configuration that maximises the Jahn-Teller energy gain ⇒ **a local version of a valence-bond (VB) insulator**

Phase diagram in DMFT: $2J = g^2/2\omega_0$

Capone et al., PRL **93**, 047001 (2004)

$$\lambda = \rho_F \left(2J - U\right)$$

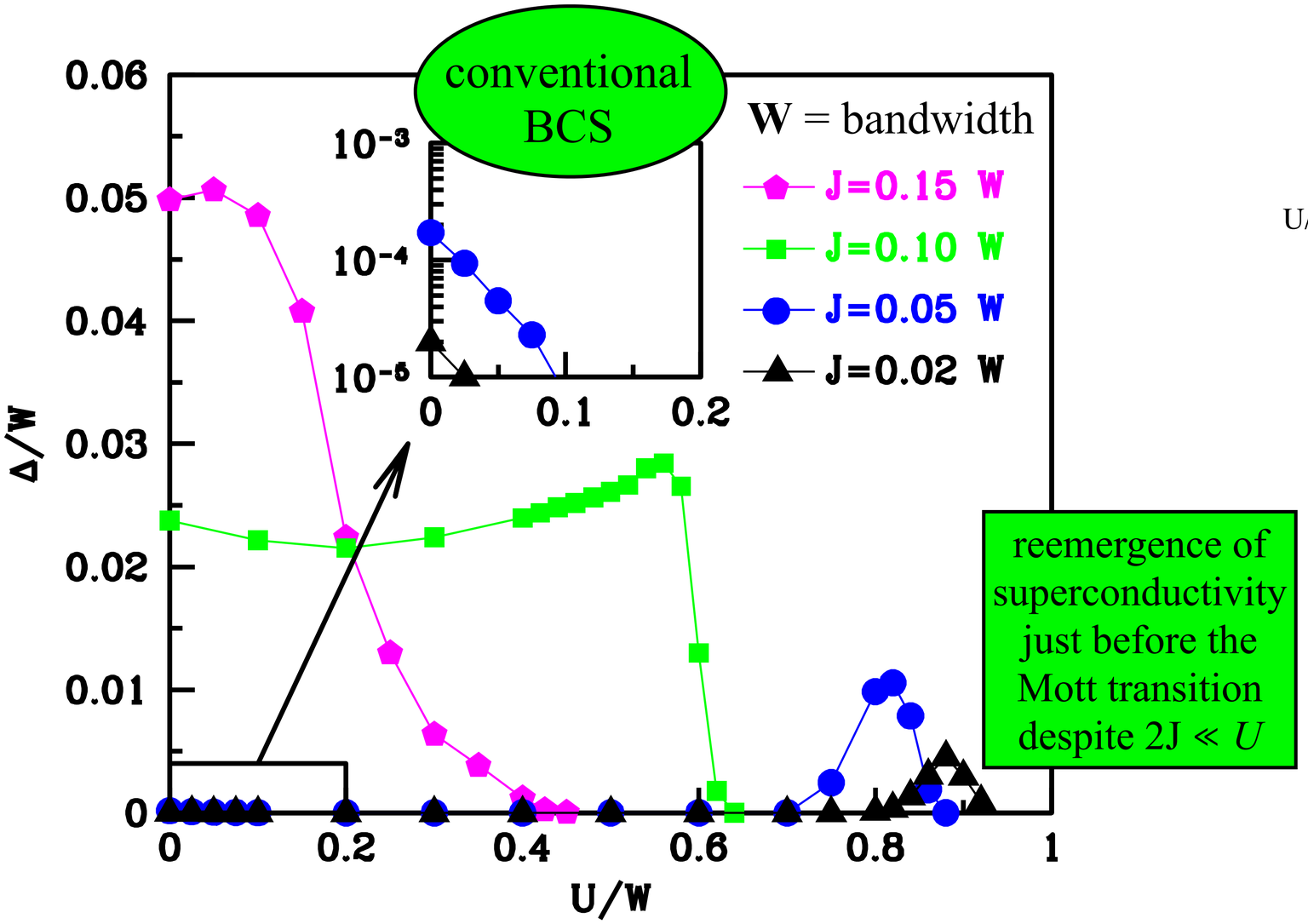

reemergence of superconductivity just before the Mott transition despite $2J \ll U$

doping the Mott insulator

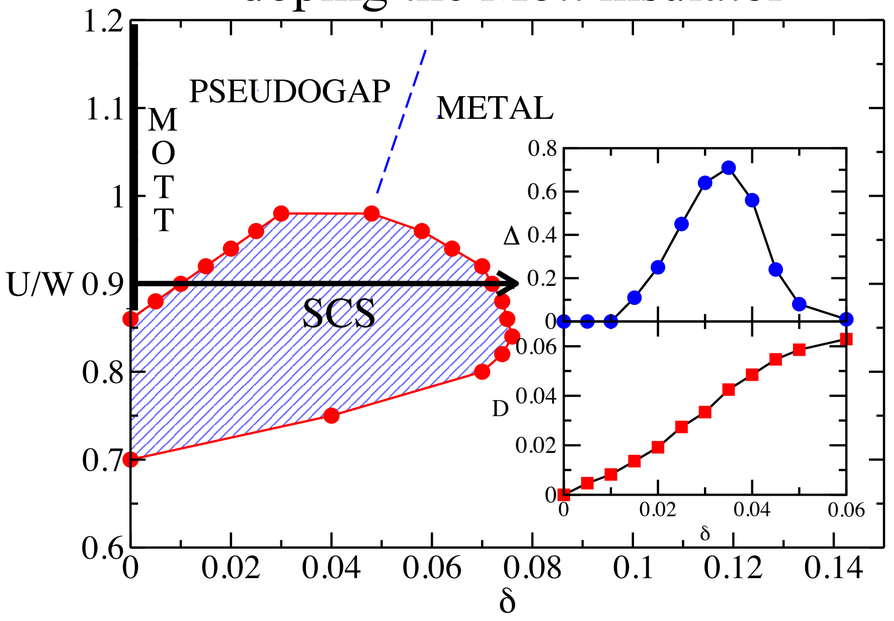

- key point: just like conventional Hund's rules, the inverted ones due to Jahn-Teller effect do not fight against charge repulsion; they just dictate how the two electrons are arranged inside the molecule

- the physical scenario is akin to Anderson's RVB and thus well captured by a projected BCS wavefunction

number of electrons

$$|\psi_N\rangle = P_{\rm G}\,|\,{\rm BCS}\rangle = P_{\rm G}\left(\Delta^\dagger\right)^N|0\rangle$$

Gutzwiller projector disfavouring U-expensive local configurations.
At large U and half-filling it yields a Mott insulator

Can we prove such conjecture rigorously, and even away from the C_{2y} invariant lines? Namely, can we actually derive the $U_v(1)$ symmetric electron-phonon coupling?

Eur. Phys. J. Plus (2020) 135:630

We use Bistritzer&MacDonald continuum model (PNAS **108**, 12233) in the equivalent representation by Song et al., PRL **123**, 036401.

Reciprocal space spanned by $\mathbf{Q} = \mathbf{Q}_A \oplus \mathbf{Q}_B$

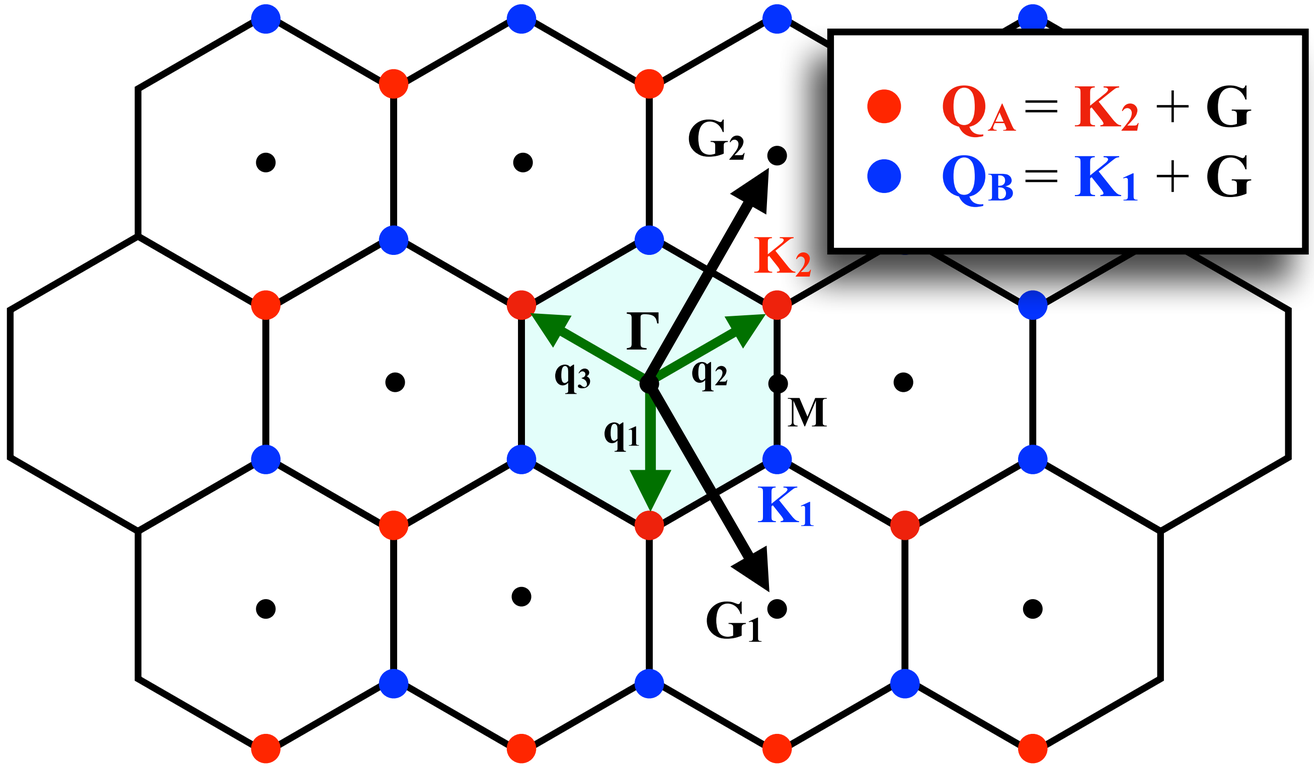

$$\Psi_{\mathbf{k},\mathbf{Q}_A,\sigma} = \begin{pmatrix} c_{2,\mathbf{k}+\mathbf{K}_2-\mathbf{Q}_A,A,\sigma} \\ c_{2,\mathbf{k}+\mathbf{K}_2-\mathbf{Q}_A,B,\sigma} \\ c_{1,\mathbf{k}-\mathbf{K}_1-\mathbf{Q}_A,B,\sigma} \\ c_{1,\mathbf{k}-\mathbf{K}_1-\mathbf{Q}_A,A,\sigma} \end{pmatrix}$$

valley +1 layer 2

valley -1 layer 1 and inverted sublattices

$$\Psi_{\mathbf{k},\mathbf{Q}_B,\sigma} = \begin{pmatrix} c_{1,\mathbf{k}+\mathbf{K}_1-\mathbf{Q}_B,A,\sigma} \\ c_{1,\mathbf{k}+\mathbf{K}_1-\mathbf{Q}_B,B,\sigma} \\ c_{2,\mathbf{k}-\mathbf{K}_2-\mathbf{Q}_B,B,\sigma} \\ c_{2,\mathbf{k}-\mathbf{K}_2-\mathbf{Q}_B,A,\sigma} \end{pmatrix}$$

valley +1 layer 1

valley -1 layer 2 and inverted sublattices

k within the reduced BZ

Single-layer Hamiltonian in the zero angle limit

$$H_{\parallel} = \sum_{\mathbf{k}\mathbf{Q}\sigma} \Psi^{\dagger}_{\mathbf{k},\mathbf{Q},\sigma} \left(v_F \, \tau_3 \left(\mathbf{k} - \mathbf{Q} \right) \cdot \boldsymbol{\sigma} \right) \Psi_{\mathbf{k},\mathbf{Q},\sigma}$$

$$\left(\sigma_1, \sigma_2 \right)$$

- τ_n, n=0,1,2,3, act in the valley space, with τ_0 the identity
- σ_n, n=0,1,2,3, act in the sublattice space, with σ_0 the identity

Inter-layer hopping

- p_z Wannier orbital in layer i=1,2, unit cell $\mathbf{R}_i$, sublattice α = A,B at position $\mathbf{r}_{i,\alpha}$:

$$\phi\left(\mathbf{r}-\mathbf{R}_i-\mathbf{r}_{i,\alpha}\right)$$

- inter-layer hopping matrix element:

$$\int d\mathbf{r}\,\phi\left(\mathbf{r}-\mathbf{R}_1-\mathbf{r}_{1,\alpha}\right)\,V_\perp(\mathbf{r})\,\phi\left(\mathbf{r}-\mathbf{R}_2-\mathbf{r}_{2,\beta}\right)\simeq T_\perp\left(\mathbf{R}_1-\mathbf{R}_2-\mathbf{r}_{1,\alpha}-\mathbf{r}_{2,\beta}\right)$$

$$T_\perp(\mathbf{r})=\frac{1}{N}\sum_{\mathbf{q}}\mathrm{e}^{i\mathbf{r}\cdot\mathbf{q}}\,T_\perp(\mathbf{q})$$

•few things worth noticing

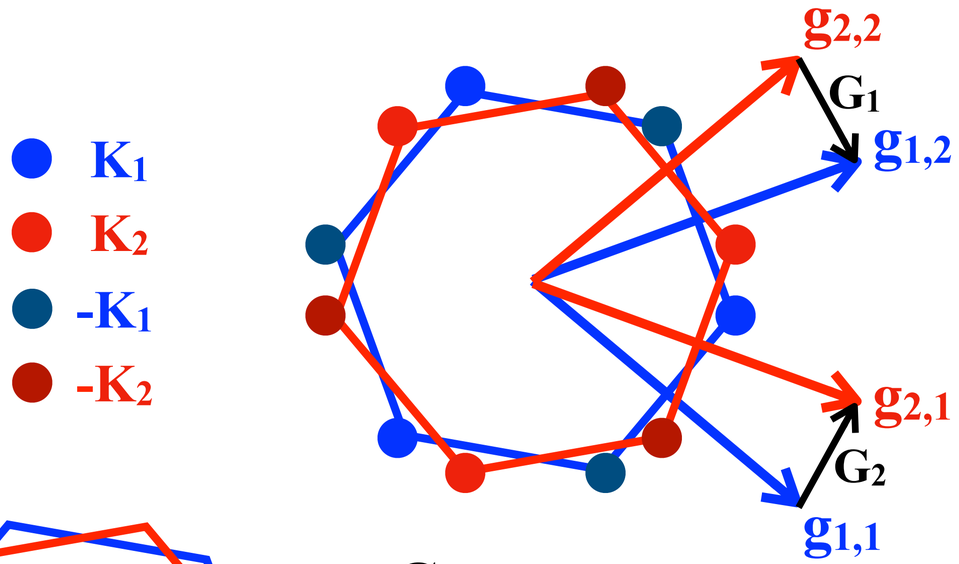

$\mathbf{g}_{n,1}$ and $\mathbf{g}_{n,2}$ are the primitive reciprocal lattice vectors, whereas $\mathbf{g}_n$ are generic reciprocal lattice vectors of layer n=1,2

$$\mathbf{K}_n = \frac{\mathbf{g}_{n,1} + \mathbf{g}_{n,2}}{3}$$

$$C_{3z}(\mathbf{K}_n) = \mathbf{K}_n - \mathbf{g}_{n,1} \quad C_{3z}^2(\mathbf{K}_n) = \mathbf{K}_1 - \mathbf{g}_{n,2}$$

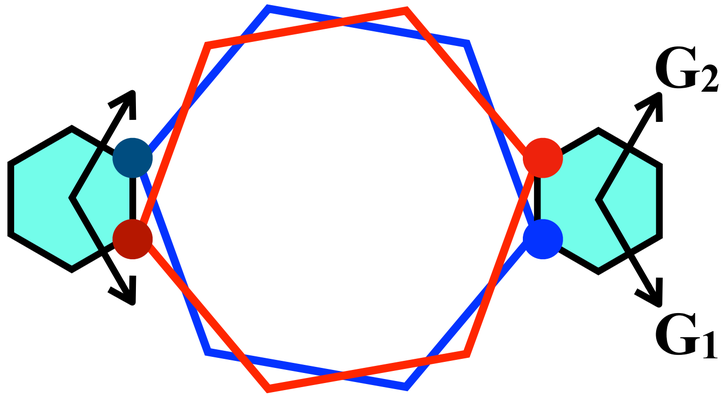

$\mathbf{G}_1$ and $\mathbf{G}_2$ are the primitive reciprocal lattice vectors of the mini Brillouin zone, while $\mathbf{G}$ a generic reciprocal lattice vector

$$\mathbf{G}_1 = \mathbf{g}_{1,2} - \mathbf{g}_{2,2} \quad \text{and} \quad \mathbf{G}_2 = \mathbf{g}_{2,1} - \mathbf{g}_{1,1}$$

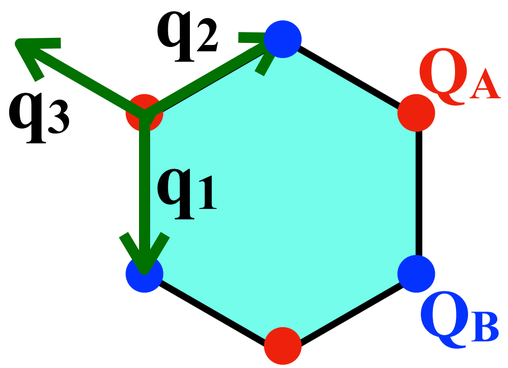

$$\mathbf{q}_1 = \mathbf{K}_1 - \mathbf{K}_2$$
$$\mathbf{q}_2 = C_{3z}(\mathbf{q}_1) = \mathbf{q}_1 + \mathbf{G}_2$$
$$\mathbf{q}_3 = C_{3z}^2(\mathbf{q}_1) = \mathbf{q}_1 - \mathbf{G}_1$$

$$\mathbf{Q}_A = \mathbf{K}_2 + \mathbf{G}$$
$$\mathbf{Q}_B = \mathbf{K}_1 + \mathbf{G}$$

• inter-layer hopping valley +1: (notice that valley -1= complex conjugate + A↔B)

$$H_{\perp}^{+1} = \sum_{\mathbf{k}\mathbf{p}\sigma} \left(c^{\dagger}_{2,\mathbf{k},\alpha,\sigma}\, T^{\alpha\beta}_{\perp\,\mathbf{k}\mathbf{p}}\, c_{1,\mathbf{p},\beta,\sigma} + H.c. \right) \quad \text{with } \mathbf{k} \sim \mathbf{K}_2 + 120^\circ \text{ rotations and } \mathbf{p} \sim \mathbf{K}_1 + 120^\circ \text{ rotations}$$

$$T^{\alpha\beta}_{\perp\,\mathbf{k}\mathbf{p}} = \frac{1}{N} \sum_{\mathbf{R}_1\mathbf{R}_2} \mathrm{e}^{-i\mathbf{k}\cdot(\mathbf{R}_2+\mathbf{r}_{2,\alpha})}\, \mathrm{e}^{i\mathbf{p}\cdot(\mathbf{R}_1+\mathbf{r}_{1,\beta})}\, T_{\perp}\left(\mathbf{R}_2 + \mathbf{r}_{2,\alpha} - \mathbf{R}_1 - \mathbf{r}_{1,\beta}\right)$$

$$= \sum_{\mathbf{g}_1\mathbf{g}_2} T_{\perp}\left(\mathbf{k} + \mathbf{g}_2\right) \delta_{\mathbf{k}+\mathbf{g}_2,\mathbf{p}+\mathbf{g}_1}\, \mathrm{e}^{i\mathbf{g}_2\cdot\mathbf{r}_{2,\alpha}}\, \mathrm{e}^{-i\mathbf{g}_1\cdot\mathbf{r}_{1,\beta}}$$

$$\mathbf{K}_1 \sim \mathbf{p} = \mathbf{k} \sim \mathbf{K}_2$$

$$C_{3z}\left(\mathbf{K}_1\right) \sim \mathbf{p} - \mathbf{g}_{1,1} = \mathbf{k} - \mathbf{g}_{2,1} \sim C_{3z}\left(\mathbf{K}_2\right)$$

$$C^2_{3z}\left(\mathbf{K}_1\right) \sim \mathbf{p} - \mathbf{g}_{1,2} = \mathbf{k} - \mathbf{g}_{2,2} \sim C^2_{3z}\left(\mathbf{K}_2\right)$$

$$\mathbf{p} = \mathbf{k}' + \mathbf{K}_1 - \mathbf{Q}_B$$
$$\mathbf{k} = \mathbf{k}' + \mathbf{K}_2 - \mathbf{Q}_A$$

$$\mathbf{Q}_B - \mathbf{Q}_A = \mathbf{K}_1 - \mathbf{K}_2 = \mathbf{q}_1$$
$$\mathbf{Q}_B - \mathbf{Q}_A = \mathbf{q}_2$$
$$\mathbf{Q}_B - \mathbf{Q}_A = \mathbf{q}_3$$

Inter-layer hopping

$$H_\perp = \sum_{\mathbf{k}\sigma} \sum_{\mathbf{Q}\mathbf{Q}'} \Psi^\dagger_{\mathbf{k},\mathbf{Q},\sigma}\, \hat{T}_{\mathbf{Q},\mathbf{Q}'}\, \Psi_{\mathbf{k},\mathbf{Q}',\sigma}$$

$$\hat{T}_{\mathbf{Q},\mathbf{Q}'} = \tau_0 \sum_{j=1}^{3} \left(\delta_{\mathbf{Q}-\mathbf{Q}',\mathbf{q}_i} + \delta_{\mathbf{Q}'-\mathbf{Q},\mathbf{q}_i} \right) \hat{T}_j\left(u_0, u_1\right)$$

$$\hat{T}_1\left(u_0, u_1\right) = u_0\, \sigma_0 + u_1\, \sigma_1$$

$$\hat{T}_{j+1}\left(u_0, u_1\right) = \mathrm{e}^{i\frac{2\pi}{3}\sigma_3}\, \hat{T}_j\left(u_0, u_1\right)\, \mathrm{e}^{-i\frac{2\pi}{3}\sigma_3} \qquad j = 1, 2$$

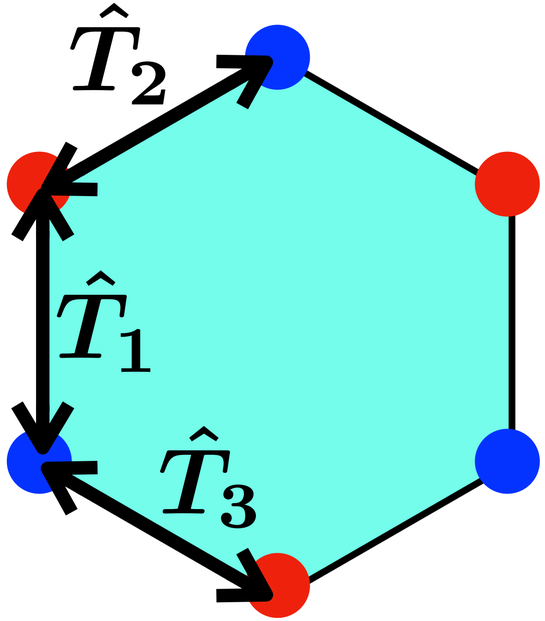

$u_1 > u_0$ takes into account atomic relaxation

Non-interacting Hamiltonian

$$H_0 = \sum_{\mathbf{k}\sigma} \sum_{\mathbf{Q}\mathbf{Q}'} \Psi^{\dagger}_{\mathbf{k},\mathbf{Q},\sigma} \hat{H}^{0}_{\mathbf{Q},\mathbf{Q}'} \Psi_{\mathbf{k},\mathbf{Q}',\sigma}$$

$$\hat{H}^{0}_{\mathbf{Q},\mathbf{Q}'} = \delta_{\mathbf{Q},\mathbf{Q}'}\, v_F\, \tau_3\, \boldsymbol{\sigma} \cdot \left(\mathbf{k} - \mathbf{Q}\right) + \tau_0 \sum_{j=1}^{3} \left(\delta_{\mathbf{Q}-\mathbf{Q}',\mathbf{q}_i} + \delta_{\mathbf{Q}'-\mathbf{Q},\mathbf{q}_i}\right) \hat{T}_j\left(u_0, u_1\right)$$

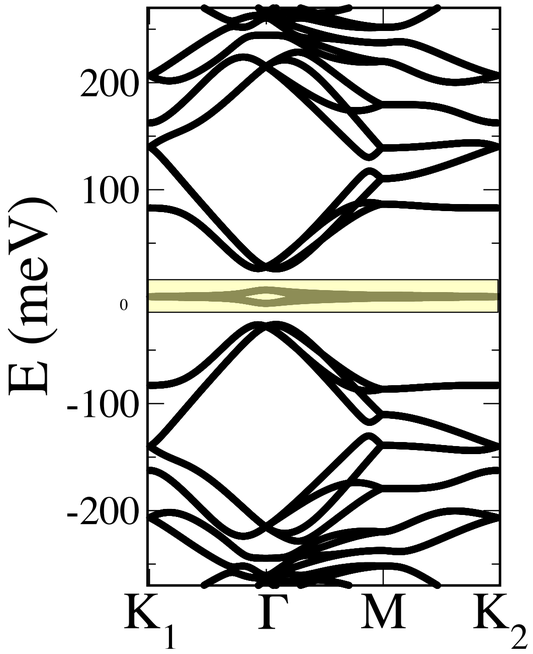

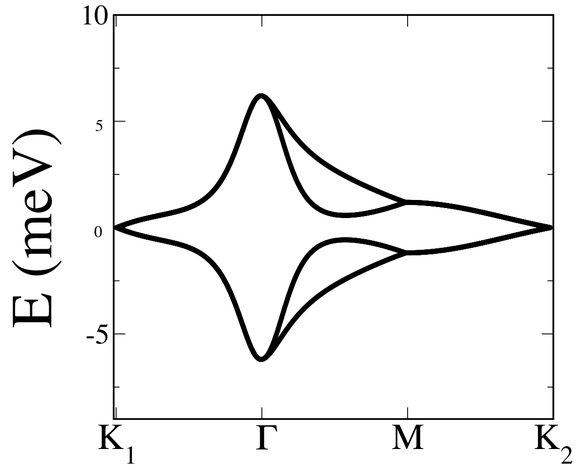

$u_0 = 0.071$ eV
$u_1 = 0.1031$ eV

Let us add the electron-phonon coupling

• position of an atom in layer n=1,2, graphene unit cell **R** and sublattice α = A,B

$$\mathbf{x}_\alpha(\mathbf{R}_n) = \mathbf{R}_n + \mathbf{r}_{n,\alpha} \longrightarrow \mathbf{R}_n + \mathbf{r}_{n,\alpha} + \boldsymbol{u}\big(\mathbf{x}_\alpha(\mathbf{R}_n)\big)$$

$$\mathrm{z}_\alpha(\mathbf{R}_n) \simeq \mathrm{z}_n$$

atomic displacement, neglecting inter-layer one

• hopping in the two-centre approximation:

$$T\Big(\mathbf{x}_\alpha(\mathbf{R}_n) - \mathbf{x}_{\alpha'}(\mathbf{R}'_{n'}), z_n - z_{n'}\Big) \simeq T\Big(\mathbf{R}_n + \mathbf{r}_{n,\alpha} - \mathbf{R}'_{n'} - \mathbf{r}_{n',\alpha'}, z_n - z_{n'}\Big) + \boldsymbol{\nabla} T\Big(\mathbf{R}_n + \mathbf{r}_{n,\alpha} - \mathbf{R}'_{n'} - \mathbf{r}_{n',\alpha'}, z_n - z_{n'}\Big) \cdot \Big(\boldsymbol{u}\big(\mathbf{x}_\alpha(\mathbf{R}_n) - \boldsymbol{u}\big(\mathbf{x}_{\alpha'}(\mathbf{R}_{n'})\big)\Big)$$

$$\boldsymbol{W}_{nm}(\mathbf{q}) = \int d\mathbf{r}\, \mathrm{e}^{-i\mathbf{q}\cdot\mathbf{r}}\, \boldsymbol{\nabla} T(\mathbf{r}, \mathrm{z}_n - \mathrm{z}_m) = -i\,\mathbf{q}\, T(\mathbf{q}, \mathrm{z}_n - \mathrm{z}_m)$$

Displacement at $\mathbf{\Gamma}$: A_1 and B_1 modes

$$\boldsymbol{u}\left(\mathbf{x}_\alpha(\mathbf{R}_n)\right) = \sum_{i,j=1}^{3} \left(\boldsymbol{u}_n(\mathbf{Q}_{ij})\, \mathrm{e}^{i\boldsymbol{Q}_{ij}\cdot\mathbf{x}_\alpha(\mathbf{R}_n)} + c.c. \right)$$

- phonon coordinates: q_1 (A_1 mode) and q_2 (B_1 mode)

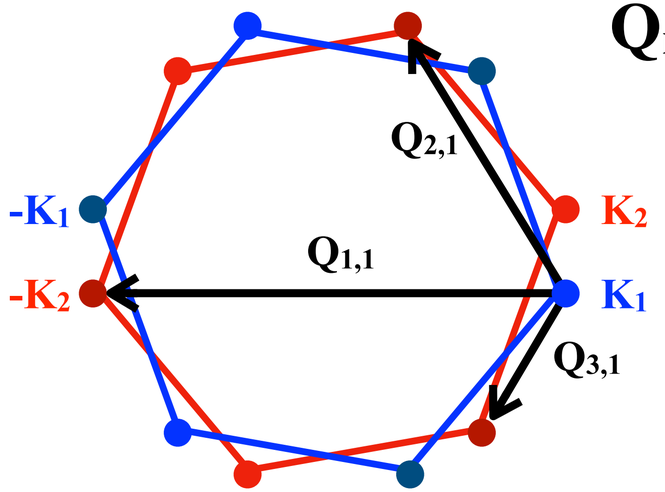

$\mathbf{Q_{n,2} = C_{3z}(Q_{n,1})}$ $\mathbf{Q_{n,3} = C_{3z}(Q_{n,2})}$ $\mathbf{n=1,2,3}$

- the set of $\{Q_{i,j}\}$ is invariant under C_{3z} and C_{2x}, and odd under C_{2y} and C_{2z}

Displacement at $\mathbf{\Gamma}$: A_1 and B_1 modes

$$\boldsymbol{u}\big(\mathbf{x}_\alpha(\mathbf{R}_n)\big) = \sum_{i,j=1}^{3} \left(\boldsymbol{u}_n(\mathbf{Q}_{ij})\, \mathrm{e}^{i\boldsymbol{Q}_{ij}\cdot\mathbf{x}_\alpha(\mathbf{R}_n)} + c.c. \right)$$

- phonon coordinates: q_1 (A_1 mode) and q_2 (B_1 mode)

$$\begin{aligned}
C_{3z}\big(\boldsymbol{u}_n(\mathbf{Q}_{ij})\big) &= \boldsymbol{u}_n\big(C_{3z}(\mathbf{Q}_{ij})\big) \\
C_{2x}\big(\boldsymbol{u}_n(\mathbf{Q}_{ij})\big) &= \boldsymbol{u}_{n'}\big(C_{2x}(\mathbf{Q}_{ij})\big) \qquad n' \neq n \\
\boldsymbol{u}_n(\mathbf{Q}_{ij})^* &= -\boldsymbol{u}_n(\mathbf{Q}_{ij}) \qquad A_1 \text{ mode} \\
\boldsymbol{u}_n(\mathbf{Q}_{ij})^* &= \boldsymbol{u}_n(\mathbf{Q}_{ij}) \qquad B_1 \text{ mode}
\end{aligned}$$

- matrix elements of the operator $c^{\dagger}_{n\mathbf{k}\alpha\sigma}\, c_{m\mathbf{p}\beta\sigma}$

$$W^{\alpha\beta}_{n\mathbf{k},m\mathbf{p}} = \frac{1}{N^2} \sum_{\mathbf{q}\mathbf{Q}_{ij}} \sum_{\mathbf{R}_n\mathbf{R}_m} \boldsymbol{W}_{nm}(-\mathbf{q}) \cdot \Big[\boldsymbol{u}_n(\mathbf{Q}_{ij})\, \mathrm{e}^{-i\left(\mathbf{k}+\mathbf{q}-\mathbf{Q}_{ij}\right)\cdot\left(\mathbf{R}_n+\mathbf{r}_{n,\alpha}\right)}\; \mathrm{e}^{i(\mathbf{p}+\mathbf{q})\cdot\left(\mathbf{R}_m+\mathbf{r}_{m,\beta}\right)}$$

$$- \boldsymbol{u}_m(\mathbf{Q}_{ij})\, \mathrm{e}^{-i(\mathbf{k}+\mathbf{q})\cdot\left(\mathbf{R}_n+\mathbf{r}_{n,\alpha}\right)}\; \mathrm{e}^{i\left(\mathbf{p}+\mathbf{q}+\mathbf{Q}_{ij}\right)\cdot\left(\mathbf{R}_m+\mathbf{r}_{m,\beta}\right)} + c.c. \Big]$$

$$= \sum_{\mathbf{q}\mathbf{Q}_{ij}} \sum_{\mathbf{G}_n\mathbf{G}_m} \boldsymbol{W}_{nm}(-\mathbf{q}) \cdot \Big[\delta_{-\mathbf{q},\mathbf{k}-\mathbf{Q}_{ij}+\mathbf{G}_n}\, \delta_{-\mathbf{q},\mathbf{p}+\mathbf{G}_m}\; \boldsymbol{u}_n(\mathbf{Q}_{ij})\, \mathrm{e}^{i\mathbf{G}_n\cdot\mathbf{r}_{n,\alpha} - i\mathbf{G}_m\cdot\mathbf{r}_{m,\beta}}$$

$$- \delta_{-\mathbf{q},\mathbf{k}+\mathbf{G}_n}\, \delta_{-\mathbf{q},\mathbf{p}+\mathbf{Q}_{ij}+\mathbf{G}_m}\; \boldsymbol{u}_m(\mathbf{Q}_{ij})\, \mathrm{e}^{i\mathbf{G}_n\cdot\mathbf{r}_{n,\alpha} - i\mathbf{G}_m\cdot\mathbf{r}_{m,\beta}} + c.c. \Big]$$

Electron-phonon coupling at $\mathbf{\Gamma}$

- interlayer:

$$\delta H_{\perp} = \sum_{i=1}^{2} q_i \sum_{\mathbf{k}\sigma} \sum_{\mathbf{Q}\mathbf{Q}'} \Psi^{\dagger}_{\mathbf{k},\mathbf{Q},\sigma} \, \tau_i \, \hat{H}_{\perp \, \mathbf{Q}\mathbf{Q}'} \, \Psi_{\mathbf{k},\mathbf{Q}',\sigma}$$

$$\hat{H}_{\perp \, \mathbf{Q}\mathbf{Q}'} = \gamma \, \sigma_0 \, \delta_{\mathbf{Q},\mathbf{Q}'}$$

- since the sublattice index is reversed for valley -1, the interlayer coupling is between different sublattice

Electron-phonon coupling at $\mathbf{\Gamma}$

- intralayer:

$$\delta H_{\parallel} = \sum_{i=1}^{2} q_i \sum_{\mathbf{k}\sigma} \sum_{\mathbf{Q}\mathbf{Q}'} \Psi^{\dagger}_{\mathbf{k},\mathbf{Q},\sigma}\, \tau_i\, \hat{H}_{\parallel\,\mathbf{Q}\mathbf{Q}'}\, \Psi_{\mathbf{k},\mathbf{Q}',\sigma}$$

$$\hat{H}_{\parallel\,\mathbf{Q}\mathbf{Q}'} = \sum_{j=1}^{3} \left(\delta_{\mathbf{Q}-\mathbf{Q}',\mathbf{q}_j} + \delta_{\mathbf{Q}'-\mathbf{Q},\mathbf{q}_j}\right) \hat{T}_j\left(g_0, g_1\right)$$

same as before with u_0 and u_1 replaced by g_0 and g_1

- since the sublattice index is reversed for valley -1, g_0 is the coupling between different sublattice, while g_1 that between same sublattice. Therefore $g_0 > g_1$

Electron-phonon coupling at $\mathbf{\Gamma}$

$$\delta H = \sum_{i=1}^{2} q_i \sum_{\mathbf{k}\sigma} \sum_{\mathbf{Q}\mathbf{Q}'} \Psi^{\dagger}_{\mathbf{k},\mathbf{Q},\sigma}\, \tau_i \left(\hat{H}_{\parallel\, \mathbf{Q}\mathbf{Q}'} + \hat{H}_{\perp\, \mathbf{Q}\mathbf{Q}'} \right) \Psi_{\mathbf{k},\mathbf{Q}',\sigma}$$

- supplied by the phonon Hamiltonian:

$$H_{\mathrm{ph}} = \frac{\omega_0}{2} \sum_{i=1}^{2} \left(p_i^2 + q_i^2 \right)$$

precisely describes an $E \times e$ Jahn-Teller coupling with conserved quantity

$$L_3 = \frac{1}{2} \sum_{\mathbf{k}\mathbf{Q}\sigma} \Psi^{\dagger}_{\mathbf{k},\mathbf{Q},\sigma}\, \tau_3\, \sigma_0\, \Psi_{\mathbf{k},\mathbf{Q},\sigma} + \boldsymbol{q} \wedge \boldsymbol{p}$$

Frozen phonon calculation

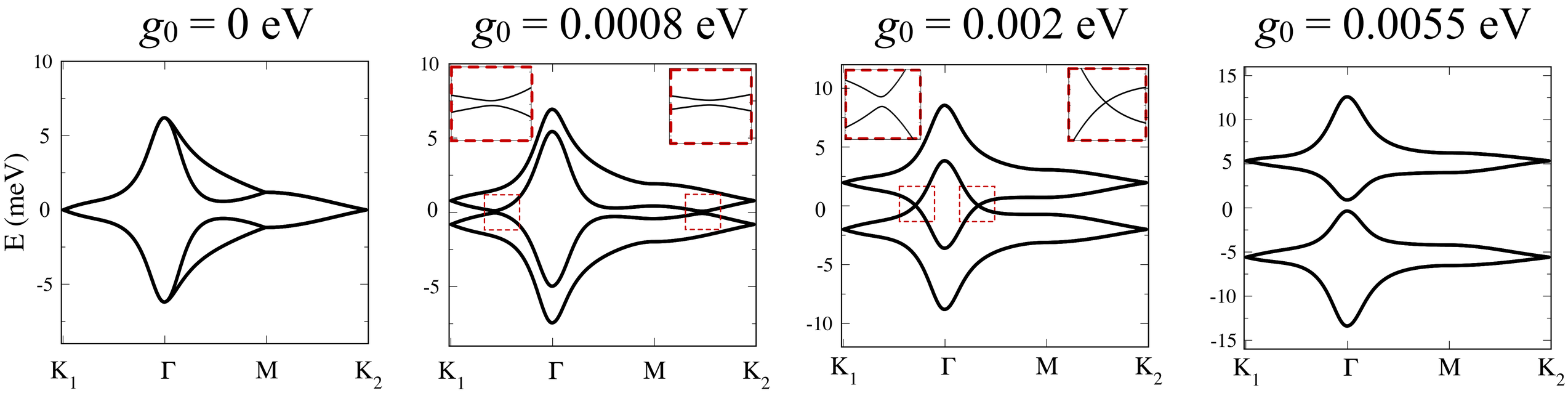

- $g_1 = g_0/10$ and $\gamma = g_0/2.5$ yield good agreement with realistic tight-binding results

Electron-phonon coupling at generic $\mathbf{q}$

- any $\mathbf{q}$ inside the mini Brillouin zone is much smaller than any $\mathbf{Q}_{ij}$
- therefore the matrix elements $\delta H_{\perp \mathbf{QQ}'}$ and $\delta H_{\parallel \mathbf{QQ}'}$ at leading order in the small twist angle are unchanged

$$H_{\text{el-ph}} = \frac{1}{\sqrt{N}} \sum_{\mathbf{q}} \sum_{i=1}^{2} q_i^\dagger(\mathbf{q}) \sum_{\mathbf{k}\sigma} \sum_{\mathbf{QQ}'} \Psi^\dagger_{\mathbf{k},\mathbf{Q},\sigma} \, \tau_i \left(\hat{H}_{\parallel \, \mathbf{QQ}'} + \hat{H}_{\perp \, \mathbf{QQ}'} \right) \Psi_{\mathbf{k}+\mathbf{q},\mathbf{Q}',\sigma}$$

$$H_{\text{ph}} = \sum_{i=1}^{2} \frac{\omega_{\mathbf{q}}}{2} \left(p_i(\mathbf{q})^\dagger \, p_i(\mathbf{q}) + q_i(\mathbf{q})^\dagger \, q_i(\mathbf{q}) \right)$$

$$L_3 = \frac{1}{2} \sum_{\mathbf{kQ}\sigma} \Psi^\dagger_{\mathbf{k},\mathbf{Q},\sigma} \, \tau_3 \, \sigma_0 \, \Psi_{\mathbf{k},\mathbf{Q},\sigma} + \sum_{\mathbf{q}} \boldsymbol{q}^\dagger(\mathbf{q}) \wedge \boldsymbol{p}(\mathbf{q})$$

Electron-phonon coupling at generic **q**

- note that the phonon dispersion is 10^{-4} the center of mass frequency: the mode is effectively dispersionless $\omega_{\mathbf{q}} \simeq \omega_0$
- we can legitimately regard it as a vibration of the moiré unit cell as if it were a huge single molecule
- given the high frequency ω_0 as compared with the flat band width, it may be safe to integrate the phonons out, and neglect retardation effects

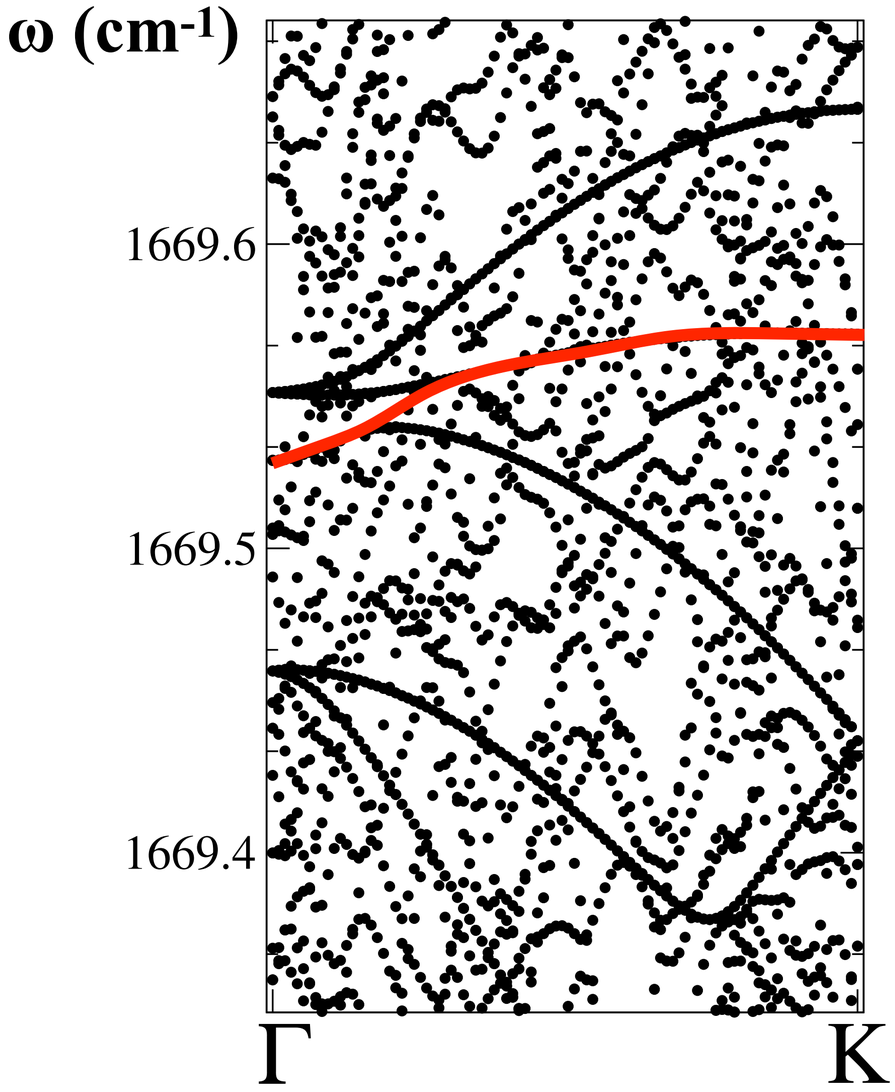

Jahn-Teller phonon-mediated attraction

$$H_{\text{J-T}} = -\frac{g}{2N} \sum_{i=1}^{2} L_i^\dagger(\mathbf{q})\, L_i(\mathbf{q})$$

$$L_i(\mathbf{q}) = \frac{1}{g_0} \sum_{\mathbf{k}\sigma} \sum_{\mathbf{Q}\mathbf{Q}'} \Psi^\dagger_{\mathbf{k},\mathbf{Q},\sigma}\, \tau_i \left(\hat{H}_{\parallel\, \mathbf{Q}\mathbf{Q}'} + \hat{H}_{\perp\, \mathbf{Q}\mathbf{Q}'} \right) \Psi_{\mathbf{k}+\mathbf{q},\mathbf{Q}',\sigma}$$

- coupling constants: $g \equiv \dfrac{g_0^2}{\omega_0} \lesssim 1.5\text{meV} \quad \dfrac{g_1}{g_0} \equiv g_1 = \dfrac{1}{10} \quad \dfrac{\gamma}{g_0} \equiv \gamma = \dfrac{2}{5}$

- $H_{\text{J-T}}$ is invariant under the P622 space group and under $\text{U}_\text{v}(1)$ with generator

$$L_3 = \frac{1}{2} \sum_{\mathbf{k}\mathbf{Q}\sigma} \Psi^\dagger_{\mathbf{k},\mathbf{Q},\sigma}\, \tau_3\, \sigma_0\, \Psi_{\mathbf{k},\mathbf{Q},\sigma}$$

Jahn-Teller phonon-mediated attraction treated on an equal footing with the Coulomb interaction

arXiv:2204.05190

Coulomb repulsion

- the charge density operators are diagonal in layer $n = 1,2$, in sublattice and valley

$$\rho_n(\mathbf{q}+\mathbf{G}) = \sum_{\mathbf{kQ}\sigma} \Psi^\dagger_{\mathbf{k},\mathbf{Q},\sigma}\, \hat{\rho}_n(\mathbf{Q})\, \sigma_0\, \Psi_{\mathbf{k}+\mathbf{q},\mathbf{Q}-\mathbf{G},\sigma}\,,$$

$$\hat{\rho}_n(\mathbf{Q}) = \delta_{\mathbf{Q},\mathbf{Q}_A}\, \frac{\tau_0 - (-1)^n\, \tau_3}{2} + \delta_{\mathbf{Q},\mathbf{Q}_B}\, \frac{\tau_0 + (-1)^n\, \tau_3}{2}$$

- Coulomb repulsion:

$$H_C = \frac{1}{2N} \sum_{\mathbf{q},\mathbf{G}} \sum_{nm} U_{nm}(\mathbf{q}+\mathbf{G})\, \rho^\dagger_n(\mathbf{q}+\mathbf{G})\, \rho_m(\mathbf{q}+\mathbf{G})$$

Fourier transforms of the interaction e^2/r screened by the high-frequency dielectric constant $\varepsilon_\infty = 9.23$ of graphene, and by the presence of a dual metal gate assumed at distance 30nm.

Let us start with the simple Hartree-Fock approximation and at charge neutrality

Coulomb interaction alone

Bultinck *et al.*, Phys. Rev. X **10**, 031034 (2020)

- without the Jahn-Teller interaction, Coulomb repulsion stabilises at charge neutrality, $\nu = 0$, an insulator, dubbed K-IVC, which breaks time-reversal, valley $U_v(1)$, and C_{2x}, with order parameter

$$\Delta_{\text{K-IVC}}(\varphi) \sim \sigma_3 \left(\cos\varphi\, \tau_1 + \sin\varphi\, \tau_2 \right)$$

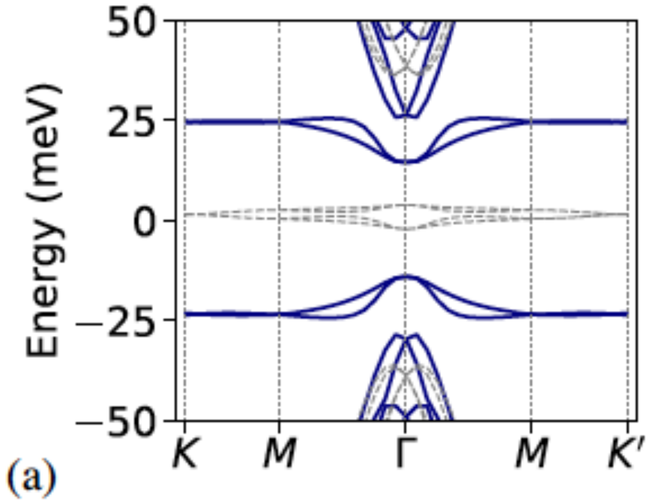

from Bultinck *et al.*, Phys. Rev. X **10**, 031034 (2020)

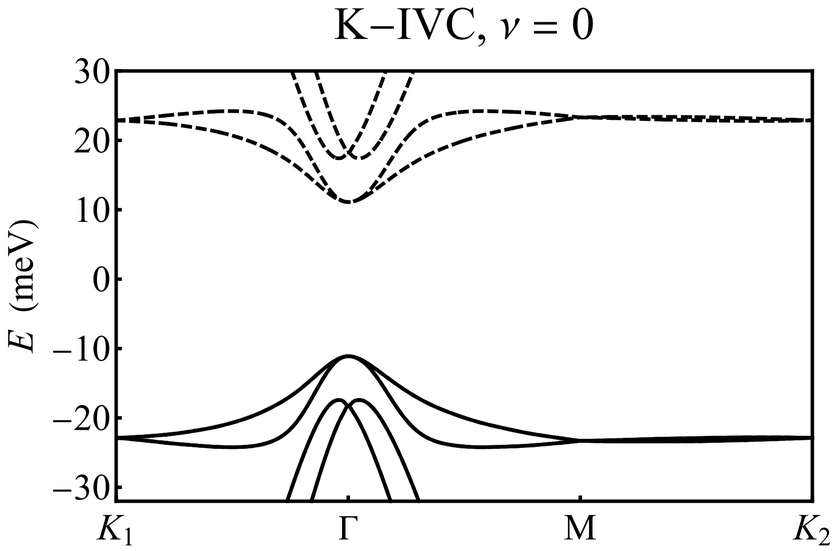

our mean-field results

Jahn-Teller phonon-mediated attraction

$$H_{\text{J-T}} = -\frac{g}{2N} \sum_{i=1}^{2} L_i^{\dagger}(\mathbf{q})\, L_i(\mathbf{q})$$

negligible

$$L_i(\mathbf{q}) = \sum_{\mathbf{k}\sigma} \sum_{\mathbf{Q}\mathbf{Q}'} \Psi^{\dagger}_{\mathbf{k},\mathbf{Q},\sigma}\, \tau_i \left(\gamma\, \sigma_0\, \delta_{\mathbf{Q},\mathbf{Q}'} + \sum_{j=1}^{3} \left(\delta_{\mathbf{Q}-\mathbf{Q}',\mathbf{q}_j} + \delta_{\mathbf{Q}'-\mathbf{Q},\mathbf{q}_j} \right) \hat{T}_j\left(1, g_1\right) \right) \Psi_{\mathbf{k},\mathbf{Q}',\sigma}$$

- already the Hartree term $-\frac{g}{N} \sum_{i=1}^{2} \langle\, L_i^{\dagger}(\mathbf{q})\, \rangle\, L_i(\mathbf{q})$ favours an order parameter

$$\Delta_{\text{st-JT}}(\varphi) \sim \sigma_0 \left(\cos\varphi\, \tau_1 + \sin\varphi\, \tau_2 \right)$$

which corresponds to a static Jahn-Teller distortion just breaking $U_v(1)$. That may be also stabilised by the Coulomb exchange, which however prefers K-IVC.

Coulomb interaction plus Jahn-Teller attraction

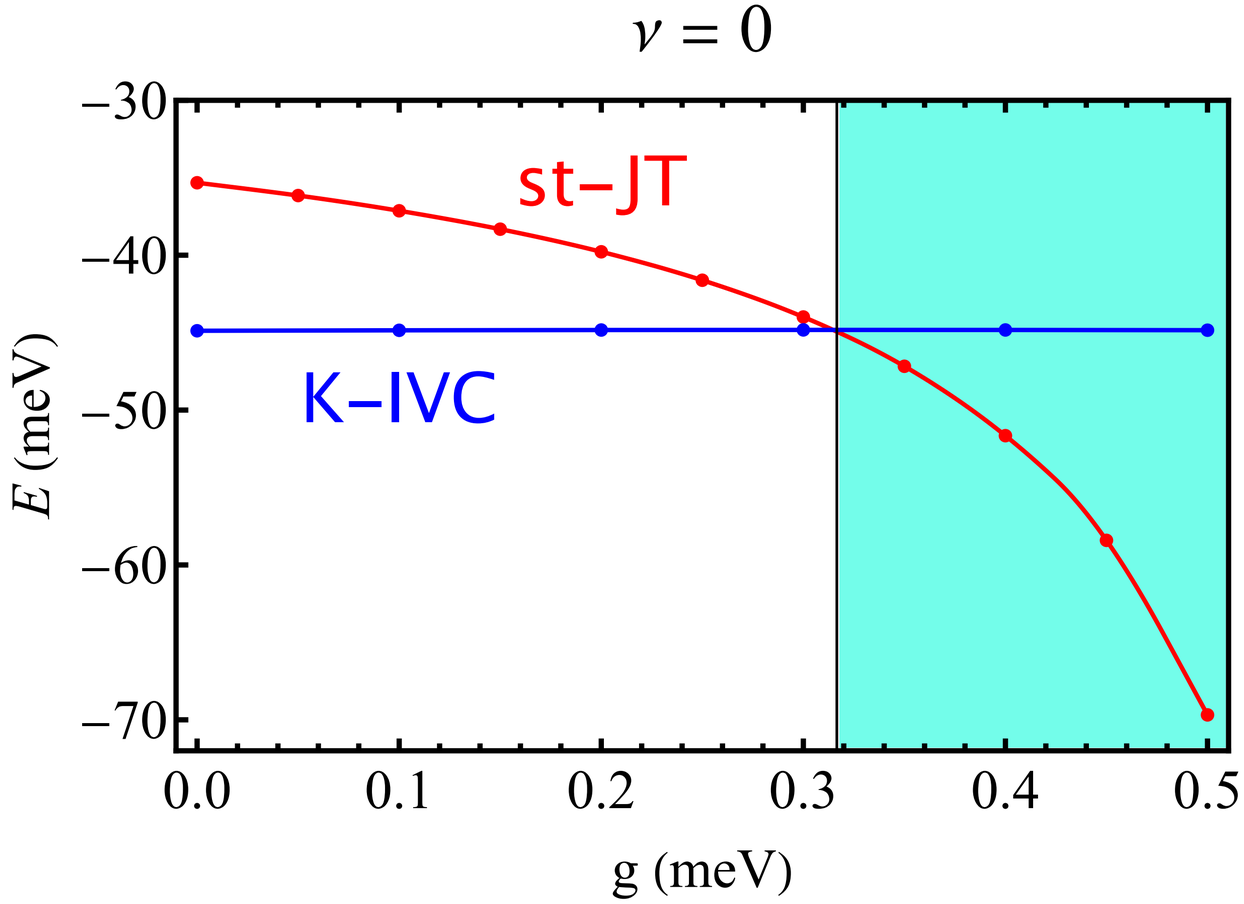

- the st-JT state is a local minimum at $g = 0$, where K-IVC is the global one. However, for $g \gtrsim 0.3$meV, thus below its estimated value, st-JT becomes the global minimum

properties of the st-JT state at ν = 0

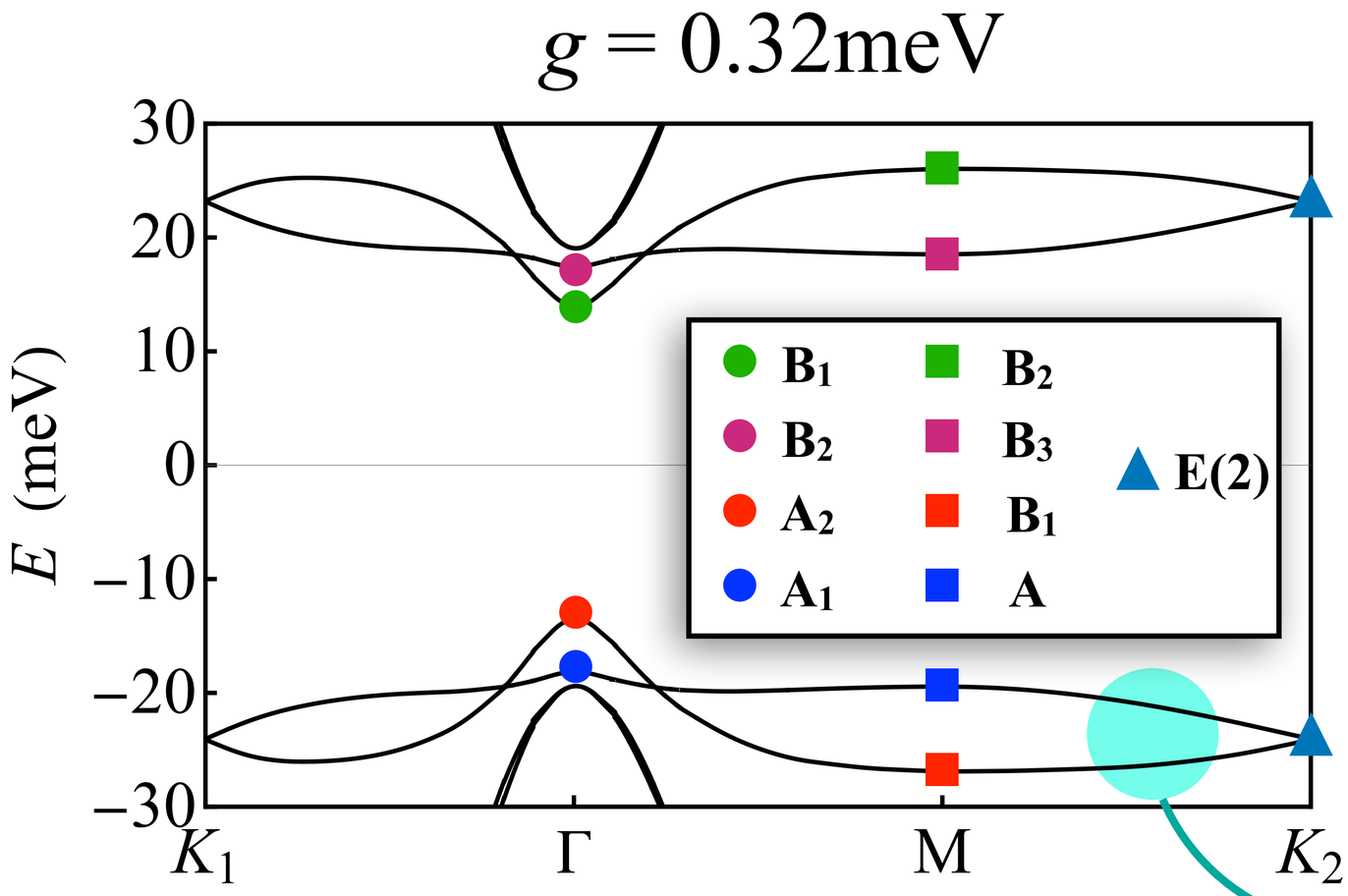

- agrees with the tight-binding results at frozen phonons
- P622 space group
- symmetry properties of the Bloch waves at the high-symmetry points still implying Wannier obstruction and non-trivial topology

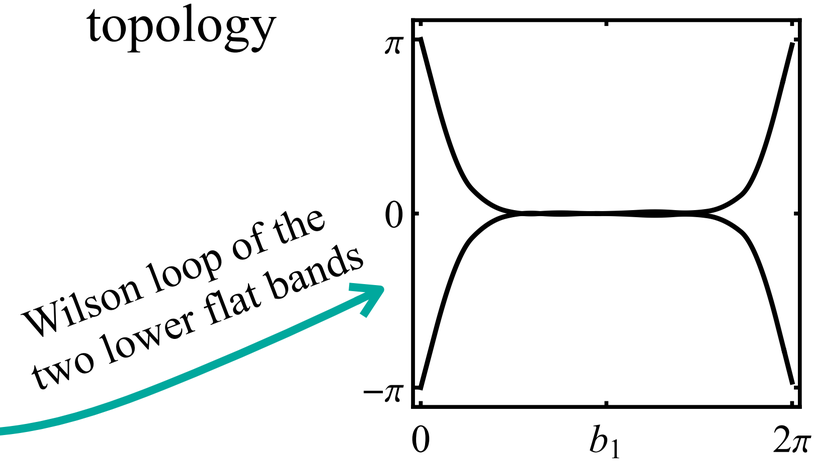

- the two lower flat bands thus carry opposite Chern numbers C = ± 2, consistently with the edge states found in the tight-binding calculation

K-IVC vs. st-JT states at $\nu = 0$ and $\varphi = 0$

$\Delta_{\text{K-IVC}}(0) \sim \sigma_3\,\tau_1$ **vs.** $\Delta_{\text{st-JT}}(0) \sim \sigma_0\,\tau_1$

- each electron carry Chern number $\sigma_3 = \pm 1$, $\tau_1 = \pm 1$, and spin

- however, K-IVC breaks time-reversal and C_{2x} while st-JT is invariant

mean-field insulating states at other integer fillings ν

st-JT

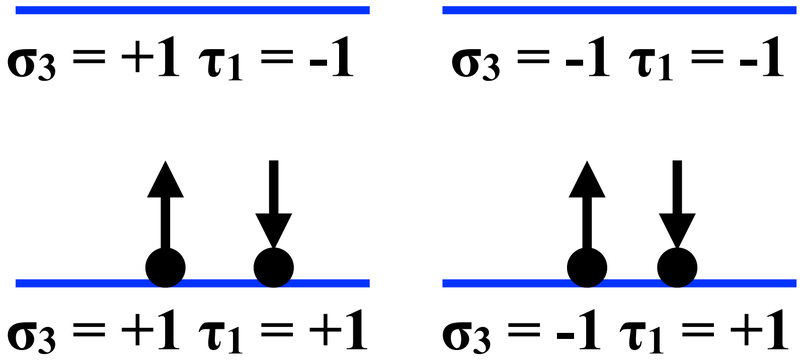

- Forcing translation symmetry, Hartree-Fock can stabilise insulators at other integer fillings only splitting spin or Chern number degeneracies
- Jahn-Teller coupling effectively inverts Hund's rules: lowest spin states are always the most favourable
- Therefore, at first instance, Chern number degeneracy is split
- Only as last resort spin degeneracy is split

st-JT: even $\nu = \pm 2$

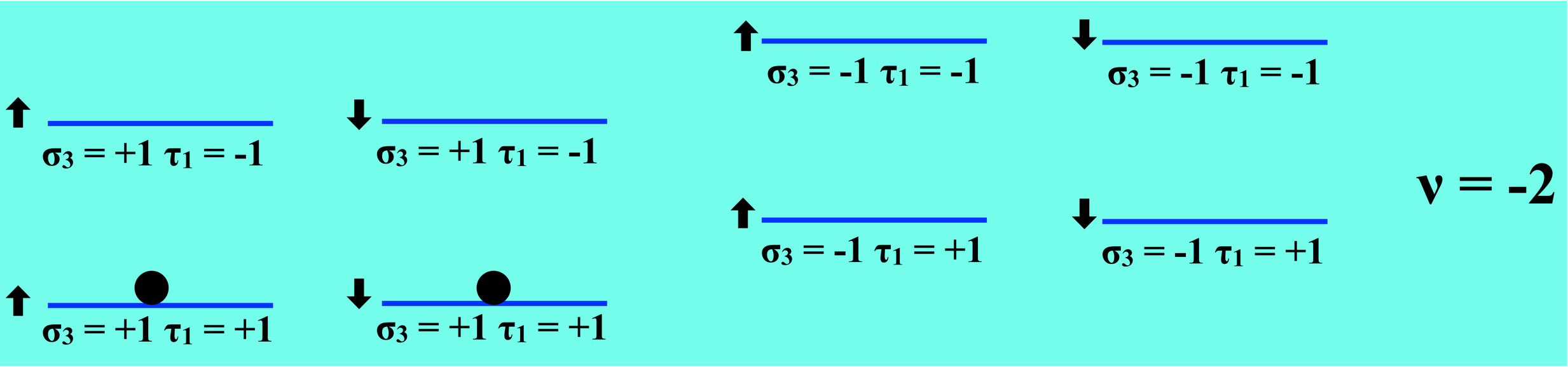

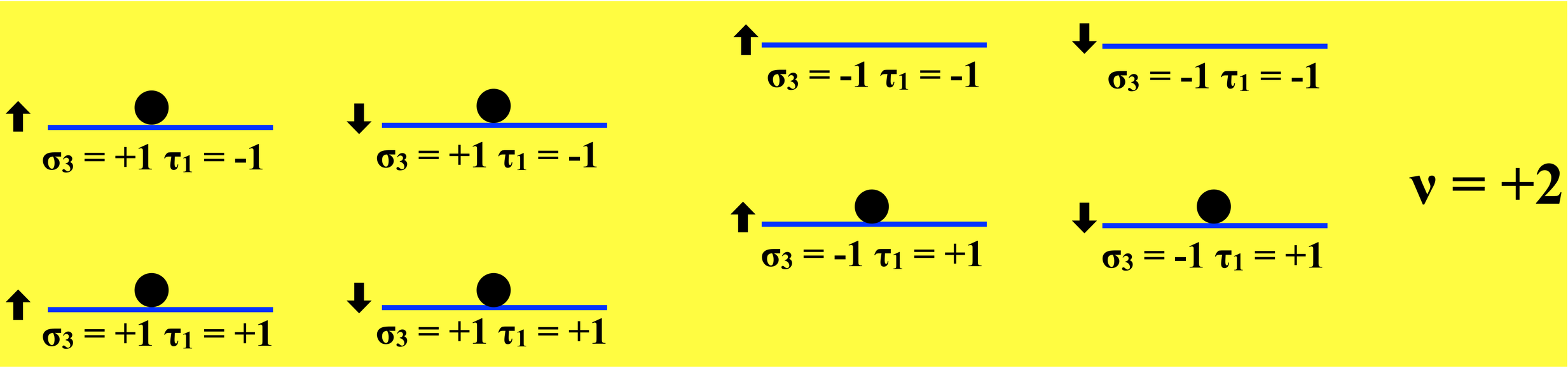

st-JT: even $\nu = \pm 2$

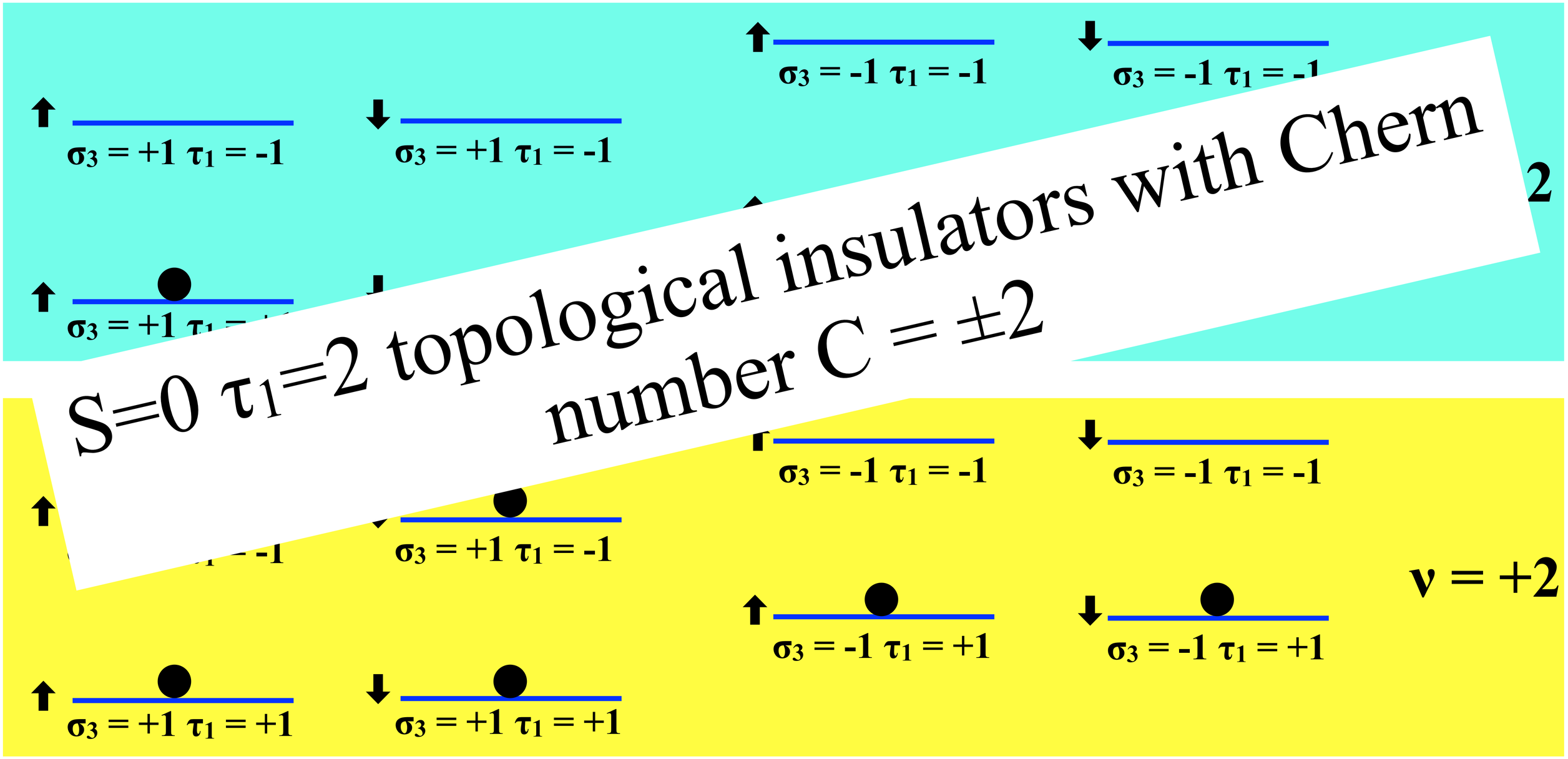

S=0 τ_1=2 topological insulators with Chern number C = ±2

Hartree-Fock bands at ν = -2

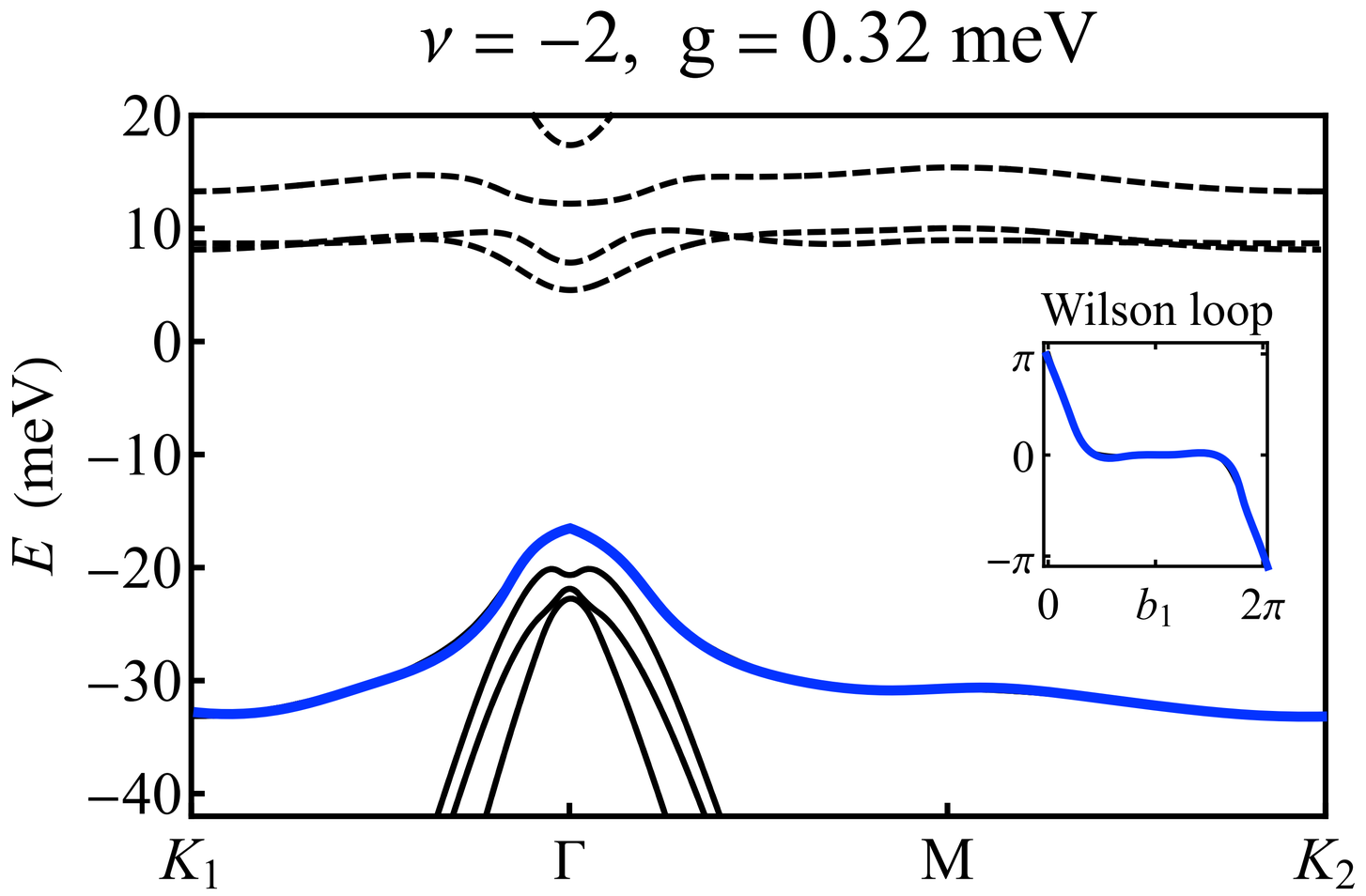

- indeed an S=0 topological insulator, in this case with C = -2, invariant just under *P*6 space group

st-JT: odd $\nu = \pm 1, \pm 3$

- at odd fillings Hartree-Fock is obliged to break spin SU(2) and spin-polarise the state

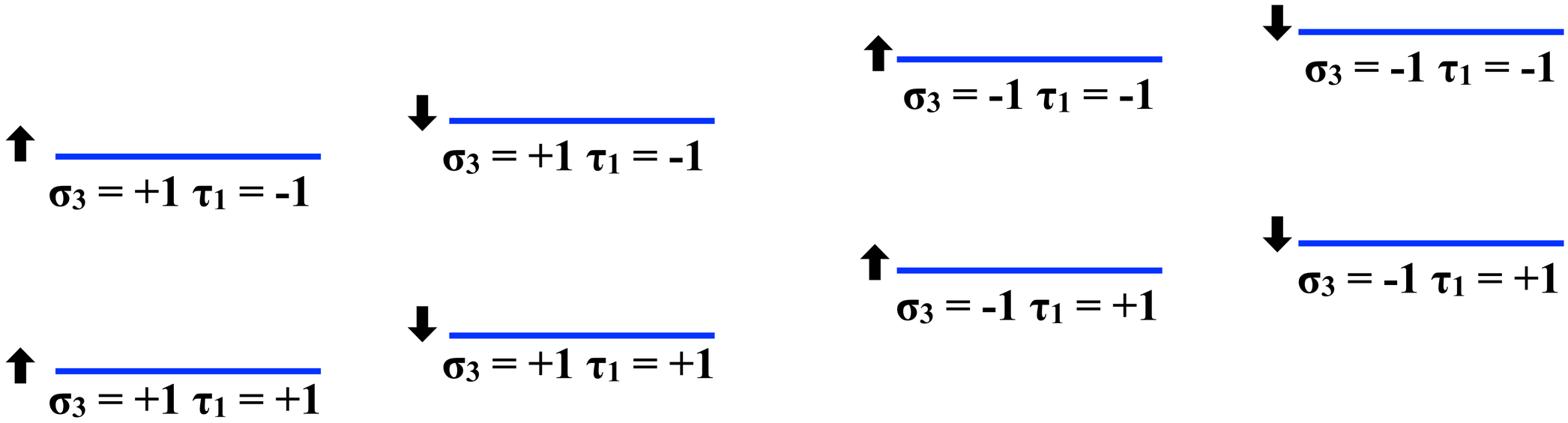

st-JT: $\nu = -3$

- $\nu = -3$: S=1/2 and τ_1=1 polarised topological insulator with C = ±1

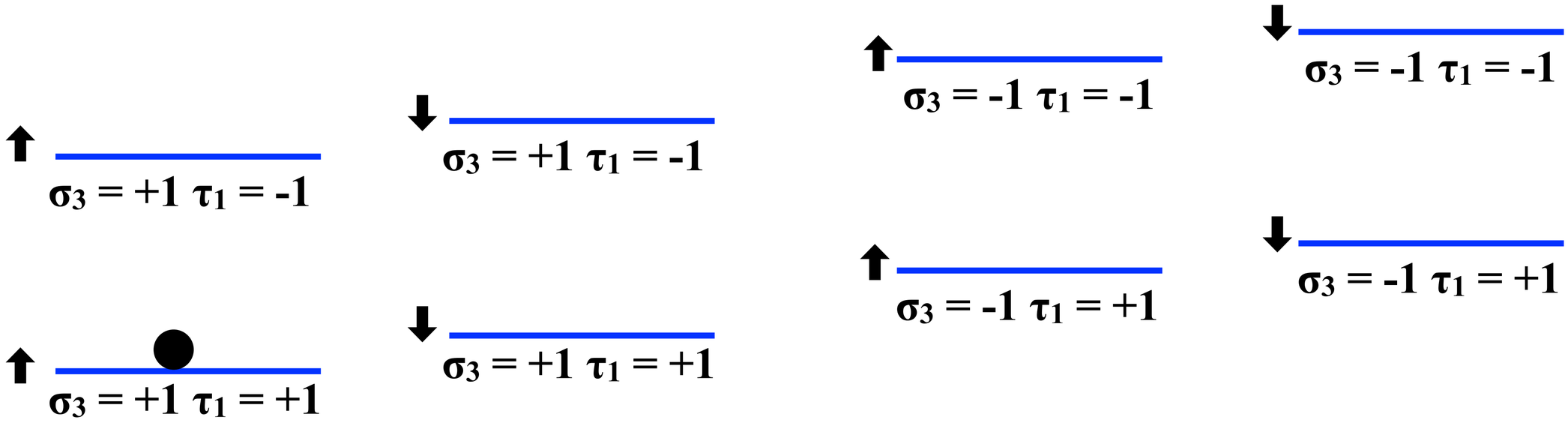

st-JT: $\nu = -1$

- $\nu = -1$: S=1/2 and τ_1=3 polarised topological insulator with C = ±1

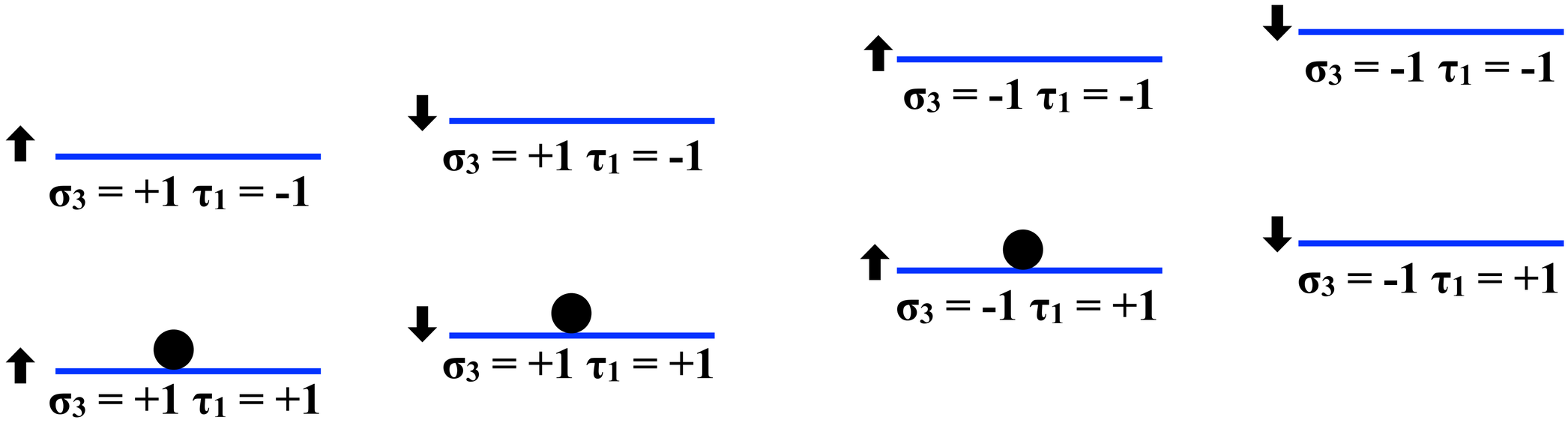

st-JT: $\nu = +1$

- $\nu = +1$: S=1/2 and τ_1=3 polarised topological insulator with C = ± 1

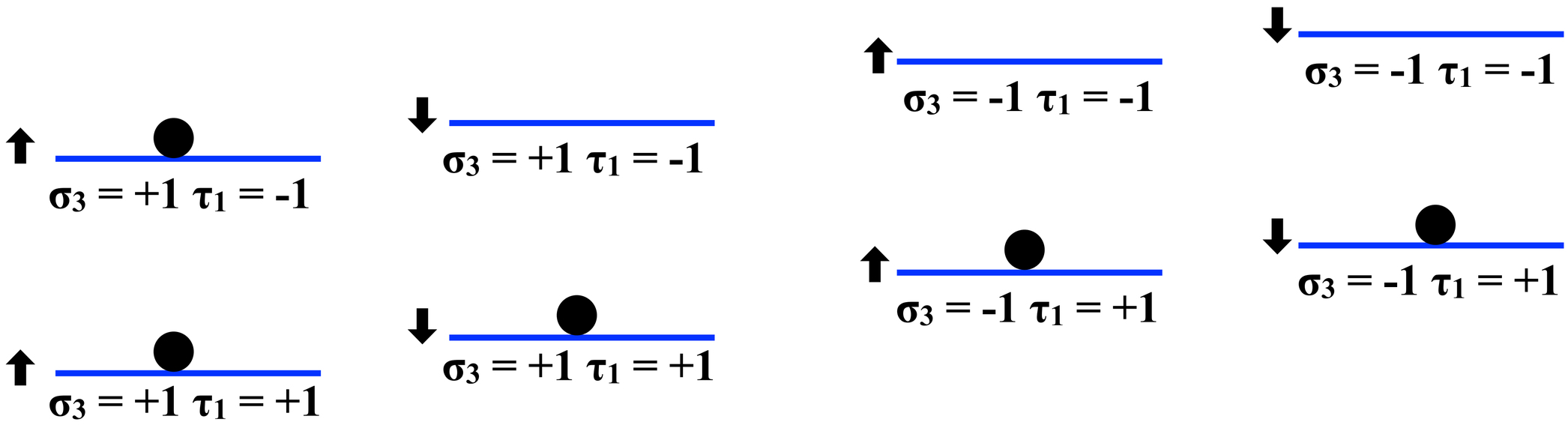

st-JT: $\nu = +3$

- $\nu = +3$: S=1/2 and τ_1=1 polarised topological insulator with C = ±1

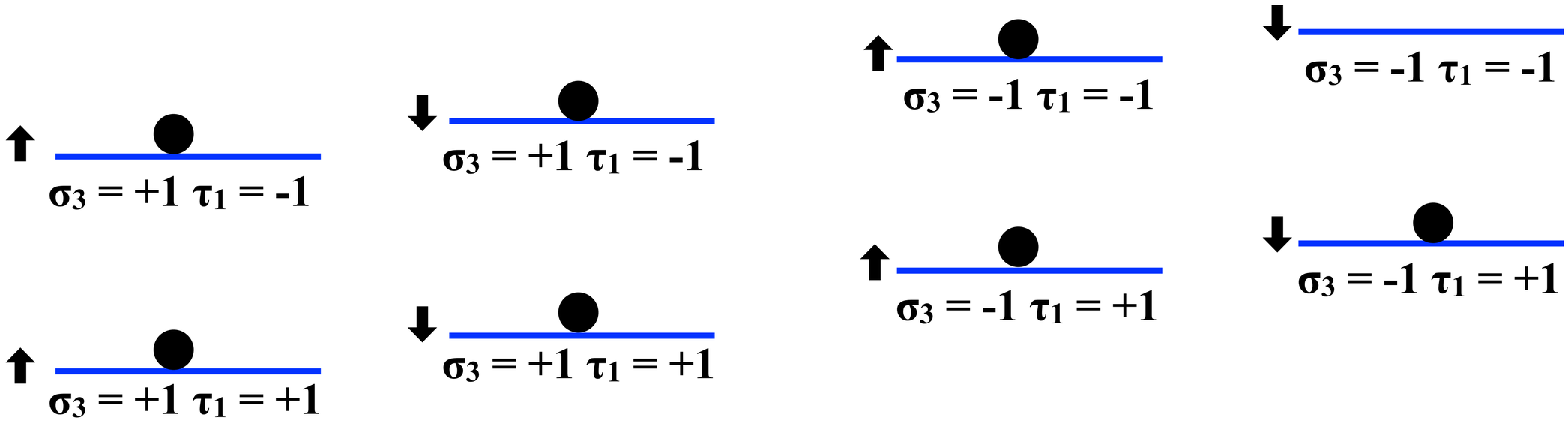

Hartree-Fock bands at ν = -1 and -3

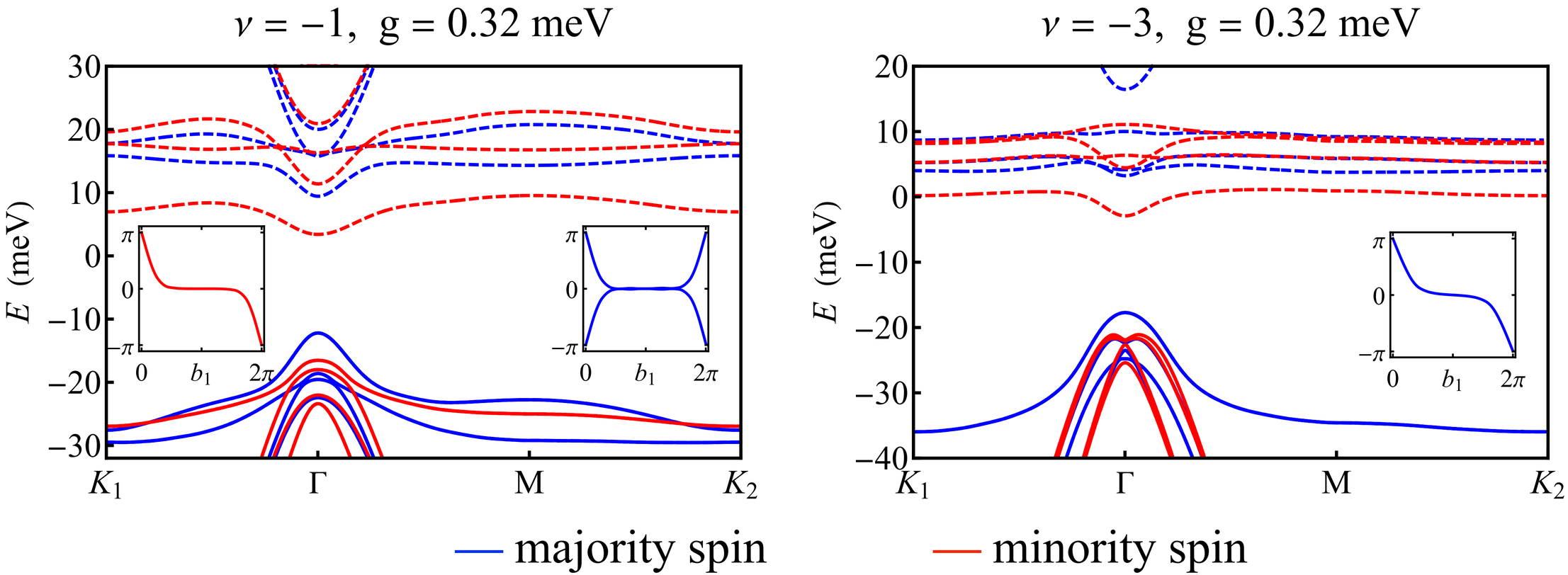

- indeed S=1/2 spin-polarised topological insulators, here with C = -1

A weak staggered potential due to a misaligned hBN substrate does not modify qualitatively the mean-field insulators

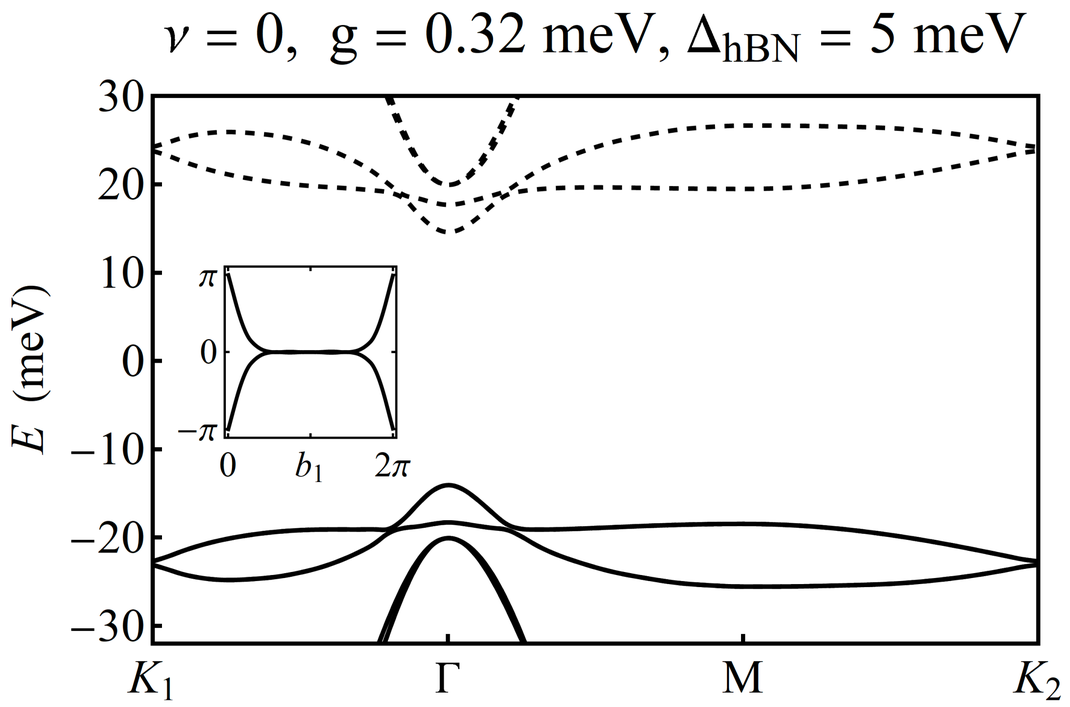

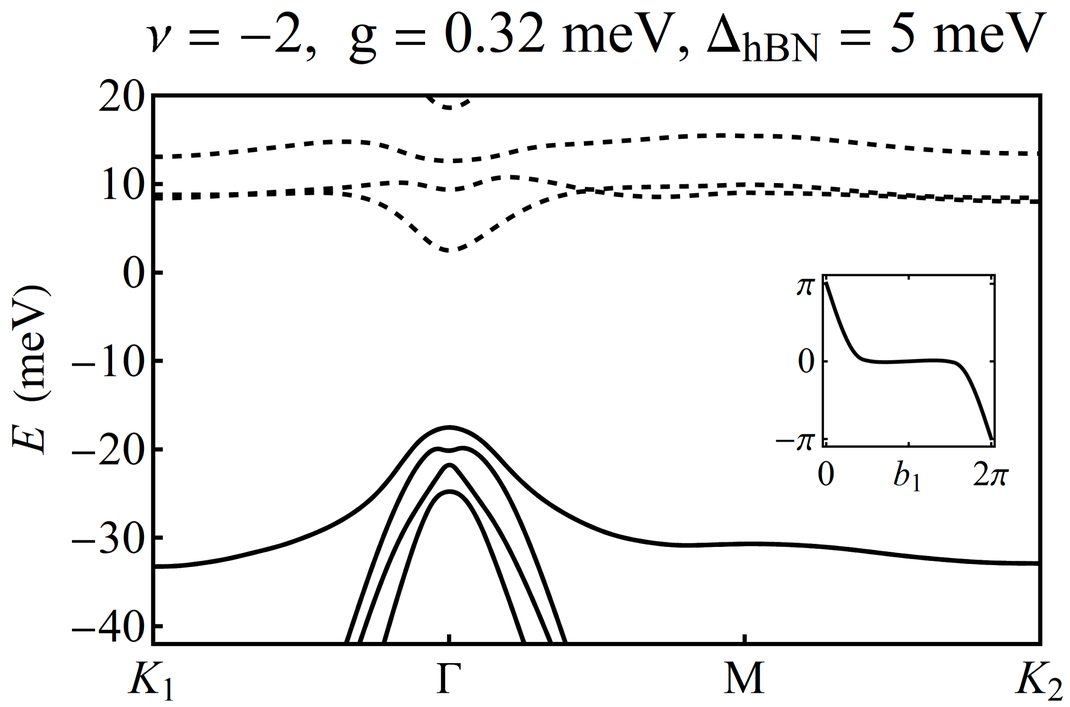

- on the contrary, close to perfect alignment, $\Delta_{hBN} \simeq 30$meV, the mean-field insulators change also qualitatively

K-IVC

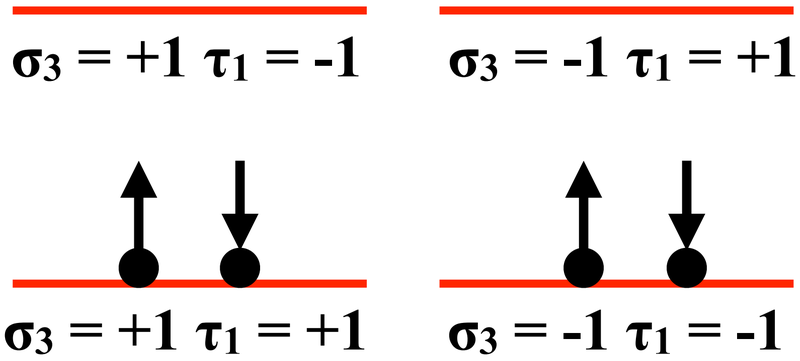

- Forcing translation symmetry, Hartree-Fock can stabilise insulators at other integer fillings only splitting spin or Chern/valley degeneracies
- Coulomb exchange leads to Hund's rules: highest spin states are always the most favourable
- Therefore, at first instance, spin degeneracy is split
- Only as last resort Chern/valley degeneracy is split

K-IVC: even $\nu = \pm 2$

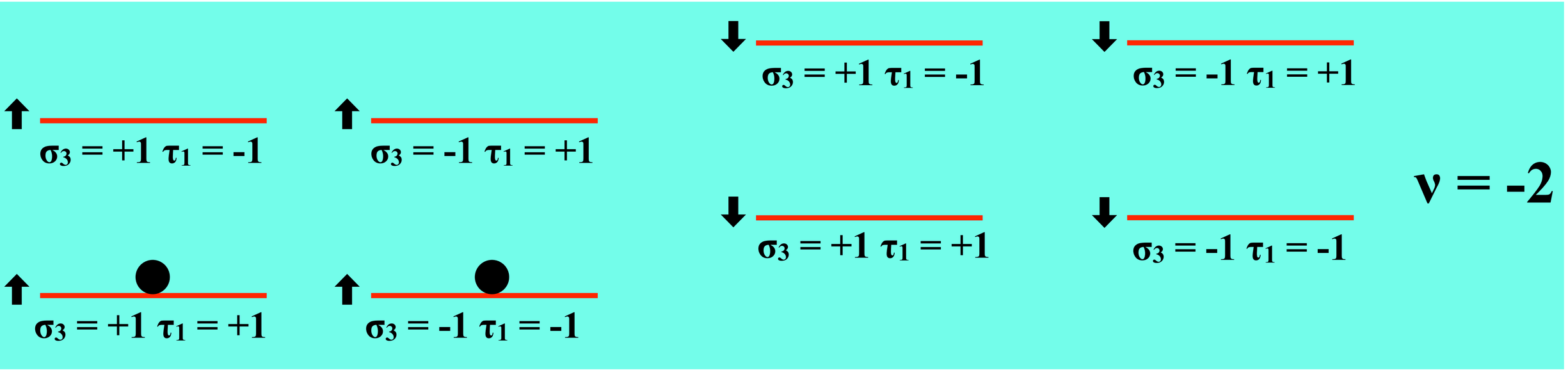

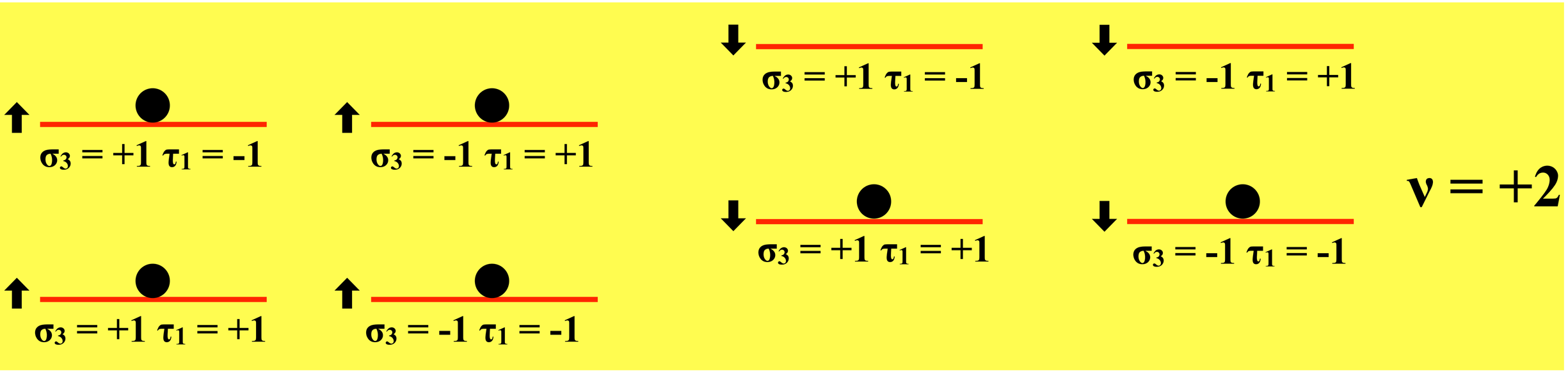

K-IVC: even $\nu = \pm 2$

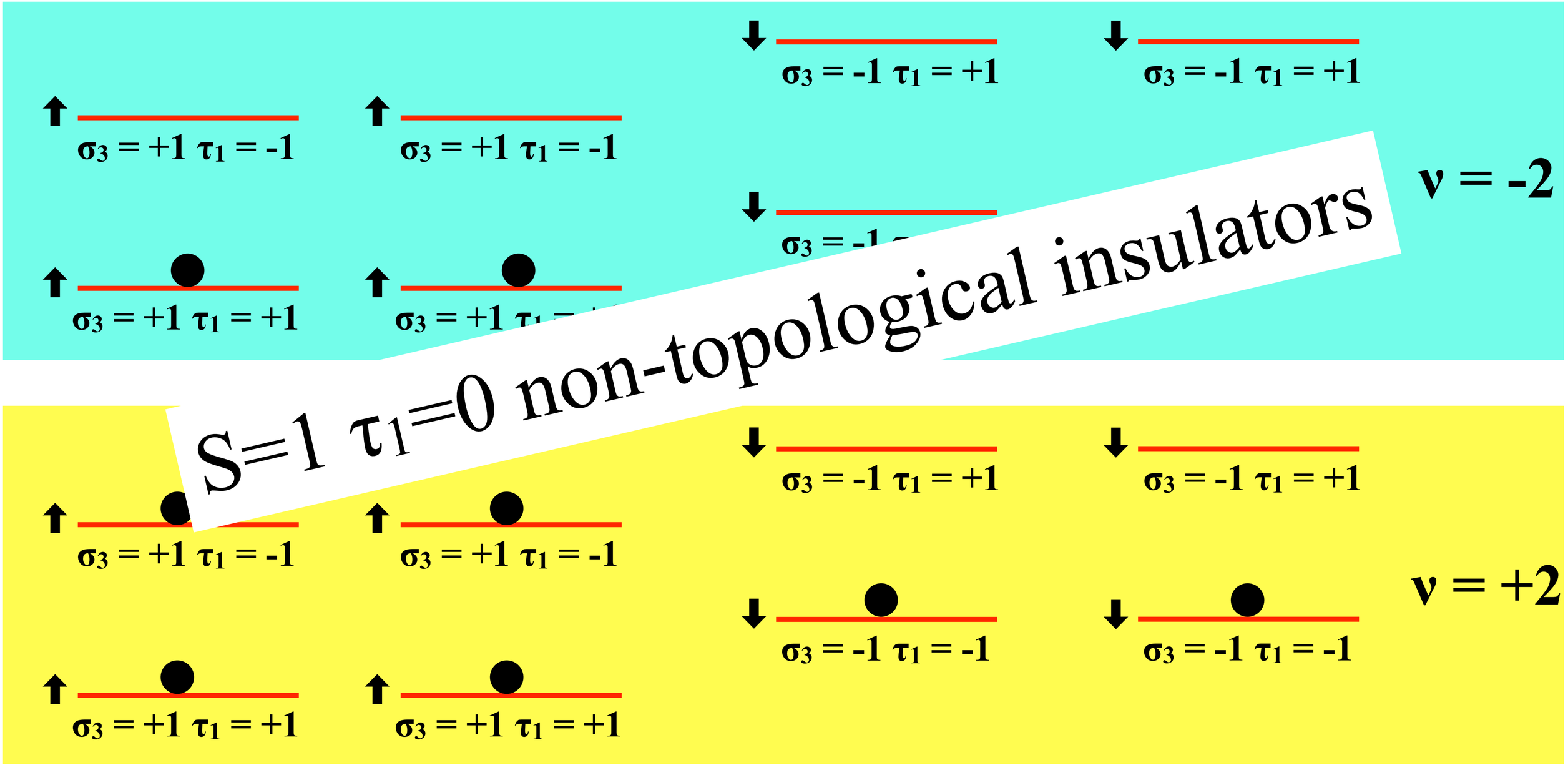

K-IVC at ν = -2

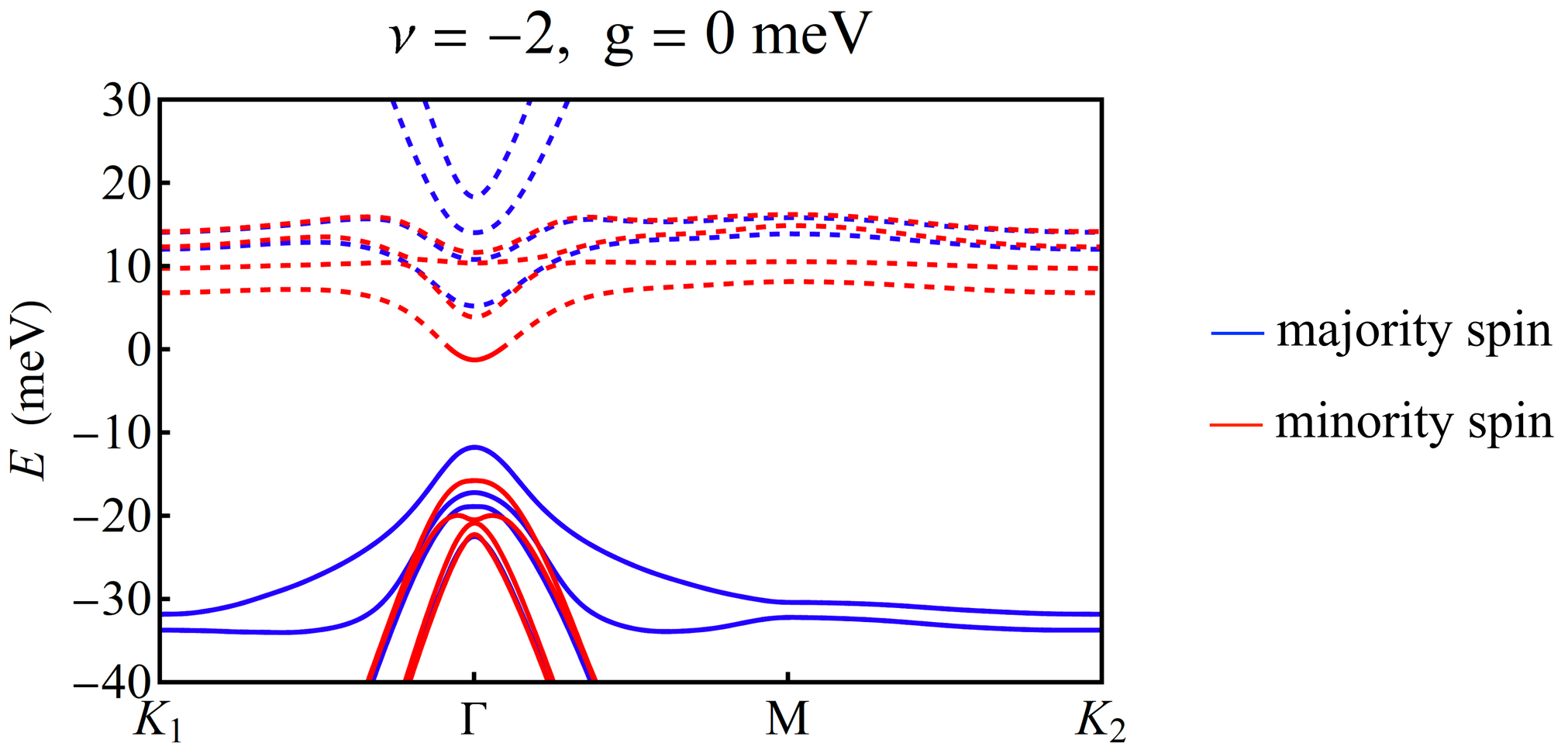

- indeed, HF stabilises a spin polarised insulator at ν = ±2, at $g = 0$ very close in energy to the unpolarised st-JT

K-IVC: odd ν

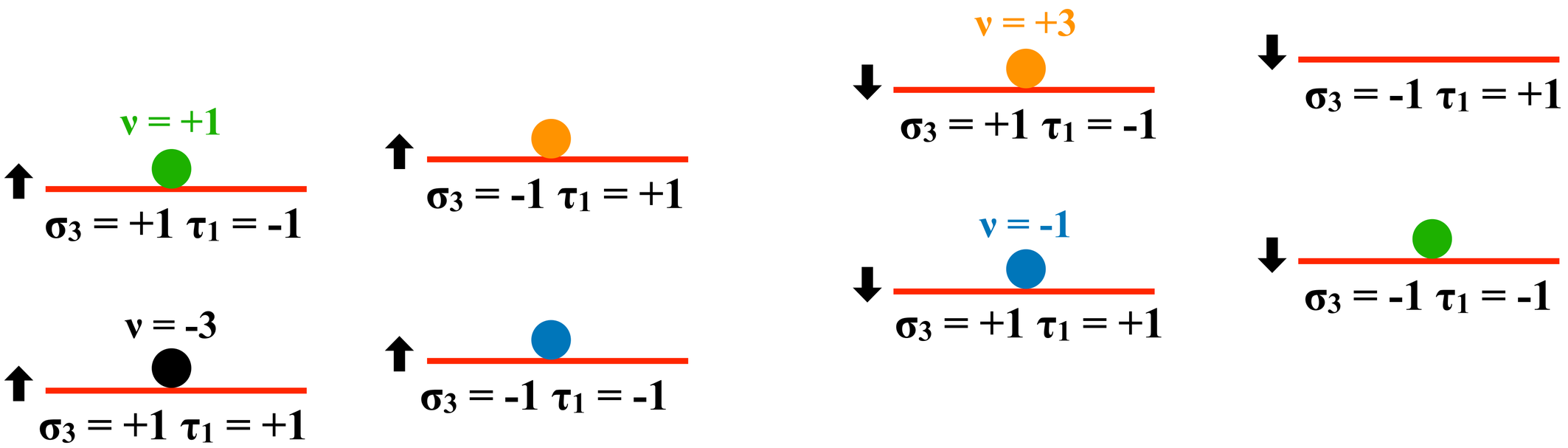

- for all odd ν we expect a S=1/2 τ_1=1 topological insulator with C = ±1, not much different from st-JT at odd fillings, apart from τ_1 at ν = ±1

st-JT vs. K-IVC

ν	C	S	time reversal
-3	±1	1/2	NO
-2	±2	0	NO
-1	±1	1/2	NO
0	0	0	YES
+1	±1	1/2	NO
+2	±2	0	NO
+3	±1	1/2	NO

- ν = 0: invariant under full *P*622 and time reversal
- ν = ±2: S=0 C=±2
- ν = ±1, ±3: S=1/2 C=±1

ν	C	S	time reversal
-3	±1	1/2	NO
-2	0	1	NO
-1	±1	1/2	NO
0	0	0	NO
+1	±1	1/2	NO
+2	0	1	NO
+3	±1	1/2	NO

- ν = 0: breaks C_{2x} and time reversal
- ν = ±2: S=1 C=0
- ν = ±1, ±3: S=1/2 C=±1

st-JT vs. K-IVC

ν	C	S	time reversal
-3	±1	1/2	NO
-2	±2	0	NO
-1	±1	1/2	NO
0	0	0	
+1	±1	1/2	
+2	±2		
+3			

• a

• ν =

• ν = ± S=1/2 C=±1

ν			sal
			O
			NO
			NO
	1	1/2	NO
	0	1	NO
+3	±1	1/2	NO

• ν = 0: breaks C_{2x} and time reversal

• ν = ±2: S=1 C=0

• ν = ±1, ±3: S=1/2 C=±1

the two scenarios could be experimentally discriminated

st-JT vs. K-IVC

ν	C	S	time reversal
-3	±1	1/2	NO
-2	±2	0	NO
-1	±1	1/2	NO
0	0	0	YES
+1	±1	1/2	NO
+2	±2	0	NO
+3	±1	1/2	NO

- ν = 0: invariant under full *P*622 and time reversal
- ν = ±2: S=0 C=±2
- ν = ±1, ±3: S=1/2 C=±1

ν	C	S	time reversal
-3	±1	1/2	NO
-2	0	1	NO
-1	±1	1/2	NO
0	0	0	NO
+1	±1	1/2	NO
+2	0	1	NO
+3	±1	1/2	NO

- ν = 0: breaks C_{2x} and time reversal
- ν = ±2: S=1 C=0
- ν = ±1, ±3: S=1/2 C=±1

- Hartree-Fock can only describe static Jahn-Teller effect
- since the phonon dispersion is order of magnitudes smaller than the center of mass frequency, it is essentially a vibration of each single moiré unit cell
- in that case is not at all unlikely that the Jahn-Teller effect might occur dynamically

Can we describe a dynamical Jahn-Teller effect?

- the interplay of static Jahn-Teller distortion and Coulomb interaction can stabilise mean-field insulating solutions at all integer fillings

- therefore dynamical Jahn-Teller effect and Coulomb interaction can well conspire to yield **Jahn-Teller Mott Insulators** at all integer fillings, i.e., states in which electron motion is halted, and each moiré supercell locks into the configuration that maximises Jahn-Teller plus Coulomb-exchange energy gain

- However, the description of a Jahn-Teller Mott insulator runs into several obstacles

  - first, the moiré unit cell contains more that 10000 atoms, and thus it is out of question a rigorous approach as in a small molecule

    to overcome that obstacle, we focus just on the flat bands, like concentrating on HOMO and LUMO in a single molecule

    ✓ weak point: the gap between the flat bands and all lower and upper ones is not very large

- However, the description of a Jahn-Teller Mott insulator runs into several obstacles

– even if we concentrate just on the flat bands, Wannier obstruction prevents building a short-range tight-binding model for the flat bands

to overcome that obstacle, we assume that a projected BCS wavefunction yields a qualitatively accurate description of Jahn-Teller Mott insulators at integer filling ν

$$|\psi(\nu)\rangle = P_{\mathrm{G}}(\nu)\,|\,\mathrm{BCS}\rangle$$

BCS wavefunction for the flat bands only

Gutzwiller projector onto the state in which each moiré supercell is strictly occupied by 4 + ν electrons

$$|\psi(\nu)\rangle = P_{\mathrm{G}}(\nu)\,|\,\mathrm{BCS}\rangle$$

- we do not optimise the wavefunction, which is practically unfeasible
- and neither we try to extract its physical properties, e.g., the topological ones, which is equally hard
- instead, we just determine the BCS wavefunction for the flat bands that is favoured by the Jahn-Teller coupling, assuming it prevails over Coulomb exchange as Hartree-Fock suggests, and pays less Coulomb charging energy
- and assume that the properties of the projected wavefunction are simply inherited by the BCS one

BCS wavefunction

$$H_{\text{J-T}} = -\frac{g}{2N} \sum_{i=1}^{2} L_i^\dagger(\mathbf{q})\, L_i(\mathbf{q})$$

- project $H_{\text{J-T}}$ onto the flat-band S=0, τ_3=0 pair operators

$$\Delta^\dagger_{\mathbf{k},nm} = \frac{1}{\sqrt{2}} \left(\Psi^\dagger_{\mathbf{k},n,\uparrow,+1}\, \Psi^\dagger{}_{-\mathbf{k},m,\downarrow,-1} + \Psi^\dagger{}_{-\mathbf{k},m,\uparrow,-1}\, \Psi^\dagger_{\mathbf{k},n,\downarrow,+1} \right)$$

- $\Psi^\dagger_{\mathbf{k},n,\sigma,\tau_3}$ creates an electron at momentum $\mathbf{k}$ inside the mini BZ, in the flat band $n = 1, 2$, with spin $\sigma = \uparrow, \downarrow$ in valley $\tau_3 = \pm 1$

- note that $\Delta^\dagger_{\mathbf{k},nn}$ and $\Delta^\dagger_{\mathbf{k},12} + \Delta^\dagger_{\mathbf{k},21}$ are even under C_{2z}, while $\Delta^\dagger_{\mathbf{k},12} - \Delta^\dagger_{\mathbf{k},21}$ is odd

BCS wavefunction

$$H_{\text{J-T}} \to -g \sum_i \lambda_i \, \Delta_i^\dagger \, \Delta_i$$

- where $\Delta_i^\dagger = \sum_{\mathbf{k}} \sum_{n,m=1}^{2} \psi_i^{nm}(\mathbf{k}) \, \Delta_{\mathbf{k},nm}^\dagger$ with $\sum_{\mathbf{k}} \sum_{n,m=1}^{2} \left|\psi_i^{nm}(\mathbf{k})\right|^2 = 1$

- if $\psi_i^{nn}(\mathbf{k}) \neq 0$ then $\psi_i^{12}(\mathbf{k}) = \psi_i^{21}(\mathbf{k})$ and $\Delta_i^\dagger$ is even under C_{2z}
- since particle-hole symmetry P is nearly satisfied, $\Delta_i^\dagger$ is (almost) even under P if $\psi_i^{11}(\mathbf{k}) \simeq \psi_i^{22}(-\mathbf{k})$ and $\psi_i^{12}(\mathbf{k}) \simeq -\psi_i^{12}(-\mathbf{k})$, and odd otherwise
- $\Delta_i^\dagger$ is even under C_{2x} if $\psi_i^{nn}\big(C_{2x}(\mathbf{k})\big) = \psi_i^{nn}(\mathbf{k})$ and $\psi_i^{12}\big(C_{2x}(\mathbf{k})\big) = -\psi_i^{12}(\mathbf{k})$, and odd otherwise
- the component of $\psi_i^{nm}(\mathbf{k})$ even under $\mathbf{k} \to -\mathbf{k}$ corresponds to the spin-singlet, valley-triplet with $\tau_3 = 0$, while that odd to the spin- and valley-singlet.

Leading pairing channel: s-wave

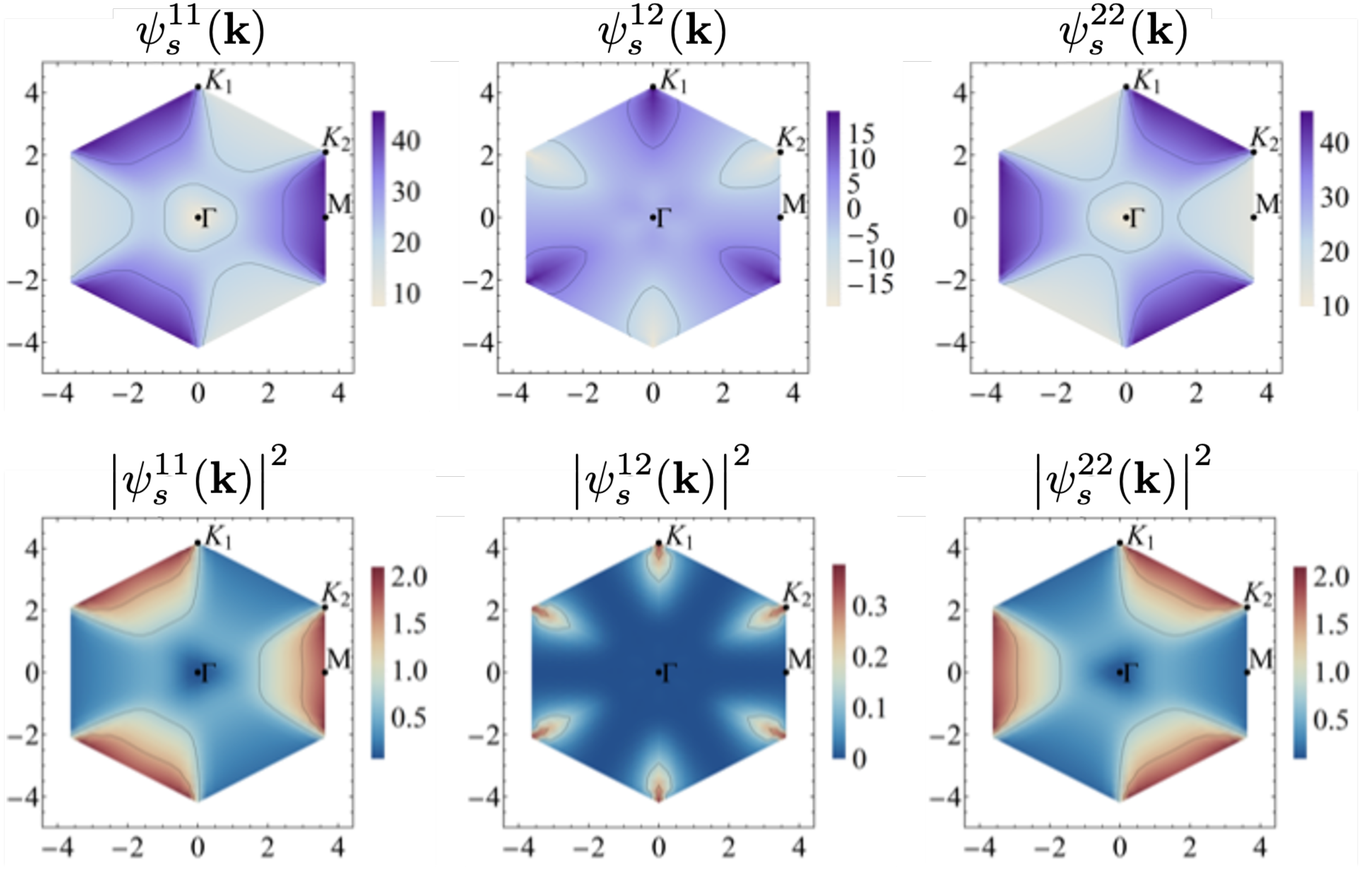

- transforms like the fully symmetric irrep of D_6
- almost even under p-h
- almost odd under **k** → **-k**: prevailing spin- and valley-singlet component

Next to leading pairing channel: d-wave

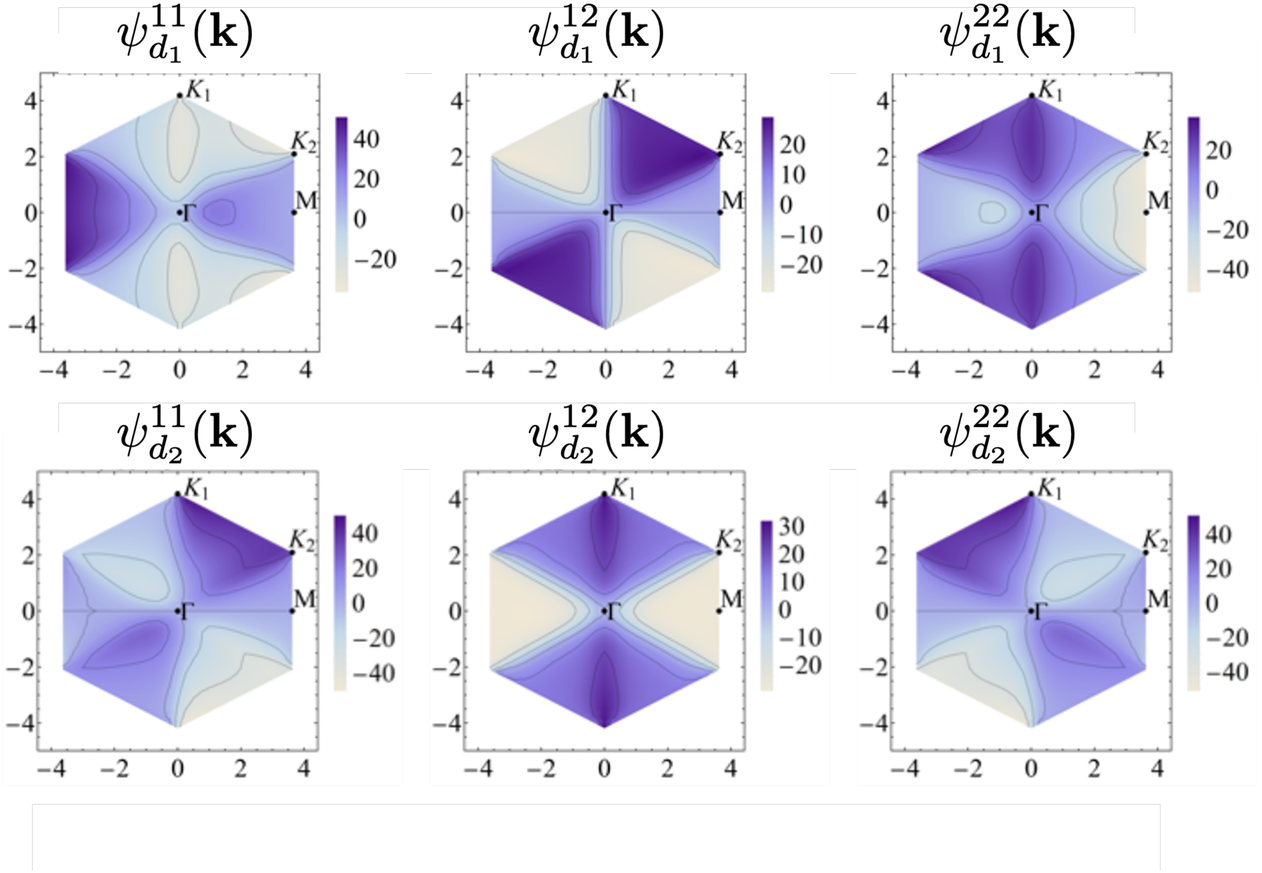

- transforms like the two-dimensional irrep E_2 of D_6, $d_1 \backsim x^2 - y^2$ and $d_2 \backsim xy$
- almost even under $\mathbf{k} \rightarrow -\mathbf{k}$: prevailing spin-singlet and valley-triplet component: $d_1 \backsim x^2 - y^2 + \alpha x$ and $d_2 \backsim xy - \alpha y$, with $\alpha \ll 1$

- almost odd under p-h symmetry, which hints at a non trivial topological character

Next to leading pairing channel: d-wave

- indeed, the combinations $d_+ = d_1 + id_2 \sim Y_{2+2}$ and $d_- = d_1 - id_2 \sim Y_{2-2}$ have finite Chern number, $C = +2$ and $C = -2$, respectively, equal to the angular momentum

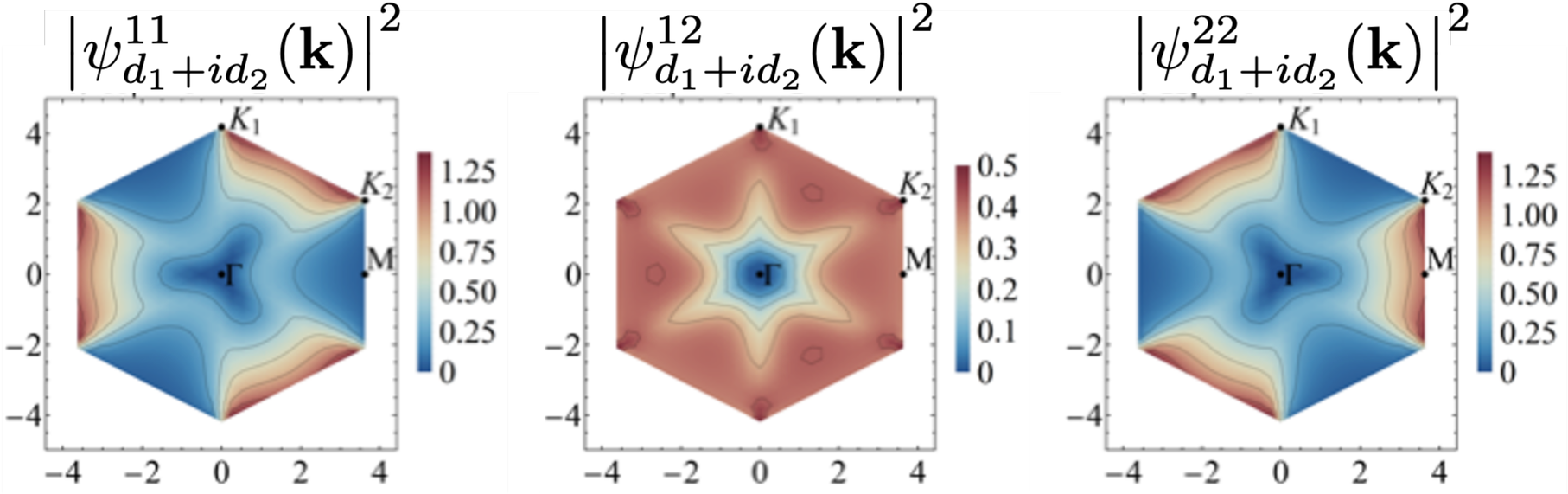

BCS wavefunction

- unsurprisingly, Jahn-Teller coupling alone favours the s-wave Cooper channel
- however, Hartree-Fock predicts topological Jahn-Teller Mott insulators at any integer filling away from charge neutrality, thus it suggests that the d-wave channel prevails
- the only reason for that can be Coulomb repulsion

indeed, Coulomb pseudo-potential, RPA-screened by all other bands, pushes the d-wave channel below the s-wave one

Projected BCS wavefunction

$$|\Psi_\nu\rangle \propto P_{\mathrm{G}}(\nu) \left(\Delta_{d_+}^\dagger\right)^{\frac{N}{2}(2+\nu_+)} \left(\Delta_{d_-}^\dagger\right)^{\frac{N}{2}(2+\nu_-)} |0\rangle$$

- the 'vacuum' $|0\rangle$ is the ground state at filling $\nu = -4$, i.e., flat bands empty
- integer $\nu_\pm \geq -2$ such that $\nu_+ + \nu_- = \nu \in [-4, 4]$
- P_{G} project onto the states where each moiré unit cell is occupied by $4 + \nu$ electrons
- Chern number $C(\nu_+, \nu_-) = (\nu_+ - \nu_-) \in [-4, 4]$
- orbital angular momentum per unit cell: $M = \mu_B \left|\nu_+ - \nu_-\right| \in [0, 4]$
- the mean-field insulators correspond to specific ν_+ and $\nu_- = \nu - \nu_+$ values

Jahn-Teller Mott insulators at $\nu = 0$

- Hartree-Fock suggests that the lowest energy state corresponds to

$$|\Psi_0\rangle \propto P_{\mathrm{G}}(0)\left(\Delta^{\dagger}_{d_+}\right)^N\left(\Delta^{\dagger}_{d_-}\right)^N|0\rangle = P_{\mathrm{G}}(0)\left(\Delta^{\dagger}_{d_1}\right)^N\left(\Delta^{\dagger}_{d_2}\right)^N|0\rangle$$

  thus, a non-magnetic and non-topological Jahn-Teller Mott insulator

- however, a magnetic field may stabilise other ν_+ and $\nu_- = \nu - \nu_+ = -\nu_+$

$$|\Psi'_0\rangle \propto P_{\mathrm{G}}(0)\left(\Delta^{\dagger}_{d_+}\right)^{\frac{N}{2}(2+\nu_+)}\left(\Delta^{\dagger}_{d_-}\right)^{\frac{N}{2}(2-\nu_+)}|0\rangle$$

  thus, topological Jahn-Teller Mott insulators with Chern numbers $C = 2\nu_+ \in [-4,4]$

Jahn-Teller Mott insulators at ν = -2 and +2

- Hartree-Fock suggests that the lowest energy states corresponds to

$$|\Psi_{-2}\rangle \propto P_{\mathrm{G}}(-2)\left(\Delta^{\dagger}_{d_{\pm}}\right)^{N}|0\rangle$$

$$|\Psi_{+2}\rangle \propto P_{\mathrm{G}}(-2)\left(\Delta^{\dagger}_{d_{\pm}}\right)^{2N}\left(\Delta^{\dagger}_{d_{\mp}}\right)^{N}|0\rangle$$

  thus, topological Jahn-Teller Mott insulators with C = ± 2

- the wavefunction also admits a non-topological insulator with $\nu_+ = \nu_-$

Jahn-Teller Mott insulators at odd filling ν

- at odd ν the projected BCS wavefunction

$$|\Psi_\nu\rangle \propto P_{\mathrm{G}}(\nu)\left(\Delta_{d_+}^{\dagger}\right)^{\frac{N}{2}(2+\nu_+)}\left(\Delta_{d_-}^{\dagger}\right)^{\frac{N}{2}(2+\nu_-)}|0\rangle$$

describes spin and valley liquid topological insulators that may have C = ± 1, ± 3, while Hartree-Fock yields polarised symmetry-breaking ones with C = ± 1

Pictorial representation of the Jahn-Teller Mott insulators

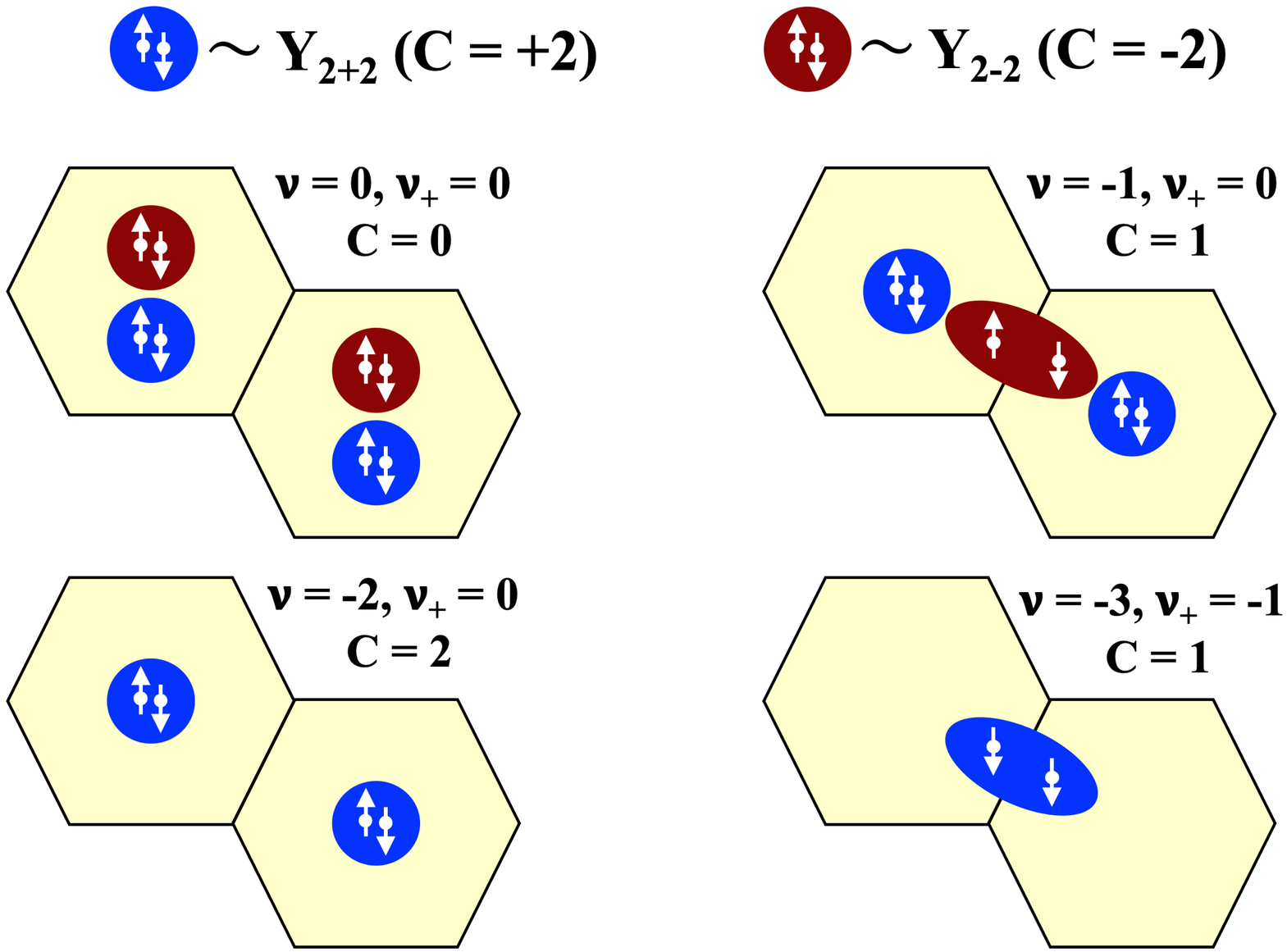

Non-topological Jahn-Teller Mott insulators

- Hartree-Fock predicts topological insulators at any $\nu \neq 0$, thus complex pair operators $\Delta^\dagger_{d_\pm}$ prevailing over real ones, $\Delta^\dagger_{d_1}$ and $\Delta^\dagger_{d_2}$
- however, we cannot exclude that in reality the real pair operators prevail, thus

$$|\Psi_\nu\rangle \propto P_{\mathrm{G}}(\nu) \left(\Delta^\dagger_{d_1}\right)^{\frac{N}{2}(2+\nu_1)} \left(\Delta^\dagger_{d_2}\right)^{\frac{N}{2}(2+\nu_2)} |0\rangle$$

Superconductivity away from integer ν

- if $\nu = n + \delta$ with integer $n \in [-3, 3]$ and $-1 \ll \delta \ll 1$, the Gutzwiller projector $P'_{\mathrm{G}}(\nu)$ admits configurations where each supercell is occupied either by n or $n + \mathrm{sign}(\delta)$ electrons

- therefore the projected wavefunction is not insulating, and most likely is superconducting

- either complex pairs: $|\Psi_\nu\rangle \propto P'_{\mathrm{G}}(\nu) \left(\Delta^\dagger_{d_+}\right)^{\frac{N}{2}(2+\nu_+)} \left(\Delta^\dagger_{d_-}\right)^{\frac{N}{2}(2+\nu_-)} |0\rangle$

  or real ones: $|\Psi_\nu\rangle \propto P'_{\mathrm{G}}(\nu) \left(\Delta^\dagger_{d_1}\right)^{\frac{N}{2}(2+\nu_1)} \left(\Delta^\dagger_{d_2}\right)^{\frac{N}{2}(2+\nu_2)} |0\rangle$

Superconductivity away from integer ν

- if complex pairs win, a chiral d-wave superconductor may appear, which has no nodes and is still topological

- on the contrary, if real pairs prevail, a conventional d-wave (spin-singlet and valley-triplet with $\tau_3 = 0$) superconductor with a weak p-wave (spin-singlet and valley-singlet) character may appear, which has nodes and is slightly nematic

Conclusions

- Jahn-Teller effect can stabilise insulating states that are only metastable in presence of the sole Coulomb repulsion
- In mean-field, the insulator at charge neutrality is invariant under *P*622 space group and time reversal, whereas those at the other integer fillings are topological: spin unpolarised with $C = \pm 2$ at $\nu = \pm 2$, spin polarised with $C = \pm 1$ at $\nu = \pm 1, \pm 3$, and all of them carry orbital magnetism
- Those topological insulators are prone to become spin-singlet superconductors upon doping, possibly topological ones. For that, Jahn-Teller effect seems crucial, as Coulomb repulsion alone seems unable to provide pairing